A systems biology approach to discover novel transcriptional regulators that influence the shoot growth by regulating cytokinin signal homeostasis in the shoot apical meristem of *Arabidopsis thaliana*

Sonal Yadav

A thesis submitted for the partial fulfillment ofthe degree of Doctor of Philosophy

Department of Biological Sciences

Indian Institute of Science Education and Research Mohali

Knowledge city, Sector 81, SAS Nagar, Manauli PO, Mohali 140306, Punjab, India.

April 2022

Dedicated to my beloved family

Declaration

The work presented in this thesis has been carried out by me under the guidance of Dr. Ram Kishor Yadav at the Indian Institute of Science Education and Research Mohali. This work has not been submitted in part or in full for a degree, a diploma, or a fellowship to any other universityor institute. Whenever contributions of others are involved, every effort is made to indicate this clearly, with due acknowledgement of collaborative research and discussions. This thesis is a bonafide record of original work done by me and all sources listed within have been detailed in the bibliography.

Sonal Yadav

Date:

Place:

In my capacity as the supervisor of the candidate's thesis work, I certify that the above statementsby the candidate are true to the best of my knowledge.

Dr. Ram Kishor Yadav

Date:

Place:

Acknowledgements

My love for plants starts from my ancestral roots in Rajasthan. I was born and brought up in the concrete jungle of Mumbai. However, my heart skipped a beat every time I was in the midst of nature. The summer trips to our ancestral village made me crave being around those luscious fields. This love drove me to hunt for a PhD position where I could work with plants. Dr Ram was the only person in India who was capable of setting up a lab where all aspects of plant development can be studied. I have spent a long time working in his lab and have learnt a lot. The skills and expertise that I have acquired here are incomparable and unrequitable. Throughout my PhD Dr Ram has pushed me to work harder and do more. He has given me the resources so that I can add so much to this thesis. For that I am thoroughly indebted to Dr Ram's mentorship and support.

I am thankful to Dr Mahak Sharma and Dr Rachna Chaba for helping and supporting me throughout my PhD. They have been with us from our 3TL2 days and I have always looked up to them for inspiration. I want to thank all my lab members for making RY lab what it is. Also, thanks to the extended family of 3TL2 and 3TL1. I am grateful for the collaborative atmosphere in the Department of Biological Sciences at IISER Mohali. I thank the IISER administration, library, instrumentation, store and purchase sections, mess staff, canteen staff, and hostel caretakers for their cooperation.

I am most grateful that I have made many friends at IISER who will stay with me as lifelong well-wishers. The first of these are my batchmates Alok, Aparajita, Richa, Namrata and Nupur. They have made me feel light and hopeful in the most difficult times of my PhD. Alok was my greatest confidante without whom so many situations would have been impossible to overcome for me. He has not only been a friend but also like a labmate because he even helped me get liquid nitrogen when all others refused to help. I want to thank Appy for her wisdom

and Richa for her infectious affections. Nupur who I thankfully connected with at the end of my PhD has helped me get back my zest for life. To Rashmi, who has been like the little sister I never had. These pandemic years have been the most difficult time of my life. But all these people have made it easier to get through the worst and keep me hoping for the best.

Finally, I have to thank my wonderful family for being my pillars of support me through these trying times. You give me courage and taught me to face any obstacles with integrity. I am truly blessed to have all of you and my one aim in life has been to never let you down. To my mother who is beautiful both inside and out. You have taught me grace and stoicism. To my father who is the epitome of everything I aspire to be. You inspire me to work hard and be true to thyself. Lastly, I want to thank my brother who is also my oldest childhood friend.

The past two years have been hard as we have been shut in the campus. I could not have gone through these trying times without so many people. I am grateful that our campus has such vast open spaces that these lockdowns have been easier to cope with. For this I will miss IISER Mohali and cherish my memories here forever.

List of Publications

- Shivani Bhatia, Harish Kumar, Monika Mahajan, **Sonal Yadav**, Prince Saini, Shalini Yadav, Sangram K. Sahu, Jayesh K. Sundaram, Ram K. Yadav (2021). "A cellular expression map of epidermal and subepidermal cell layer-enriched transcription factor genes integrated with the regulatory network in Arabidopsis shoot apical meristem" **Plant Direct**

- **Sonal Yadav**, Sangram K. Sahu and Ram Kishore Yadav (2022). "Abiotic stress induced transcription factors orchestrate cytokinin signal homeostasis in *Arabidopsis* shoot apex" (**Manuscript under preparation**)

Table of Contents

Synopsis

Introduction

Among the classical phytohormones, cytokinin (CK) and auxin are considered the most important. The early work of many pioneering plant biologists revealed the role of auxin in trophic movements in plants. The quest to grow plant cells in tissue culture led to the discovery of CK. In the beginning, plant tissue culture experiments were performed using the CK-like compounds that were obtained from the yeast extract (Robbins et al., 1922) and autoclaved herring sperm DNA (Miller & Skoog, 1953). The naturally occurring CKs, zeatin and ribosylzeatin were extracted from maize endosperm (Letham et al., 1964) and coconut milk (Overbeek et al., 1941), respectively. The term "cytokinin" was proposed based on the cell division promoting activity of CKs, which was tested on tobacco cells (Miller and Skoog, 1962).

Cytokinins have a key role to play in initiating cell division by regulating the expression of the D-type cyclins (CYCD), which are important for G_1/S phase transition (Riou-Khamlichi et al., 1999). The role of cytokinins in the G_2/M phase transition has not yet been determined due to the lack of a direct molecular link. However, cytokinin levels peak twice during the cell cycle, at the end of S phase and then again during mitosis (Redig et al., 1996). Therefore, an optimal amount of cytokinins at precise junctions of the cell cycle are required to promote cell division. The development of Murashige and Skoog (MS) media enabled a surge in possible applications of plant tissue culture. This also led to the discovery of an interesting phenomenon in the formation of shoots from callus cultures. It was observed that CKs have an inherent shoot promoting effect, as a higher CK-to-auxin ratio led to the formation of shoots from the undifferentiated callus. The Two-Component signalling Sensor new (TCSn) is the most stable CK response reporter and in the shoot apical meristem (SAM) it is expressed within the

organizing center (OC). The *TCSn* reporter was constructed by combining concatemeric binding sites of the Type-B ARRs with endoplasmic reticulum targeted GFP reporter protein (Zürcher et al., 2013). Interestingly, type-B ARRs bind to the *WUS* promoter and activate its expression in the zone of highest cytokinin response within the OC (Wang et al., 2017; Xie et al., 2018; Zhang et al., 2017; Zubo et al., 2017). Thus, the shoot forming ability of CK response is mediated by its direct activation of *WUS* expression.

Cytokinin biosynthesis, degradation and signalling genes in the shoot apical meristem

To understand the genes responsible for maintaining CK levels and response in the SAM, I have generated transcriptional reporters of all relevant CK biosynthesis, degradation and signalling genes. The first committed step in cytokinin biosynthesis is catalyzed by ISOPENTENYLTRANSFERASEs (IPTs) to create inactive nucleotides or nucleosides. In plants, there are two types of IPTs based on their substrate specificity namely the ATP/ADP IPTs and tRNA IPTs (Miyawaki et al., 2004). I have studied the expression of both kinds of *IPTs* in the SAM and found that they also vary in expression pattern.

The enzymes responsible for creating active cytokinin nucleobases were first characterized in rice (*Oryza sativa*). These were coined as LONELY GUY (LOG) enzymes and basically, they are cytokinin riboside 5'-monophosphate phosphoribohydrolases (Kuroha et al., 2009). I have made the transcriptional reporters of *LOG4* and *LOG7* to determine the regions in the SAM where active CKs are synthesized. Cytokinins are degraded by a group of enzymes that are biochemically different but commonly known as CYTOKININ OXIDASEs /DEHYDROGENASEs (CKXs) (Werner et al., 2003). The *CKX3* and *CKX5* are expressed in different domains of the SAM but are functionally complementary as observed in the double

mutant (Bartrina et al., 2011). The transcriptional reporter of *CKX5* was shown to have an expression in the domains of the SAM where CK response is minimal.

The two-component signal transduction pathway begins with the transmembrane ARABIDOPSIS HISTIDINE KINASEs (AHKs) (To & Kieber, 2008). I have studied the expression pattern for transcriptional reporters of *AHK2*, *AHK3* and *AHK4* in the SAM. After the autocatalytic activation of the AHKs, the phosphorelay system transduces the signal further with the help of certain intermediate molecules known as the HISTIDINE PHOSPHOTRANFER PROTEINs (AHPs). I have studied the expression of *AHP5* in the SAM with the help of its transcriptional reporter lines. Similarly, the expression pattern of pseudo-phosphotransfer gene *AHP6* was also observed in the SAM.

The AHPs that are phosphorylated translocate into the nucleus will in turn activate a group of ARABIDOPSIS RESPONSE REGULATORS (ARRs). These ARRs are of two types, namely the Type-A ARRs and the Type-B ARRs (D'Agostino et al., 2000). The type-B ARRs are transcription factors and of these, I generated transcriptional reporters of two genes (*ARR1* and *ARR10*). The type-A ARRs are negative regulators of CK response since they function as quenchers. Among the type-A ARRs, I have studied the expression pattern of *ARR4*, *ARR5*, *ARR7*, *ARR9* and *ARR15* in the SAM. Using this approach, I have been able to study the functional relevance of each gene in maintaining optimum levels of CK molecules and CK response within the SAM.

Identifying novel transcription factors responsible for maintaining cytokinin homeostasis

While the downstream effect of CK signalling has been well studied, there is a lacuna in our understanding of the upstream factors that influence CK response. The CK biosynthesis, degradation and signalling genes are also regulated by several transcription factors that induce

or repress their expression. I employed a network biology approach to identify the upstream transcription factors that are involved in Cytokinin Gene Regulatory Network (CKGRN) in the shoot apex of *Arabidopsis thaliana*. I constructed the promoter baits consisting of the 3kb upstream promoter sequence for thirty-five genes, encoding ISOPENTENYL TRANSFERASEs (IPT2, 3 7, 9), LONELY GUYs (LOG1, 2, 3, 4, 5, 6, 7), CYTOKININ OXIDASEs (CKX3, 5, 6), ARABIDOPSIS HISTIDINE KINASEs (AHK, 2, 3, 4, 5), HISTIDINE PHOSPHOTRANSFER PROTEINs (AHP2, 3, 5, 6), Type-A ARRs (ARR 4, 5, 7, 9, 15), and Type-B ARRs (ARR1, 2, 10, 12, 14, 18, 20, 21). In total 11445 interactions were screened with 327 transcription factor preys and 25 bait promoters, after excluding the baits exhibiting high autoactivation. I have obtained an eY1H protein-DNA network consisting of 49 transcription factors binding to the 23 target gene promoters involving 164 interactions.

To further validate the CKGRN the T-DNA insertion lines for interacting transcription factors were isolated and characterized. These lines were further used to characterize the *in-planta* effect of an interacting TF on the expression of its target gene using RT-qPCR. In this way, a part of the CKGRN network was validated and the nature of the interactions was determined. The phenotype in single and double mutants of various transcription factors was studied for shoot growth defects. Change in the CK response also has a direct effect on bolting time, flowering and other factors that determine the growth of the plant (Bartrina et al., 2017; Riefler et al., 2006; Tokunaga et al., 2012). This shoot promoting property of CKs was also used to screen for mutants that could be defective in CK response.

NAC062 regulates shoot growth by maintaining cytokinin biosynthesis and signalling

NAC062/NAC WITH TRANSMEMBRANE MOTIF1 (NTM1)-LIKE6 (NTL6) was identified as a part of the CKGRN in the eY1H screen. NAC062/NTL6 is a membrane-bound

transcription factor (MTF) that is activated by changes in membrane fluidity. The cleavage of NAC062/NTL6 is enhanced by cold, drought, salt and UPR stress. Its cleavage is also promoted by Abscisic acid (ABA) (Kim et al., 2007; Seo et al., 2010; Yang et al., 2014). NAC062/NTL6 modulates CK response by binding to the *LOG4* and *AHK4* promoters. The CK signalling output is reduced in the stem cell niche of *nac062*/*ntl6* mutant plant SAM, and as a result size of the shoot is also reduced. Conversely, constitutive overexpression of the nuclear form of NAC062 led to delayed senescence and severe growth defects due to enhanced CK signalling. NAC062/NTL6 is present throughout the SAM and has a minimal effect on growth even in ambient conditions. The changes in membrane fluidity caused by exposure to colder temperatures further stimulate NAC062/NTL6 cleavage from the membrane. I have also shown that CK response increases in cold, and this is mediated by NAC062. However, since the membrane stabilizes approximately 24 hours after initial cold exposure, NAC062 cannot be activated for an extended duration. Therefore, to observe the long-term effects of NAC062 in the SAM it was expressed constitutively and transiently in the shoot. This resulted in several shoot defects such as loss of apical dominance and arrested shoot growth. These morphological defects were due to the rapid increase in CK response within the SAM such that it fails to undergo senescence.

Bibliography

Bartrina, I., Jensen, H., Novák, O., Strnad, M., Werner, T., & Schmülling, T. (2017). Gain-of-function mutants of the cytokinin receptors AHK2 and AHK3 regulate plant organ size, flowering time and plant longevity. *Plant Physiology*, *173*(3), 1783–1797. https://doi.org/10.1104/pp.16.01903

Bartrina, I., Otto, E., Strnad, M., Werner, T., & Schmülling, T. (2011). Cytokinin regulates the activity of reproductive meristems, flower organ size, ovule formation, and thus seed yield in Arabidopsis thaliana. *The Plant Cell*, *23*(1), 69–80. https://doi.org/10.1105/tpc.110.079079

D'Agostino, I. B., Deruère, J., & Kieber, J. J. (2000). Characterization of the response of the Arabidopsis response regulator gene family to cytokinin. *Plant Physiology*, *124*(4), 1706–1717. https://doi.org/10.1104/pp.124.4.1706

Kim, S. Y., Kim, S. G., Kim, Y. S., Seo, P. J., Bae, M., Yoon, H. K., & Park, C. M. (2007). Exploring membrane-associated NAC transcription factors in Arabidopsis: Implications for membrane biology in genome regulation. *Nucleic Acids Research*, *35*(1), 203–213. https://doi.org/10.1093/nar/gkl1068

Kuroha, T., Tokunaga, H., Kojima, M., Ueda, N., Ishida, T., Nagawa, S., Fukuda, H., Sugimoto, K., & Sakakibara, H. (2009). Functional analyses of LONELY GUY cytokinin-activating enzymes reveal the importance of the direct activation pathway in Arabidopsis. *The Plant Cell*, *21*(10), 3152–3169. https://doi.org/10.1105/tpc.109.068676

Letham, D. S., I. S. Shannon and I. R. McDonald. 1964. The structure of zeatin, a factor inducing cell division. Proc. Chem. Soc. 230-231.

Miller, C., & Skoog, F. (1953). Chemical Control of Bud Formation in Tobacco Stem Segments. *American Journal of Botany*, *40*(10), 768–773. https://doi.org/10.2307/2438273

Miyawaki, K., Matsumoto-Kitano, M., & Kakimoto, T. (2004). Expression of cytokinin biosynthetic isopentenyltransferase genes in Arabidopsis: Tissue specificity and regulation by auxin, cytokinin, and nitrate. *Plant Journal*, *37*(1), 128–138. https://doi.org/10.1046/j.1365-313X.2003.01945.x

Murashige, T. and F. Skoog. 1962. A revised medium for rapid growth and bioassays with tabacco tissue cultures. Physiol. Plant. 15: 473-497. https://doi.org/10.1111/j.1399-3054.1962.tb08052.x

Redig, P., Shaul, O., Inze, D., Van Montagu, M., & Van Onckelen, H. (1996). Levels of endogenous cytokinins, indole-3-acetic acid and abscisic acid during the cell cycle of synchronized tobacco BY-2 cells. *FEBS letters*, *391*(1-2), 175–180. https://doi.org/10.1016/0014-5793(96)00728-4

Riefler, M., Novak, O., Strnad, M., & Schmülling, T. (2006). Arabidopsis cytokinin receptors mutants reveal functions in shoot growth, leaf senescence, seed size, germination, root development, and cytokinin metabolism. *Plant Cell*, *18*(1), 40–54. https://doi.org/10.1105/tpc.105.037796

Riou-Khamlichi, C., Huntley, R., Jacqmard, A., & Murray, J. A. (1999). Cytokinin activation of Arabidopsis cell division through a D-type cyclin. *Science (New York, N.Y.)*, *283*(5407), 1541–1544. https://doi.org/10.1126/science.283.5407.1541

Robbins, W. J. (1922a). Cultivation of excised root-tips and stem tips under sterile conditions. *Bot. Gaz*. 73, 376-390. https://doi.org/10.1086/333010

Seo, P. J., Kim, M. J., Song, J. S., Kim, Y. S., Kim, H. J., & Park, C. M. (2010). Proteolytic processing of an Arabidopsis membrane-bound NAC transcription factor is triggered by cold-induced changes in membrane fluidity. *Biochemical Journal*, *427*(3), 359–367. https://doi.org/10.1042/BJ20091762

To, J. P. C., & Kieber, J. J. (2008). Cytokinin signaling: two-components and more. *Trends in Plant Science*, *13*(2), 85–92. https://doi.org/10.1016/j.tplants.2007.11.005

Tokunaga, H., Kojima, M., Kuroha, T., Ishida, T., Sugimoto, K., Kiba, T., & Sakakibara, H. (2012). Arabidopsis lonely guy (LOG) multiple mutants reveal a central role of the LOG-dependent pathway in cytokinin activation. *Plant Journal*, *69*(2), 355–365. https://doi.org/10.1111/j.1365-313X.2011.04795.x

Van Overbeek, J., Conklin, M. E., & Blakeslee, A. F. (1941). Factors in coconut milk essential for growth and development of very young datura embryos. *Science (New York, N.Y.)*, *94*(2441), 350–351. https://doi.org/10.1126/science.94.2441.350

Wang, J., Tian, C., Zhang, C., Shi, B., Cao, X., Zhang, T. Q., Zhao, Z., Wang, J. W., & Jiao, Y. (2017). Cytokinin signaling activates WUSCHEL expression during axillary meristem initiation. *Plant Cell*, *29*(6), 1373–1387. https://doi.org/10.1105/tpc.16.00579

Werner, T., Motyka, V., Laucou, V., Smets, R., Onckelen, H. van, & Schmuelling, T. (2003). Cytokinin-Deficient Transgenic Arabidopsis Plants Show Functions of Cytokinins in the Regulation of Shoot and Root Meristem Activity. *The Plant Cell*, *15*(November), 2532–2550. https://doi.org/10.1105/tpc.014928.)

Xie, M., Chen, H., Huang, L., O'Neil, R. C., Shokhirev, M. N., & Ecker, J. R. (2018). A B-ARR-mediated cytokinin transcriptional network directs hormone cross-regulation and shoot development. *Nature Communications*, *9*(1), 1–13. https://doi.org/10.1038/s41467-018-03921-6

Yang, Z. T., Lu, S. J., Wang, M. J., Bi, D. L., Sun, L., Zhou, S. F., Song, Z. T., & Liu, J. X. (2014). A plasma membrane-tethered transcription factor, NAC062/ANAC062/NTL6, mediates the unfolded protein response in Arabidopsis. *Plant Journal*, *79*(6), 1033–1043. https://doi.org/10.1111/tpj.12604

Zhang, F., May, A., & Irish, V. F. (2017). Type-B ARABIDOPSIS RESPONSE REGULATORs Directly Activate WUSCHEL. *Trends in Plant Science*, *22*(10), 815–817. https://doi.org/10.1016/j.tplants.2017.08.007

Zubo, Y. O., Blakley, I. C., Yamburenko, M. v., Worthen, J. M., Street, I. H., Franco-Zorrilla, J. M., Zhang, W., Hill, K., Raines, T., Solano, R., Kieber, J. J., Loraine, A. E., & Schaller, G. E. (2017). Cytokinin induces genome-wide binding of the type-B response regulator ARR10 to regulate growth and development in Arabidopsis. *Proceedings of the National Academy of*

Sciences of the United States of America, *114*(29), E5995–E6004. https://doi.org/10.1073/pnas.1620749114

Zürcher, E., Tavor-Deslex, D., Lituiev, D., Enkerli, K., Tarr, P. T., & Müller, B. (2013). A robust and sensitive synthetic sensor to monitor the transcriptional output of the cytokinin signaling network in planta. *Plant Physiology*, *161*(3), 1066–1075. https://doi.org/10.1104/pp.112.211763

List of figures

List of tables

List of abbreviations

%	Percent
mg	Miligram
M	Molar
mL	Mililitre
mM	Millimolar
µM	Micromolar
min	Minute
GRN	Gene regulatory network
PCR	Polymerase chain reaction
SAM	Shoot apical meristem
bHLH	basic helix loop helix
TF	Transcription factor
WT	Wild type
Y1H	Yeast-one-hybrid

Chapter 1

General Introduction

1.1 From cell theory to plant hormones

The search for plant hormones began unbeknownst to several pioneering plant biologists because they were obsessed with the classical cell theory as defined by Schwann, Schleiden and Virchow. This hunt started in 1838 with Matthias Schleiden's work on the microscopic nature of plant tissues (Schleiden, M. J. 1838). After Schwann's work with animal cells, it was proposed that a common cell theory can be applied to all organisms. This theory was later expanded to include the principle that "omnis cellula e cellula" or "all cells come from cells", as stated by Rudolf Virchow in 1858.

These were the principles that led Gottlieb Haberlandt to first introduce the concept of plant tissue culture in 1902. He was able to keep single cells alive in nutrient media but could not promote cell division within these cultures (Haberlandt, G. 1902). The significance of Haberlandt's contribution was recognized after the groundbreaking work of A. Carrel in establishing the method of animal tissue culture (Carrel, A. 1912). This reinvigorated the hunt for micronutrients that could promote unlimited division and propagation of plant cells.

The first phytohormone discovered by F. W. Went (1926) was defined as a "growth-substance" that promotes elongation of cells in *Avenia* coleoptile tip. Frits Went coined this substance as "auxin" and even discovered polar auxin transport (Went, F. W. 1926). But it was Kögl and coworkers who isolated and characterized the common auxin known as Indole Acetic Acid (IAA) in 1934. The discovery of auxin led to the possibility of plant tissue culture with *Nicotiana* and carrot tissue by Gautheret, White and Nobécourt (1939).

The presence of another plant growth substance was unknowingly discovered by Robbins (1922) in the yeast extract, but the nature of this compound was yet to be defined. This natural growth substance was also discovered in coconut milk by J. van Overbeek and Marie E. Conklin, who were culturing *Datura* embryo for Albert Blakslee to help in his experimentation with colchicine. As it happens this natural cell division promoting factor termed "cytokinin"

was the key to proving that infinite cells can arise from existing cells as proposed in the cell theory. Cytokinins were thus discovered and characterized by Miller, Skoog and coworkers in their experimentation with autoclaved herring sperm DNA and yeast extract (Miller and Skoog, 1962). They discovered that a derivative of adenine known as Kinetin, or 6-furfurylaminopurine, induced the proliferation of tobacco cells. The naturally occurring cytokinins, zeatin and ribosylzeatin, were isolated from maize endosperm and coconut milk respectively by David S. Letham.

These discoveries have demonstrated that all cells are genetically the same but have different characteristics and in plants the auxin-cytokinin interplay is the key to reverting cells from one state to the other.

1.2 Cytokinin: A cell division promoting phytohormone

The initial tissue culture explants maintained by Gautheret that were grown on only auxin substituted media, displayed stressed growth and eventual habituation. This was overcome by the addition of cytokinins in the media developed by Murashige and Skoog. The plant explants grown on the Murashige and Skoog media containing both auxin and cytokinin form a callus (Murashige and Skoog, 1962). The callus is formed as the cells start to dedifferentiate and subsequently start dividing rapidly, thus leading to the growth of the callus. The ratio of cytokinin and auxin is varied to induce the formation of shoot or root, respectively. Thus, a higher cytokinin-to-auxin ratio will promote shoot formation from the undifferentiated callus.

Cytokinins have a key role to play in initiating cell division by regulating the expression of the D-type cyclins (CYCD) which are important for G_1/S phase transition (Riou-Khamlichi et al., 1999). There are three genes of CYCD3 in *Arabidopsis thaliana* and when all of these are disrupted, there is no greening or shoot formation in response to cytokinin (Dewitte et al., 2007). Conversely, the constitutive expression of CYCD3 promotes callus formation in

explants on media that are only substituted with auxin. Moreover, the cytokinin induced greening of callus can also be activated by the expression of CYCD3 in the absence of cytokinin (Riou-Khamlichi et al., 1999).

The role of cytokinins in the G_2/M phase transition has not yet been determined due to the lack of a direct molecular link. Using synchronized tobacco BY-2 cell cultures it is possible to determine that cytokinin levels peak twice during the cell cycle, at the end of S phase and then again during mitosis (Redig et al., 1996). The cells of microalga *Chlorella variabilis* also have a naturally synchronized cell cycle, which is linked to the circadian cycle. Increasing the cytokinin biosynthesis in these microalgae cells led to an extended cell cycle, larger cell size and delayed senescence (Saraswati Nayar, 2021). All these changes were attributed to the delay in progression into G_2/M phase (Orchard et al., 2005). Therefore, an optimal amount of cytokinins at precise junctions of the cell cycle are required to promote cell division.

1.3 Architecture of shoot apical meristem

The shoot apical meristem (SAM) of all higher plants displays an indeterminate growth. This growth is due to the capacity of pluripotent stem cells to self-renew. The stem cells in the meristem remain mitotically active throughout the life cycle of a plant. The stem cells in the SAM are defined during embryogenesis and will give rise to all above-ground organs of the plant. The SAM in angiosperms can be sub-divided into three distinct zones, namely, the central zone (CZ), peripheral zone (PZ) and rib zone (RZ) (Figure 1.1B). The CZ is also called the zone of initials as it consists of a group of slow dividing cells that are involved in the maintenance of the meristem. These cells divide and give rise to the cells of the PZ and RZ. The PZ consists of rapidly dividing cells that give rise to lateral organs such as leaves, axillary meristems and flowers. In *Arabidopsis thaliana,* the CZ is flanked by leaf primordia during the vegetative phase. However, as the reproductive phase is initiated the cells of the PZ start

generating flower primordia. Below the central zone is the RZ which consists of highly active cells that divide to form the growing stem and vasculature. Thus, it is the mitotically active cells of the CZ and RZ that allow the plants to grow laterally and upwards.

The SAM of *Arabidopsis thaliana* can also be distinguished by three distinct cell layers (Figure 1.1). The outermost L1 cell layer is defined from the time of embryogenesis and is perpetuated as the epidermal cell layer. The L1 epidermal precursor cell division is always anticlinal such that new cell walls are formed perpendicular to the surface and therefore there is no intermixing with inner layers. The L2 layer consists of the subepidermal precursor cells and in the CZ this layer is distinct. In the CZ the L2 cell division is anticlinal, however in the zones where organs are initiated some L2 cells start to divide periclinal such that new cell walls are formed parallel to the cell surface. This mixture of cell divisions of the L2 layer gives rise to the distinct bump in the periphery that will later form a leaf or flower. The L3 layer is also called the corpus, and it has no specific organization as the cells in this layer divide in all possible orientations. The L3 layer gives rise to the vasculature of the lateral organ and stem (Meyerowitz et al. 1997).

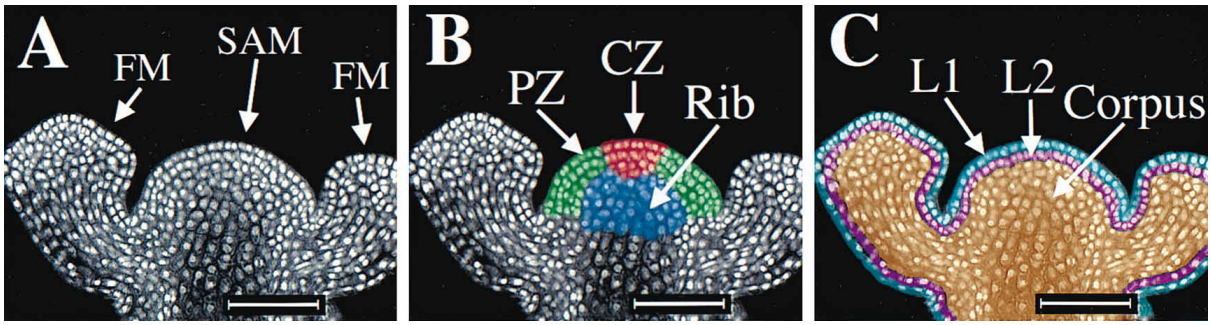

Figure 1.1 : The shoot apical meristem organization (SAM)

SAM labelled and divided based on the (A) organs with floral meristem (FM) in reproductive stage shoot; (B) zones including Central Zone (CZ), Perpheral Zone (PZ) and Rib meristem ; and (C) layers including the epidermal layer (L1), sub-epidermal layer (L2) and Corpus layers. (Courtesy: Meyerowitz et al. 1997)

1.4 Genes that maintain the shoot: CLAVATA and WUS

The SAM consists of very few truly pluripotent stem cells and this stem cell pool is maintained by the signals emanating from the underlying organizing center (OC). The stem cells express *CLAVATA3* (*CLV3*) which forms a short peptide that binds to a Leucine-Rich Repeat (LRR) receptor kinase encoded by the *CLAVATA1* (*CLV1*) gene. The CLV3-CLV1 pathway is responsible for negatively influencing the rate of stem cell division in the CZ and organ primordia. When either of these genes is mutated, there is uncontrolled proliferation throughout the lifecycle of the plant and the size of the SAM enlarges to 1000 times larger than the normal SAM (Clark et al., 1993, 1995). The CORYNE-CLAVATA2 receptor kinase complex has also been shown to act simultaneously in parallel to CLV1 in transducing the CLV3 signal (Müller et al., 2008).

The expression of *WUSCHEL* (*WUS*) gene marks the OC within the shoot apex, and it encodes a homeodomain-containing transcription factor. *WUS* is required for the maintenance of the stem cells within the CZ. Transcription of *WUS* is repressed by the CLV3-CLV1 mediated signalling receptor kinase pathway in the OC due to the presence of CLV1 in this region. It was observed that silencing of *CLV3* led to a marked increase in the *WUS* expression domain (Reddy and Meyerowitz, 2005) and overexpression of *CLV3* led to the rapid decrease of *WUS* expression (Brand et al., 2000; Müller et al., 2006). Conversely, when WUS was overexpressed in the SAM this led to an increase in the number of *CLV3* expressing cells (Schoof et al., 2000). Thus, a negative feedback loop is operating between *CLV3* and *WUS* that is responsible for maintaining the constant number of stem cells and shoot size in higher plants (Brand et al. 2000; Schoof et al., 2000). The signals originating from the OC specify the fate of stem cells in the meristem. Contrary, the repression signal emanating from within the stem cells is responsible for delimiting the stem cell pool. This theory was further expanded by showing the movement of WUS protein from the OC to the overlying stem cells and to the

PZ cell types. Thus, WUS can directly activate the expression of *CLV3* (Yadav et al., 2011). A recent study has also shown that higher levels of *WUS* inhibit *CLV3* expression in the RM. This may explain why *CLV3* is repressed in the cells where *WUS* is normally active (Perales et al., 2016). Further, the nuclear export of WUS protein is mediated by its interaction with EXPORTINs, and this is also negatively regulated by CLV3 signalling (Plong et al., 2021). During embryogenesis, WUS expression is initiated in the 16-cell stage OC progenitor cells (Mayer et al., 1998). The homozygous *wus1* mutant seedlings fail to form a shoot meristem (Laux et al., 1996). The *CLV3* expression in these is completely absent in the bent cotyledon stage. But in the early heart shape stage *CLV3* expression is initiated by the WOX2 module that consists of WUSCHEL-RELATED HOMEOBOX (WOX) transcription factors (Zhang et al., 2017).

1.5 Genes that define the shoot: Epidermal factors

Many genes have been attributed as epidermis-specific based on their expression and activity in the outermost layers of *Arabidopsis thaliana*. However, two homologous HD-ZIP class IV transcription factors ARABIDOPSIS THALIANA MERISTEM LAYER 1 (ATML1) and PROTODERMAL FACTOR 2 (PDF2) are most important for epidermal cell fate specification in the shoot and leaf epidermis (Session et al., 1999; Ogawa et al., 2015). These factors contain a highly conserved StAR-related lipid-transfer (START) domain which has a lipid-sterol binding property that allows them to interact with the cell wall. They also consist of a leucine zipper motif for dimerization and a DNA binding homeodomain (Schrick et al., 2004).
The expression of *ATML1* was observed starting from the apical cell of the zygote till the adult SAM of the vegetative and reproductive shoot. In the 16-cell stage proembryo, the *ATML1* transcript is restricted to the protodermal cells. This continues till the torpedo stage where *ATML1* expression is repressed and then resurges in the L1 layers cells of the adult embryo (Lu

et al., 1996; Sessions et al., 1999). The *PDF2* transcript was present in proembryo and reproductive shoot, but unlike *ATML1* it is absent in the vegetative shoot (Abe et al., 2003). The epidermal expression of the majority of HD-ZIP class-IV transcription factors is attributed to the cis-regulatory element called the L1 box, which is present in their promoters (Abe et al., 2001).

The single mutant plants of *ATML1* and *PDF2* do not show a discernible phenotype, but the *atml1 ; pdf2* double mutant plants develop severe defects in the shoot epidermal cells (Abe et al., 2003). When strong mutant alleles of both *atml1* and *pdf2* were combined the homozygous double mutant embryos were arrested in the globular stage (Abe et al., 2003). The double mutant created by combining the weak alleles of *pdf2-1* and *atml1-1* showed an irregular epidermal surface in the shoot apex and the orientation of the cell division plane was perturbed. In the postembryonic development, the double mutant plants showed malformed cotyledons. The epidermal cell layer was completely missing from young leaves. Instead, the outermost adaxial and abaxial surfaces of these leaves contain palisade and mesophyll cells, respectively (Abe et al., 2003; Ogawa et al., 2015).

1.6 Genes that define the shoot: Organ initiation factors

The cells entering the periphery of the shoot start to accumulate auxin and this leads to organogenesis. The organ primordia initiation sites in the SAM display a positive feedback loop between polar auxin transport and the downstream factors. First, auxin maxima is established by the polar localization of PIN-FORMED (PIN) proteins and the regulation of *PIN* expression (Reinhardt et al., 2003; Bhatia et al., 2016). The increase of auxin levels in the periphery of the SAM also leads to the activation of AUXIN RESPONSE FACTORS (ARFs) transcription factors (Barton M. K., 2010). In response to auxin signalling the two transcription factors, MONOPTEROS (MP/ARF5) and NONPHOTOTROPIC HYPOCOTYL4

(NPH4/ARF7), regulate several downstream genes responsible for apical-basal polarity and lateral organ formation in *Arabidopsis* (Berleth and Jurgens, 1993; Hardtke and Berleth, 1998; Hardtke et al., 2004). Moreover, alteration in MP activity also changes the PIN1 polarity in the peripheral zone (Bhatia et al., 2016).

Apart from organ initiation factors, genes that regulate the patterning of emerging organ primordia are very critical for achieving the final shape of the mature organ. The transcription factors whose expression marks the adaxial and abaxial cells of organs have a pre-established pattern of expression in the CZ and PZ of the SAM (Emery et al., 2003; Kerstetter et al., 2001; McConnell et al., 2001; Yadav et al., 2013). The Class-III homeodomain-leucine zipper (HD-ZIPIII) transcription factors are expressed in the central zone of apical meristem and adaxial surfaces of organ primordia (McConnell et al., 2001; Otsuga et al., 2001). The triple mutant of the HD-ZIPIII family genes *PHABULOSA*, *PHAVOLUTA*, and *REVOLUTA* have no apical meristem and can develop a single abaxialized cotyledon with no apparent bilateral symmetry (Emery et al., 2003).

The *FILAMENTOUS FLOWER* (*FIL*) is a YABBY family transcription factor that is expressed in the abaxial surfaces of lateral organs and it is important for flower symmetry (Sawa et al., 1999; Watanabe et al. 2003). The GARP-domain containing *KANADI* transcription factors are expressed in the organ circumference, abaxial side of leaf primordia and abaxial surface of flower primordia (Kerstetter et al., 2001). The triple mutants of *KANADI* genes develop radialized lateral organs that has lost their abaxial identity. The *kan1 kan2 kan4* triple mutant plants have leaf-like organs on the hypocotyl and outgrowths in the abaxial side of the cotyledons (Eshed et al., 2004; Izhaki and Bowman, 2007).

KANADI and HD-ZIPIII genes function antagonistically to each other in such a way that the organ is specified at the boundary between their expression domains. Determining which came first in the organ primordia, dorsoventral identity transcription factors or establishment of auxin

maxima, is like solving the chicken and egg conundrum. The high levels of auxin play a critical role in organizing the expression of *HD-ZIPIII* and *KAN1* genes in the PZ (Caggiano et al., 2017). Conversely, members of the *KANADI* gene family establish dorsoventral patterning by regulating the PIN1 localization (Izhaki and Bowman, 2007).

1.7 Cytokinin biosynthesis and degradation

The naturally occurring cytokinins consist of an adenine substituted at the N^6 position by an isoprenoid or aromatic side chain (Figure 1.2) (Mok and Mok, 2001). The various forms of cytokinins can also have nucleosides, nucleotides and amino acid conjugates. The N^7 and N^9 positions can also be glycosylated to form N-glycosides. The hydroxyl group can also be modified by glycosylation or xylosylation to form the O-glycosides. These glycosylated forms of cytokinin are inactive but easily transported throughout the plant (Sakakibara et al. 2006). The most abundant and biologically active CKs present in higher plants are a group of isoprenoid cytokinins, namely isopentenyladenine (iP)-, trans-zeatin (tZ)-, cis-zeatin (cZ)- and dihydrozeatin-type (Novak, O., et al. 2008).

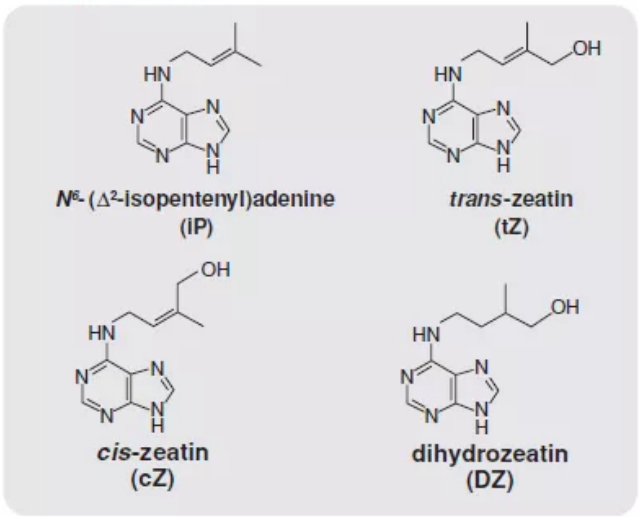

Figure 1.2 : Structure of isoprenoid cytokinins

The dynamic sites of cytokinin production are the root and shoot meristems. The root meristem is enriched with the tZ-type cytokinins, and these can be translocated upwards via the xylem. Conversely, the major cytokinins in the shoot meristem are the iP-type which are transported basipetally via the phloem (Zhang, K., et al. 2014). Thus, cytokinins have local and long-distance effects that are almost indistinguishable from each other.

The first committed step in cytokinin biosynthesis is catalyzed by ISOPENTENYLTRANSFERASEs (IPTs) to create inactive nucleotides or nucleosides (Figure 1.3). In plants, there are two types of IPTs based on their substrate specificity (Miyawaki K., et al. 2004). The ATP/ADP IPTs can use dimethylallyl diphosphate (DMAPP) as the side-chain donor to isopentenylate ATP and ADP (Kakimoto et al., 2001; Sun et al., 2003). The tRNA IPTs are responsible for the synthesis of cZ-type cytokinins by degradation of cis-hydroxy isopentenyl tRNAs. These tRNA IPTs are found in bacteria, animals and plants but they are better understood for their role in cytokinin production in bacteria (Koenig et al., 2002). In *Arabidopsis*, there are two such homologous tRNA IPTs, namely *IPT2* and *IPT9* (Golovko et al., 2002). However, seven genes encode for the ATP/ADP IPTs (*IPT1,3,5,6,7,8*) and these are responsible for generating the iP- and tZ-type of cytokinins (Takei et al., 2004; Kakimoto et al., 2001).

The overexpression of ATP/ADP IPTs leads to an increase in the iP-type cytokinins and cytokinin independent formation of shoots in callus (Kakimoto et al., 2001; Sun et al., 2003; Sakakibara et al., 2005). The *ipt 1,3,5,7* quadruple mutant show severe growth defects due to reduced levels of iP and tZ-type cytokinins. The double mutant of tRNA IPTs (*ipt 2,9*) had undetectable levels of cZ-type cytokinins and a chlorotic phenotype (Miyawaki et al., 2006).

The enzymes responsible for creating active cytokinin nucleobases were first characterized in rice (*Oryza sativa*). These were coined as LONELY GUY (LOG) enzymes and basically, they are cytokinin riboside 5'-monophosphate phosphoribohydrolases (Figure 1.3). They are

responsible for catalyzing the reaction that removes the ribose 5'-monophosphate to release the active cytokinin nucleobase (Figure 3) (Kurakawa et al., 2007). In *Arabidopsis thaliana,* there are 9 such LOG genes (*LOG 1-9*), but *LOG6* and *LOG9* are non-functional due to premature stop codons. Of these LOG 1, 3, 4 and 7 have high enzymatic activities and are functionally redundant. The *log 3,4,7* triple mutant exhibits delayed flowering, smaller shoot meristem size, and increased adventitious root formation (Kuroha et al., 2009). The *log* septuple mutant has even further exaggerated shoot and root meristem defects, further highlighting the redundancy within the *LOG* genes (Tokunaga et al., 2012).

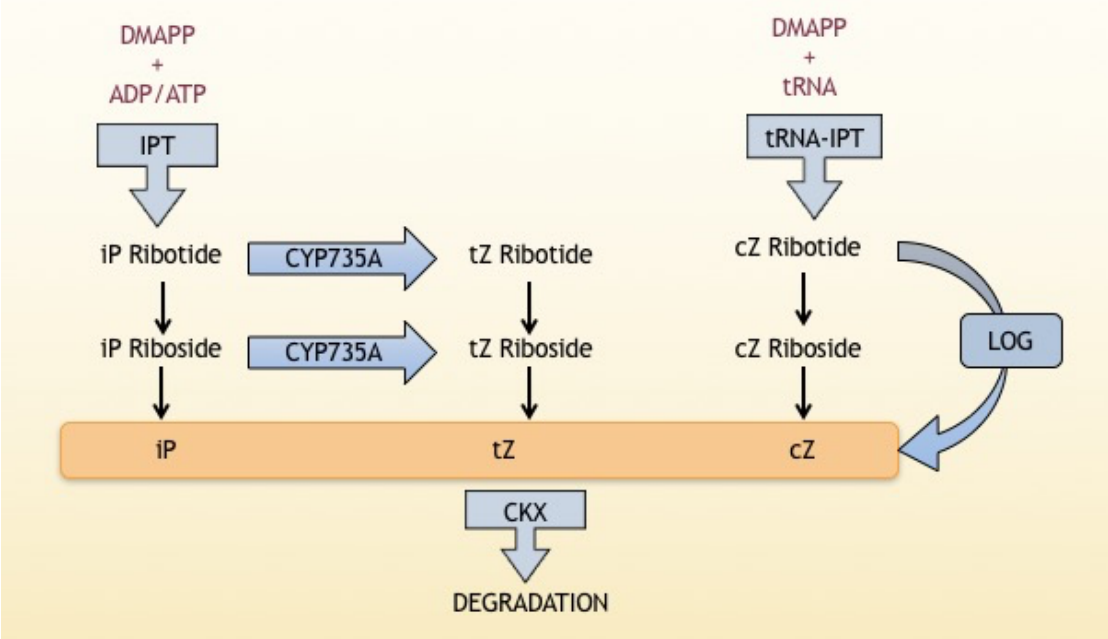

Figure 1.3 : Cytokinin biosynthesis and degradation

Schematic representation of various steps of cytokinin biosynthesis and activation by ISOPENTENYLTRANSFERASEs (IPTs) and LONELY GUY (LOG) enzymes, followed by degaradation by CYTOKININ OXIDASE/DEHYDROGENASEs (CKXs).

While transport is necessary for cytokinins to be translocated to sink tissues, other checkpoints regulate cytokinin homeostasis. After its biosynthesis cytokinin can be degraded or

conjugated, in order to maintain an optimum level of cytokinin response in the cells. Cytokinins are degraded by a group of enzymes that are biochemically different but commonly known as CYTOKININ OXIDASE/DEHYDROGENASEs (CKXs) (Figure 1.3) (Werner T., *et al*. 2003). The *CKX3* and *CKX5* are expressed in different domains of the SAM but are functionally complementary as observed in the double mutant. The *ckx3,5* double mutant had a larger meristem and increased seed yield due to enhanced cytokinin levels in the SAM (Bartrina et al., 2011). However, when *CKX1* expression in the L1 layer where no *CKX* is expressed, there was a reduction in seed yield and other cytokinin deficient defects (Werner et al. 2021). Thus cell-type and tissue-specific degradation of cytokinins can be modulated to control grain yield in plants.

1.8 Cytokinin reception and intermediate molecules

The two-component signal transduction system was first discovered in the bacterial response to chemotaxis, osmoregulation, photosensitivity and microbial pathogenesis (Appleby et al., 1996). This system consists of a phosphorelay between two or more multidomain signal transducers. Each component of this system contains two types of domains that are required for sensing the signal (sensor domain) and downstream transmission that receives the signal (receiver domain). The sensor domain consists of a histidine (HIS)-kinase which has the ability to use ATP to *trans*-phosphorylate a specific substrate histidine residue on the adjacent subunit within the homodimer. The receiver domains have the ability to phosphorylate their own aspartate residue by accepting a phosphoryl group from a cognate phosphorylated histidine phosphodonor (Hwang and Sheen, 2001). The signal transduction pathway consists of molecules that transfer the signal from the cell surface into the nucleus via a multi-step histidine to aspartate phosphorelay (Figure 1.4). This His-Asp phosphorelay system is conserved

throughout species and it is utilized to respond to external and internal stimuli (Appleby et al., 1996; Mizuno 1997, 1998).

The two-component system in Arabidopsis was first discovered by studying the His-kinase ethylene receptors (Hua and Meyerowitz, 1998). The His-kinases responsible for cytokinin-mediated signal transduction were isolated due to their similarity with bacterial His-kinases. The first receptor to be discovered was CYTOKININ INDEPENDENT 1 (CKI1) for its ability to constitutively regenerate shoot in calli. It was later characterized that CKI1 has no cytokinin binding activity, but it can constitutively activate the cytokinin two-component signalling (TCS) pathway (Hwang and Sheen, 2001; Yamada et al., 2001; Kakimoto, 1996).

The canonical His-kinases were isolated due to their ability to function as cytokinin-sensors in *Escherichia coli*. These genes were able to complement the His-kinase bacterial mutant (*rscB*) in the bacterial two-component signalling pathway and activate the endogenous *lacZ* expression in response to exogenous cytokinin (Suzuki et al., 2001; Takeda et al., 2001). In *Arabidopsis* three such transmembrane His protein kinases have been isolated and they are the ARABIDOPSIS HISTIDINE KINASEs (*AHK2*, *AHK3* and *AHK4*). The AHKs contain an extracellular binding domain which is called the Cyclin His kinase-Associated Sensory (CHASE) domain. They also contain two transmembrane domains that are followed by the cytoplasmic C-terminal end that consists of a His-kinase and receiver domain for transduction of the signal inwards (Figure 1.4) (Inoue et al., 2001; Ueguchi et al., 2001; Yamada et al., 2001). The X-ray crystallography of AHK4 protein has revealed that it exists as dimers and binds cytokinin with the Per-Arnt-Sim (PAS)-like domain. This receptor can bind all forms of cytokinin nucleobases but the heavier conjugated cytokinins cannot enter the binding pocket (Hothorn et al., 2011). The AHKs are localized in the plasma membrane and endoplasmic reticulum with a cytokinin binding site facing out towards the extracellular matrix or ER lumen (Wulfetange et al., 2011; Caesar et al., 2011). Upon binding with cytokinin the cytoplasmic

kinase domain is activated, and it gets autophosphorylated at the His residue. This activates the phosphorelay mechanism and the high energy phosphoryl group can then be transferred to the receiver domain Asp residue in the same molecule (Hwang and Sheen, 2001).

The *woodenleg* mutant of the *AHK4/CRE1* gene was identified in a genetic screen for mutants that were defective for shoot induction in response to cytokinin. In the *wol* mutants, there is a single amino acid substitution that leads to the conversion of threonine into isoleucine. This threonine residue in *AHKs* is present at the entry of the binding pocket and is essential for cytokinin binding. The *wol* mutant had a unique xylem differentiation phenotype when compared to higher-order *AHK* mutants (Scheres et al., 1995). When weak alleles of *ahk2, ahk3* and *ahk4* were combined, the resultant triple mutants were viable but had severe shoot defects and dwarfed stature. However, these were not null mutants therefore the cytokinin response was still slightly active. When stronger alleles of *AHK*s were combined, there were sporophytic defects that led to no seeds being formed (Nishimura et al., 2004; Higuchi et al., 2004).

After the autocatalytic activation of the AHKs, the phosphorelay system transduces the signal further with the help of certain intermediate molecules known as the HISTIDINE PHOSPHOTRANFER PROTEINs (AHPs). The AHPs are histidine-containing phosphotransmitters (HPt) that do not have any catalytic activity, rather they are involved in accepting and transferring the phosphoryl group from one receiver domain to another (Figure 1.4) (Appleby et al., 1996). The *AHP*s were first characterised for their ability to complement a yeast histidine phosphotransfer protein mutant and in *E.coli* they were capable of accepting and donating the phosphoryl groups (Imamura et al. 1999). There are five canonical *AHP*s in *Arabidopsis* (*AHP1,2,3,4,5*) and these vary in their binding affinity with the receptors (Urao et al., 2000; Suzuki et al., 2001). In the presence of cytokinin, these AHPs are phosphorylated by the AHKs, and this leads them to translocate into the nucleus. A pseudo-phosphotransfer

protein AHP6 has been identified as a negative regulator of cytokinin signalling. The AHP6 is capable of binding with the receptors but it lacks the His residue that is required to accept the phosphoryl group (Figure 1.4). While AHP6 competes for binding with the receptors and blocks the signal transduction, its expression is negatively regulated by cytokinin signalling. The *ahp6* mutant was able to partially suppress the vascular differentiation phenotype of the *wol* mutant (Mahonen et al., 2006). The *ahp1,2,3,4,5* quintuple mutant had severe morphological defects and reduced sensitivity to cytokinin (Hutchison et al., 2006).

1.9 Cytokinin signalling response regulators

The AHPs that are phosphorylated translocate into the nucleus will in turn activate a group of ARABIDOPSIS RESPONSE REGULATORS (ARRs). These ARRs are of two types, namely the Type-A ARRs and the Type-B ARRs. There are 11 type-B ARRs in *Arabidopsis* and these are redundant in function. The type-B ARRs have a receiver domain and a carboxyl output domain. The carboxyl domain consists of the DNA-binding GARP domain and an activation domain (Kakimoto et al., 2003). The receiver domain contains the Asp residue that is phosphorylated by the AHPs. These ARR transcription factors have a unique binding motif (G/A)GGAT(T/C) and their binding to the primary response genes is conferred as cytokinin response. The type-A ARRs are known as primary cytokinin response genes because their expression is further induced by the type-B ARRs (Figure 1.4) (Mason et al., 2005). *ARR1*, *ARR10* and *ARR12* overexpression led to shoot regeneration without the presence of cytokinin and the opposite was observed in the triple mutant.

There are 10 genes in Arabidopsis that encode for the type-A ARRs. These type-A ARRs contain a receiver domain but no DNA-binding domain. Due to this anomaly, the type-A ARRs compete for the phosphoryl group donated by AHPs. They will get phosphorylated at the Asp residue but these quenchers of cytokinin signalling have no downstream effect (Figure 1.4).

Mutational studies by substituting the Asp with Ala lead to the loss of their ability to get phosphorylated. However, when the Asp was replaced by a phosphomimic Glutamine this led to enhanced protein stability (To et al., 2007; Ferreira et al., 2005).

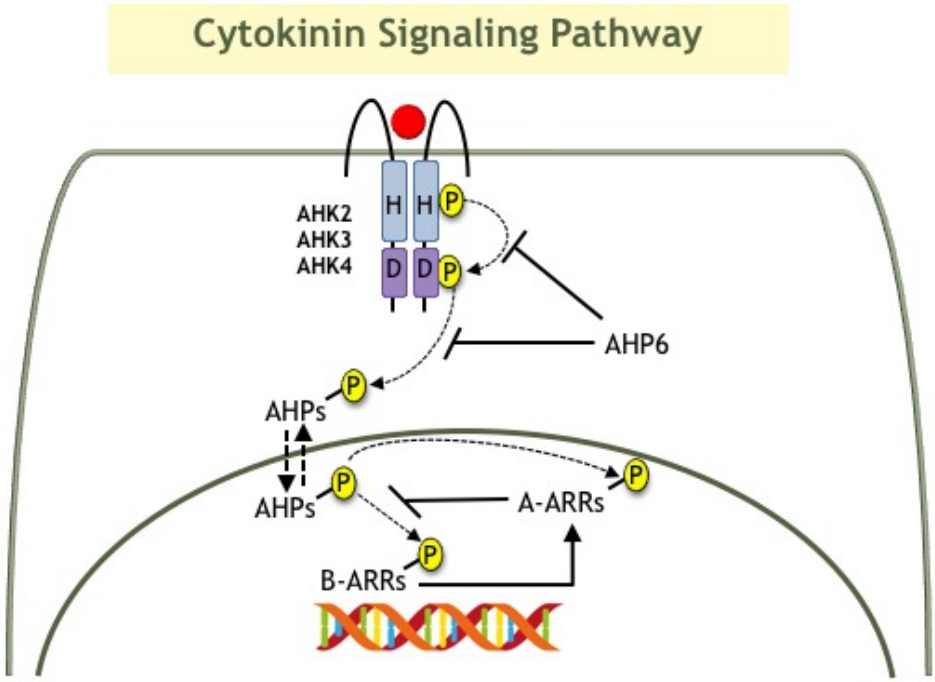

Figure 1.4 : Cytokinin signalling pathway

Schematic representation of various steps of cytokinin signalling pathway consisting of the ARABIDOPSIS HISTIDINE KINASE (AHK) receptors, HISTIDINE PHOSPHOTRANFER PROTEINs (AHPs) and ARABIDOPSIS RESPONSE REGULATORS (ARRs).

Thesis Objective

The endogenous CK levels in plants are dependent on their biosynthesis and degradation activity. The CK response within the plants is dependent on the presence of the CK signalling genes within a particular tissue. While the CK response increase with moderate concentrations of CK, if the CK levels exceed a particular level there is a reduction in CK response. The effect of CK response in the SAM is to promote cell division and differentiation. The optimum levels of CK in the SAM are maintained throughout the life cycle, however, it decreases as the plant undergoes senescence.

To understand the most important genes for maintenance of CK response in the SAM, I have first performed a comprehensive analysis of their gene expression. The transcriptional reporters of all relevant CK biosynthesis, degradation and signalling genes were made to observe their expression pattern in the SAM. The knowledge that I have gained from looking at their expression pattern was essential for interpreting the results of subsequent objective.

Next, I have performed a reverse genetics screen to identify the upstream regulators of all the shoot specific CK genes. This screen was performed by using many shoot specific transcription factors. Using this approach, I was able to identify several novel binding partners of the promoters of CK genes. The transcription factors are induced and activated by several developmental and environmental signals. Therefore, these transcription factors can be responsible for the change in CK response in accordance with internal and external signals.

One such transcription factor that I have focused on was NAC062/NTL6 which interacts with *LOG4* and *AHK4* promoters. With the help of several molecular and genetic approaches, I was able to determine that NAC062/NTL6 activates the expression of these genes in the SAM. Also, by characterizing the mutant and overexpression lines I was able to understand the role that *NAC062* plays in modulating the shoot growth. Lastly, I have shown how NAC062 induces CK response to halt growth in colder temperatures.

CHAPTER 2

Elucidating the diversity of expression patterns within cytokinin biosynthesis, degradation and signalling genes in the shoot apical meristem of *Arabidopsis thaliana*

2.1 Summary

Transcriptional reporters based on fluorescent protein are valuable resources required to understand the regulation of cytokinin biosynthesis, degradation and signalling genes in *Arabidopsis thaliana* shoot apical meristem (SAM). In this chapter, I present the findings related to the spatiotemporal expression pattern of shoot-enriched cytokinin biosynthesis, degradation and signalling genes. These reporter lines were studied using confocal microscopy to visualize their gene expression in various cell types of the SAM. The 18 transcriptional reporters that were studied included three *IPTs*, two *LOGs*, one *CKX*, three *AHKs*, two *AHPs*, five type-A *ARRs* and two type-B *ARRs*. By analyzing the reporter expression data, I was able to discern the inherent complexity involved in maintaining optimum cytokinin levels for input and the regions in the SAM where cytokinin signalling is activated.

2.2 Introduction

Cytokinin (CK) signalling has wide-ranging effects on the overall growth and development of higher plants. CK signalling also influences the plant's ability to respond to biotic and abiotic signals. The CK response is mediated by influencing the level of cytokinin and the activation of the two-component signalling pathway. There is major functional redundancy within homologous genes of each gene family for all the components of CK biosynthesis, degradation and signalling. This was apparent in studies where single and double mutants of CK biosynthesis, degradation and receptor genes either had a weak phenotype or did not have a clear phenotype. Whereas, when the higher-order mutants of an entire gene family were combined there were drastic growth defects due to a lack of CK response (Higuchi et al., 2004; Hutchison et al., 2006; Kuroha et al., 2009; Mason et al., 2004; Miyawaki et al., 2006; Tokunaga et al., 2012). Therefore, the tissue- and cell-specific expression of these genes is regulated in plants to elicit a specific CK response in a particular tissue or cell type. In the CK

deficient mutants or the mutants lacking CK signalling components, there was a common phenotype such that the SAM size was reduced (Ishida et al., 2008; Tokunaga et al., 2012; Werner et al., 2003). Due to the increase of CK levels in the *ckx3,5* mutant, the SAM size was enlarged which led to an increase in the yield (Bartrina et al., 2011). Initially, one of the genes encoding a Type-A ARR, *ARR5* was used previously to study the sites of active CK signalling in plants. This was because the type-A ARR expression is induced by CK signalling due to the presence of type-B ARR binding sites in its promoter. The Two-Component signalling Sensor new (TCSn) was constructed by combining concatemeric binding sites of the Type-B ARRs with endoplasmic reticulum targeted GFP reporter protein (Zürcher et al., 2013). The *TCSn::GFP-ER* reporter is considered better for studying the CK response compared to the *ARR5* reporter because it utilised the unique binding motifs of type-B ARRs and also there was no possibility of influence by other transcription factors. In the SAM it has been shown that *TCSn* is expressed in a domain that is overlapping with the OC and extends beyond it. The region with the highest activity of *TCSn* overlaps with *WUS* expression, as cytokinin signalling positively regulates *WUS*. This is mediated by the activation of AHK2 or AHK4 which then leads to the activation of type-B ARRs (Gordon et al., 2007). The type-B ARRs bind to the *WUS* promoter and activate its expression in the zone of highest cytokinin response within the OC (Wang et al., 2017; Zhang et al., 2017; Zubo et al., 2017; Xie et al., 2018). The *arr1,10,12* and *wus* mutants lose their ability to regenerate shoots from callus in cytokinin-rich shoot induction medium (SIM). However, by inducing ectopic *WUS* expression in the *arr1,10,12* mutant the shoot formation can be induced from the callus (Meng et al., 2017). Thus, the shoot forming ability of CK response is mediated by its direct activation of *WUS* expression.

Among the *LOGs*, *LOG1*, *LOG4* and *LOG7* are expressed in different domains of the shoot apex (Yadav et al., 2014; Gruel et al., 2016). By looking at the spatial expression pattern of these genes in the inflorescence meristem it is apparent that CK levels are highest in the L1

layer. From the L1 layer, CKs are either actively or passively transported into the inner layers of the meristem. The receptor genes (*AHK*s) are expressed in a broad domain consisting of the OC and rib meristem (Figure 2.1). None of these canonical AHK receptors are expressed in the L1 layer of the SAM. Therefore, the CK signalling is activated in the overlapping region where there are optimum levels of CKs and receptors present (Gruel et al., 2016).

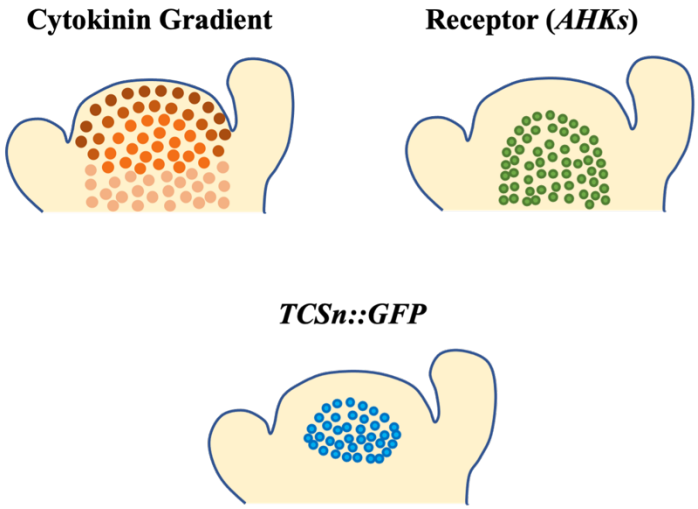

Figure 2.1 : Cytokinin response in the SAM

Diagrammatic representation of regions within the SAM where cytokinin hormone is present and where it is perceived.

2.3 Results

2.3.1 Expression pattern of *IPT*s in the inflorescence meristem

To study the expression pattern of *IPT* genes in the SAM the transcriptional reporters were generated for *IPT2*, *IPT3*, *IPT7* and *IPT9*. The 3kb upstream promoters of the cytokinin biosynthesis *IPT* gene family were amplified from the wild type (WT) *Landsberg erecta* (Ler) genomic DNA. These were combined with a nuclear-localized H2B::YFP in the pGreen vector and this was used to make transcriptional reporters. Several lines of each reporter transgene were followed to determine the best transgenic line.

The previous studies have shown tissue-specific expression of ATP/ADP type *IPT3* was highly enriched in the rosette and cauline leaves than in the open flowers and floral buds (Miyawaki et al., 2004; Takei et al., 2004). By creating a fluorescence based transcriptional reporter of *IPT3*, I was able to observe its expression in the peripheral zone of the shoot and in the floral primordia (Figure 2.2A). The expression of *IPT3* is highest in the corpus layer or vasculature of the flowers (Figure 2.2B). In the flower, *IPT3* expression begins from the stage-II floral primordia. This implies that iP- and tZ-type of cytokinins are present primarily in the organs.

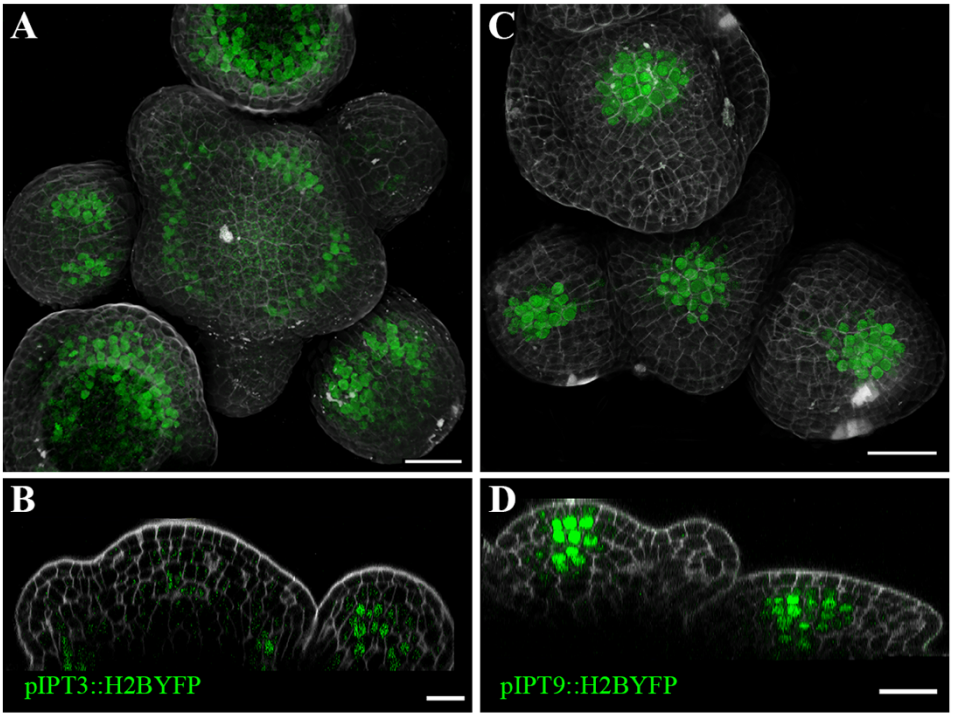

Figure 2.2 : Expression of ATP/ADP and tRNA type *IPTs* in the SAM

(A, B) *pIPT3::H2BYFP* (green) top view (A) and side view (B). PI (grey); Scale bar = 25µm

(C, D) *pIPT9::H2BYFP* (green) top view (C) and side view (D). PI (grey); Scale bar = 25µm

Conversely, tRNA type *IPT9* is expressed in the OC of the shoot but not in the L1 layer of the SAM (Figure 2.2C, D). In the floral primordia, *IPT9* starts expressing in the OC of the stage-II floral primordia and it progressively expands towards the epidermal cell layer in the later stages of development (Figure 2.2D). This implies that the cZ-type of CKs is present in the

center of the shoot and the flower primordia. It has been reported that the cZ-type of CKs are the predominant species in the shoot tip. Preliminary analysis of the reporter has shown that *pIPT9::H2BYFP* has a higher fluorescence intensity than *pIPT3::H2BYFP*, thus supporting the previous reports (Miyawaki et al., 2004).

There was no visible expression of *pIPT7::H2BYFP* in the SAM using the 3kb promoter, indicating that this promoter is not sufficient to drive the expression. There was a very weak expression of the tRNA type IPT, *pIPT2::H2BYFP*, in the RM (Figure 2.3). The GUS reporters of all *IPTs* have been studied previously and they exhibit unique expression patterns. The expression of the tRNA *IPTs*, *IPT2* and *IPT9*, was high in the proliferating tissues with *IPT9* having a higher expression among the two (Miyawaki et al., 2004).

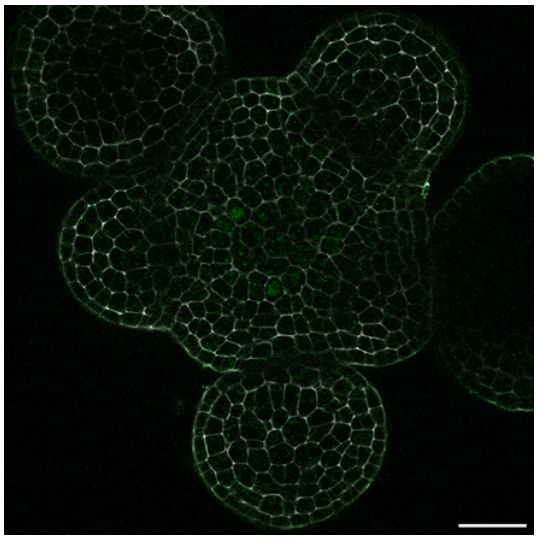

Figure 2.3 : Expression of the tRNA type *IPT2* in the SAM

Slice view of SAM from 25 day old plant. *pIPT2::H2BYFP* (green) and PI (grey); z = 46;

Scale bar = 25μm

2.3.2 Expression pattern of *LOG*s in the inflorescence meristem

The *H2BYFP* fusions for cytokinin activation genes *LOG1*, *LOG4*, *LOG5* and *LOG7* were also created in the pGreen vector backbone. These were transformed in WT-L*er*, selected for BASTA resistance and finally screened for fluorescence activity in the SAM. As reported in

the previous study by Gruel et al. (2016), *LOG4* is expressed in the L1 layer throughout the SAM. The expression of LOG4 is highest in the central zone and decreases in the cells towards the periphery. The *LOG4* levels begin to increase again at the tip of the primordia. Starting with the stage-II floral primordia *LOG4* is restricted to the tip and gets depleted from the organ boundaries (Figure 2.4A, B).

The *pLOG7::H2BYFP* reporter expression was not detected in the shoot apex, but it was active in the flower primordia. In stage-II flower primordia, expression of *LOG7* was dynamic from the onset, and as the primordia mature and enters stage-III, *LOG7* expression starts decreasing from the floral meristem, suggesting that *LOG7* expression is strongly linked to stage-II of flower primordia (Figure 2.4C and D). In the later stage of flower primordia, it is restricted towards the adaxial surface (Figure 2.4D). These two genes indicate that the sites for cytokinin activation are the L1 layer of the central zone and throughout the organ primordia.

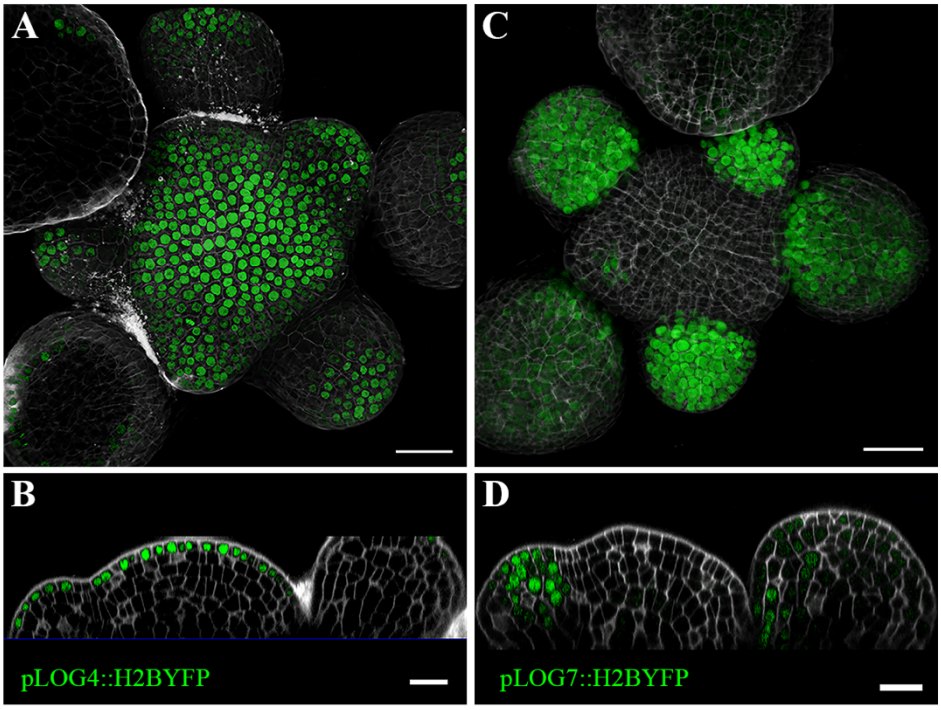

Figure 2.4 : Expression of *LOGs* in the SAM

(A, B) *pLOG4::H2BYFP* (green) top view (A) and side view (B). PI (grey); Scale bar = 25µm

(C, D) *pLOG7::H2BYFP* (green) top view (C) and side view (D). PI (grey); Scale bar = 25µm

There was no expression of H2BYFP observed in the SAM of *pLOG1::H2BYFP* and *pLOG5::H2BYFP* transgenic lines. For *LOG1,* in situ hybridization studies clearly indicate its expression in the CZ of SAM (Yadav et al., 2009; Aggarwal et al., 2010). The expression of *LOG5* has not been reported in the shoot apex, but GUS reporter indicates it is activated in the vasculature (Kuroha et al., 2009).

2.3.3 Expression pattern of *CKX*s in the inflorescence meristem

The transcriptional reporters of cytokinin degradation genes *CKX3*, *CKX5* and *CKX6* were screened for expression in the SAM. Based on the cell type-specific microarray study, all three genes are enriched in the SAM. Of these, only the expression of pCKX5::H2BYFP was observed in the SAM. The *CKX5* expression was broad in the floral meristem and shoot apex (Figure 2.5A). In the side view of SAM, the expression of *CKX5* can be seen in the L3 cell layer and below expanding to RM (Figure 2.5B). In the shoot apex, *CKX5* expression radiates into the periphery but it is excluded from the early-stage primordia. This *CKX5* expression reappears in the stage-II primordia where it is again restricted to the L3 layer and RM. However, in later stages of flower primordia, *CKX5* is excluded from sepal primordia (Figure 2.5A, B).

Previous studies have shown using *in-situ* hybridization that *CKX3* expression overlaps with the niche cells, therefore the 3kb promoter was not sufficient for eliciting this expression pattern (Aggarwal et al., 2010; Bartrina et al., 2011). Using GUS reporter Werner et al., (2003) have shown that *CKX6* is expressed in the vasculature of developing cotyledons, leaves and roots. Therefore, there is a possibility that *CKX6* has no discernible expression in the SAM.

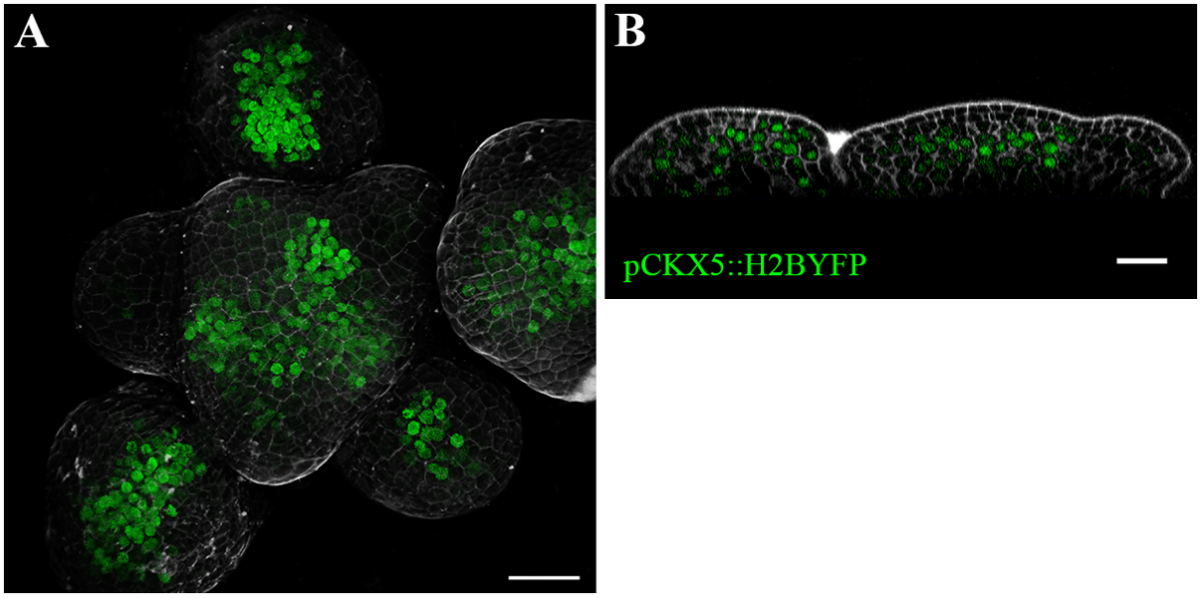

Figure 2.5 : Expression of *CKX5* in the SAM

(A, B) *pCKX5::H2BYFP* (green) top view (A) and side view (B). PI (grey); Scale bar = 25µm

2.3.4 Expression pattern of *AHK*s in the inflorescence meristem

Previous studies have shown that genes encoding for CK receptor proteins, *AHK2*, *AHK3* and *AHK4*, are differentially expressed in shoot and flower primordia (Chickarmane et al., 2012; Gordon et al., 2009). In the reporter lines made for this study, *AHK2* displayed a very weak expression in the RM, indicating that it is active in the vasculature (Figure 2.6C). The *AHK3* expression is specifically confined to stage-II and stage-III flower primordia (Figure 2.6D). However, *AHK4* expression was confined to stem cell niches in flower and shoot apex. In the SAM and flower, *AHK4* expression is weak in the L2 layer but highest in the L3 layer and below. Just as the cytokinin biosynthesis and degradation genes, *AHK4* expression is activated in the stage-II flower primordia. This expression pattern also overlaps with the *TCSn::GFP* reporter in SAM and flower, indicating the pivotal role played by AHK4 in CK responses in plants. CK signalling is vital for establishing functional stem niches both in the flower and shoot apex. From this study, it appears that *AHK2*/*AHK4* is required for the SAM niche, whereas *AHK3*/*AHK4* together specify stem cell niche in flower meristem.

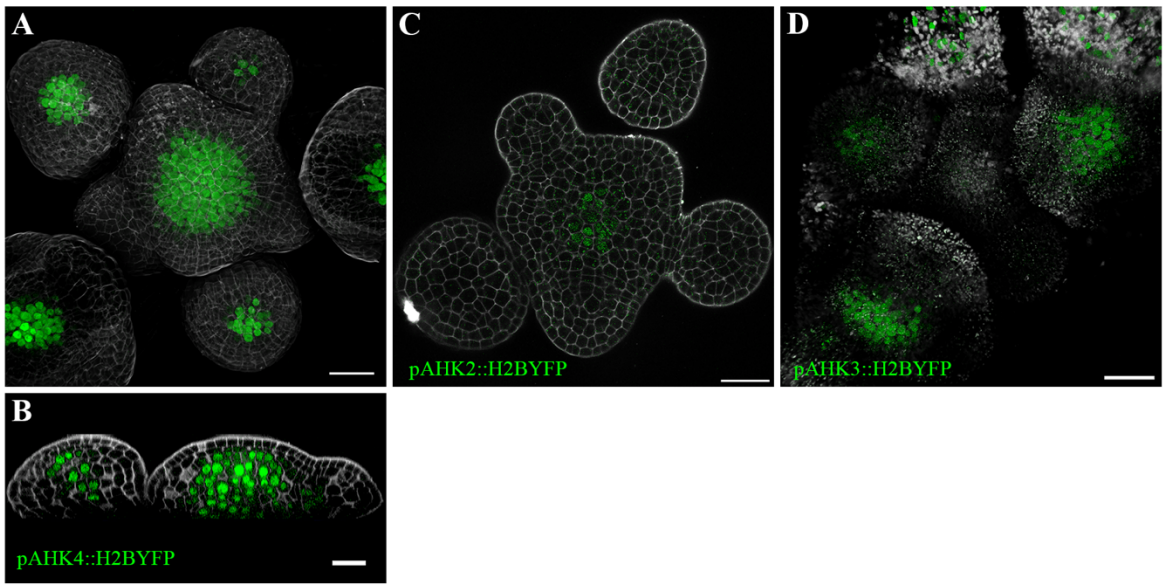

Figure 2.6 : Expression of *AHKs* in the SAM

(A, B) *pAHK4::H2BYFP* (green) top view (A) and side view (B). PI (grey); Scale bar = 25µm

(C) *pAHK2::H2BYFP* (green) slice view (C). PI (grey); z = 49; Scale bar = 25µm

(D) *pAHK2::H2BYFP* (green) top view (D). Autofluorescence (grey); Scale bar = 25µm

2.3.5 Expression pattern of *AHP*s in the inflorescence meristem

Expression of the canonical phosphotransfer genes *AHP2*, *AHP3* and *AHP5* has been reported in the female gametophyte and the vasculature with the help of GUS transcriptional reporters (Liu et al., 2017). We created the transcriptional reporters for all three canonical *AHPs* (*AHP2*, *AHP3* and *AHP5*) genes but only *pAHP5::H2BYFP* activity was detectable in the SAM. Using confocal microscopy, I found *AHP5* is broadly expressed throughout the CZ and PZ of the SAM, but it is absent in the epidermal cells. *AHP5* expression is absent in the stage-I primordia, but from the stage-II floral primordia it is restricted to the CZ of the primordia. The expression of *pAHP5::H2BYFP* in the stage-II and stage-III floral primordia is weak as compared to its expression in the SAM (Figure 2.7A, B). Thus, *AHP5* expression is highest in the regions of maximum cytokinin response in the SAM, however it is repressed in the epidermal layers of the SAM.

The transcriptional reporter for the pseudo-phosphotransfer gene *AHP6* was created with a larger promoter than the translational reporter that has been previously reported, and it shows the same pattern of expression in the primordia (Besnard, Rozier, et al., 2014). *AHP6* is a negative regulator of cytokinin signalling and plays an essential role in organ initiation. As expected the *pAHP6::H2BYFP* reporter marks the emerging organ primordia in the SAM and floral meristem (Figure 2.7C and D). Within the early primordia, it is restricted to L1 and L2 layer of the stage-I floral primordia. In stage-II floral primordia, its expression extends deeper into the L3 layer (Figure 2.7D). *AHP6* is not expressed in the CZ of stage-III floral primordia, however, it is expressed in the emerging sepal primordia in this stage (Figure 2.7C, D).

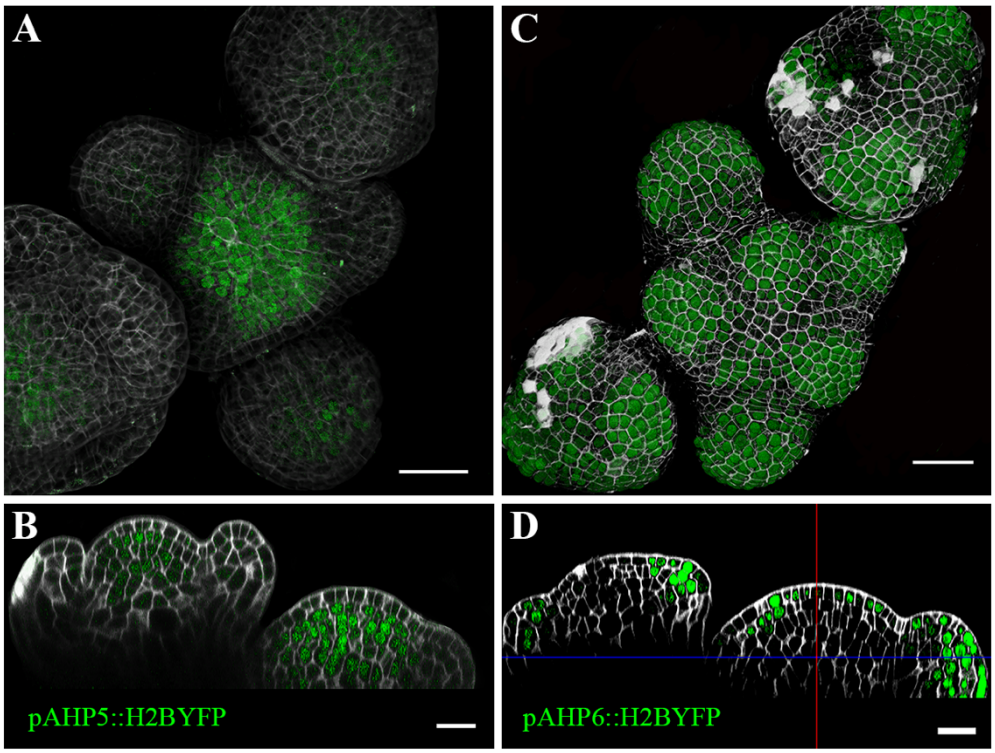

Figure 2.7 : Expression of *AHPs* in the SAM

(A, B) *pAHP5::H2BYFP* (green) top view (A) and side view (B). PI (grey); Scale bar = 25µm

(C, D) *pAHP6::H2BYFP* (green) top view (C) and side view (D). PI (grey); Scale bar = 25µm

2.3.6 Expression pattern of type-B *ARR*s in the inflorescence meristem

The type-B ARRs that I was interested to pursue this study were: ARR1, ARR10, ARR12 and ARR14. These genes were short-listed based on the cell-type specific transcriptome dataset (Yadav et al., 2014). The transcriptional reporter of *ARR1* had an expected overlap with the domain where CK response reporter *TCSn::GFP* is activated in the SAM. The expression of *ARR1* was noticeable throughout the SAM and flower primordia, but it was absent in the epidermal cell layers (Figure 2.8A, B). Unlike the other ARRs, the single mutant of *ARR1* has a phenotype such that it displays reduced CK sensitivity (Sakai et al., 2001). Altogether the reporter data and mutant analysis suggest that *ARR1* is the most crucial gene for CK response in the SAM. *ARR10* is expressed in the form of foci that coincide with the emerging organ primordia in inflorescence meristem. This could indicate, a possible cell-type specific CK response elicited by ARR10 during organ initiation (Figure 2.8C, D).

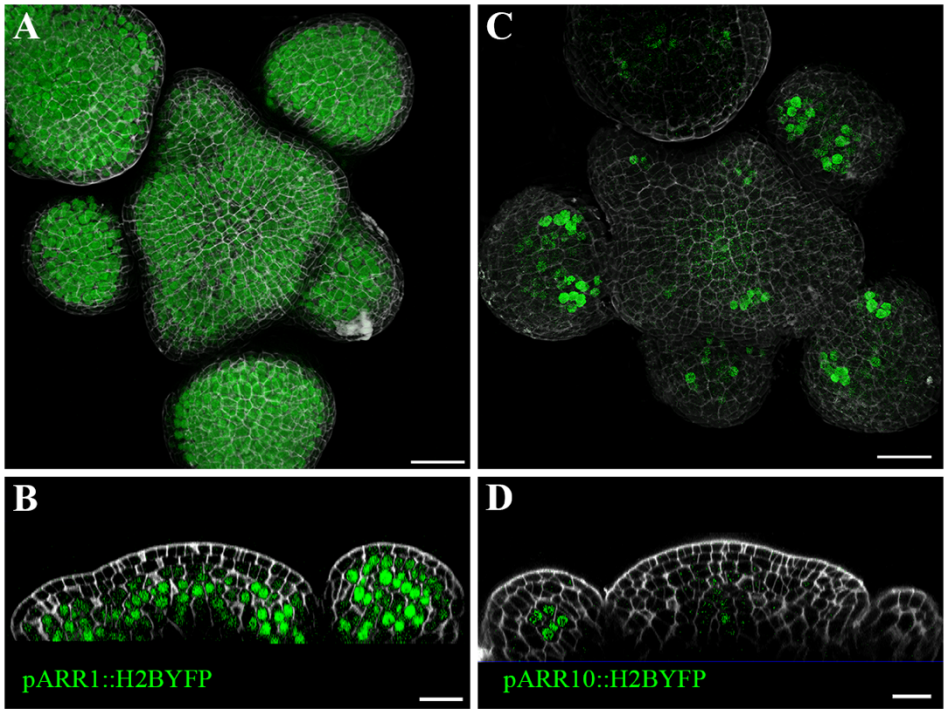

Figure 2.8 : Expression of type-B *ARR*s in the SAM

(A, B) *pARR1::H2BYFP* (green) top view (A) and side view (B). PI (grey); Scale bar = 25µm

(C, D) *pARR10::H2BYFP* (green) top view (C) and side view (D). PI (grey); Scale bar=25µm

The transgenic lines for *pARR12::H2BYFP* and *pARR14::H2BYFP* had no reporter activity in the SAM.

2.3.7 Expression pattern of type-A *ARR*s in the inflorescence meristem

The type-A *ARR*s can be classified into various sub-groups based on homology (To et al., 2004). One such group of type-A *ARRs*, *ARR7* and *ARR15* are expressed throughout the shoot and their expression is regulated by *WUS* and *AUXIN RESPONSE FACTOR5/MONOPTEROS (MP)* (Leibfried et al., 2005; Zhao et al., 2010). *pARR7::H2BYFP* is expressed throughout the SAM but the expression is lower in the L2 layer compared to L1 layer (Figure 2.9A, B). The *pARR15::H2BYFP* is expressed highly in the L1 and L3/corpus layers but, reduced in the L2 layer (Figure 2.9C, D).

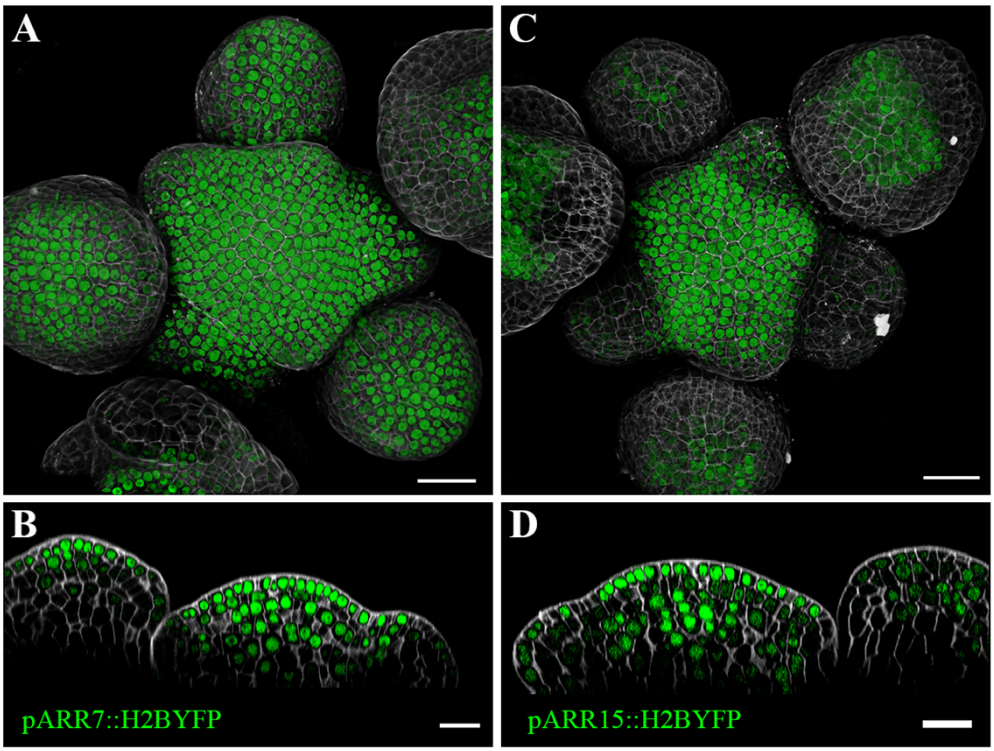

Figure 2.9 : Expression of type-A *ARRs* (*ARR7*/*ARR15*) in the SAM

(A, B) *pARR7::H2BYFP* (green) top view (A) and side view (B). PI (grey); Scale bar = 25µm

(C, D) *pARR15::H2BYFP* (green) top view (C) and side view (D). PI (grey); Scale bar=25µm

These reporters indicate that *ARR7* is expressed broadly, while *ARR15* is restricted to center of the primordia after the P2 stage. *ARR7* and *ARR15* are highly similar in structure and these reporters show that they are also similar in their expression pattern.

ARR3 and *ARR4* are a group of atypical type-A ARRs that are also involved in PhyB signalling, by binding to the PhyB protein and increasing its sensitivity to red light (Sweere et al., 2001). Based on the cell-type specific transcriptome dataset it was determined that *ARR3* is not expressed in the shoot (Yadav et al., 2014). However, the transcriptional reporter of *ARR4* was created as it shows high expression in the transcriptome dataset (Yadav et al., 2014) and the ARR4 protein accumulates in the aerial parts of the plants one day after germination (Sweere et al. 2001). The *pARR4::H2BYFP* reporter shows high activity in the OC and floral primordia of the shoot (Figure 2.10A, B). The *ARR4* expression in the flower meristem begins from the stage-II primordia in the floral niche cells.

Another group consists of *ARR5* and *ARR6*, of which ARR6 is not expressed in the shoot (Yadav et al., 2014). *ARR5* is also known as Induced By Cytokinin 6 (IBC6) and its expression is positively regulated by Type-B *ARRs* (Brandstatter & Kieber, 1998; Mason et al., 2004). The protein turnover of some type-A ARRs (ARR5, ARR6 and ARR7) is also stabilized by CK-mediated activation (To et al., 2007). In this study, I have created the transcriptional reporter of *ARR5* it is also expressed in the OC and flower primordia (Figure 2.10C, D). Both ARR4 and ARR5 have overlapping expression domains, but ARR4 expression also extends to the rib meristem in the center.

The type-A ARRs, ARR8 and ARR9 are structurally quite dissimilar compared to the other type-A ARRs. Among the two, only *ARR9* is relevant in the context of the shoot, as *ARR8* is not expressed in the different cell-types of the SAM (Yadav et al., 2014). I created the transcriptional reporter for *ARR9* as its expression has not been studied in the context of the

shoot. *pARR9::H2BYFP* is expressed in the lower rib meristem and organ boundaries (Figure 2.10E, F).

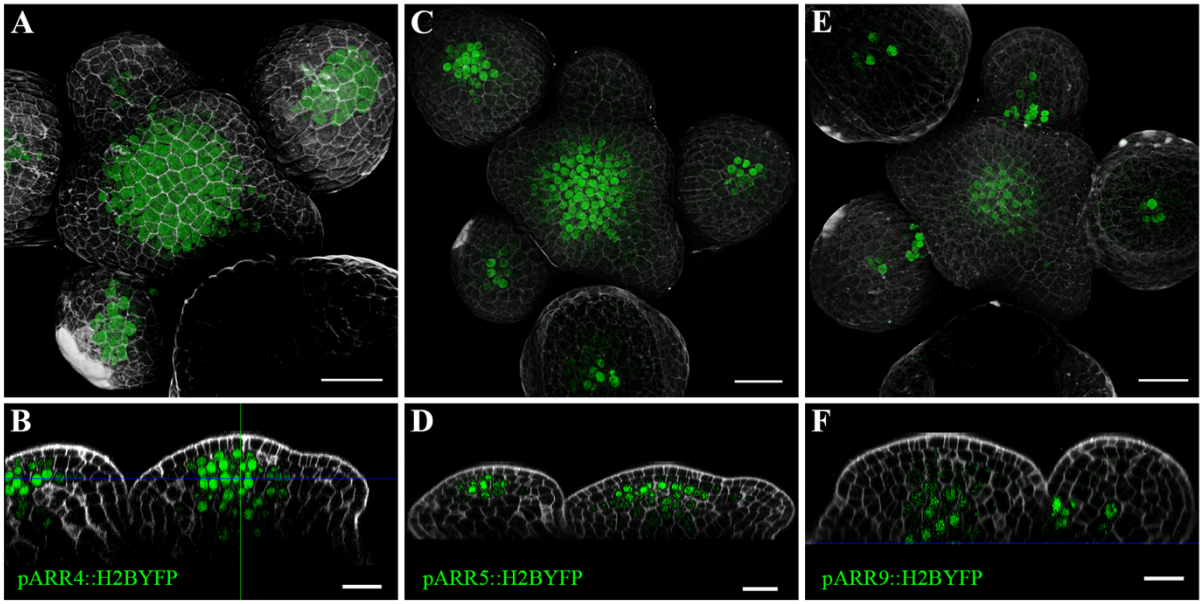

Figure 2.10 : Expression of type-A *ARRs* (*ARR4*/*ARR5*/*ARR9*) in the SAM

(A, B) *pARR4::H2BYFP* (green) top view (A) and side view (B). PI (grey); Scale bar = 25µm

(C, D) *pARR5::H2BYFP* (green) top view (C) and side view (D). PI (grey); Scale bar = 25µm

(E, F) *pARR9::H2BYFP* (green) top view (E) and side view (F). PI (grey); Scale bar = 25µm

2.4 Discussion

The transcriptional reporters of the CK biosynthesis, degradation and signalling genes have highlighted the diversity within their expression pattern. While there is redundancy in the expression of some genes, surprisingly other homologous genes have very little expression overlap even though they are known to be functionally redundant.

The first step of CK biosynthesis in the SAM is catalyzed by the ATP/ADP type *IPT3* and tRNA type *IPT2*/*IPT9*. These three *IPT* genes have a distinct expression in the shoot apex based on their transcriptional reporters. Their expression gives us an insight into the zones of synthesis for the inactive cZ, iP- and tZ-type of CKs. While *IPT3* leads to synthesis of iP- and

tZ-type of inactive CKs in the flower primordia, the cZ-type of inactive CKs are synthesized by *IPT9* in the niche cells of the SAM (Figure 2.11). The cZ-type of CKs have lower biological activity in *Arabidopsis* as seen in the complementation assay with *AHK4* expressed in *sln1* mutant of *S. cerevisiae* (Inoue et al., 2001). However, the maize CK receptors (*ZmHKs*) have a higher affinity toward the cZ-type of CKs (Yonekura-Sakakibara et al., 2004). In Arabidopsis, the *ipt2 ; ipt9* double mutant also has a chlorotic phenotype, indicating that the cZ-type of CKs have some functional significance in shoot growth (Miyawaki et al., 2006). Based on the H2BYFP transcriptional reporters it can be hypothesized that the cZ-type of CKs are locally inducing CK response in the OC of the SAM. However, for the iP- and tZ-type of CKs to have any influence, they must be transported from the flower primordia towards the OC of the SAM. There are several Equilibrative Nucleoside Transporters (ENTs) that could be involved in the local transport of iP- and tZ-type CK nucleosides but these must be investigated in the context of the SAM (Liu et al., 2019).

The active CK nucleobases are synthesized by the LOG enzymes throughout the plant. In the shoot there are two major *LOGs* responsible for CK activation, these are *LOG4* and *LOG7*. The expression domain of *LOG4* and *LOG7* in the SAM indicates that the active pool of CKs is in the epidermal layer and flower primordia (Figure 2.11). However, these CK nucleobases must be actively transported or diffuse passively into the lower layers so that the CK response can be activated in the OC of the SAM. Studies have shown the activity of several Purine Permeases (PUPs) in actively transporting CK nucleobases (Liu et al., 2019). *PUP14* is responsible for shoot morphogenesis, and it can transport apoplastic CKs into the cell where they will activate ER-localized receptors (Zürcher et al., 2016). Future studies will hopefully be able to elucidate the relevant CK transporters in the shoot of *Arabidopsis*.

Cytokinin degradation plays a key role in maintaining CK homeostasis in all plants. Previous studies have shown by using in-situ hybridization that *CKX3* was expressed in the OC of the

SAM and flower primordia, whereas *CKX5* was expressed in the procambium and flowers (Aggarwal et al., 2010; Bartrina et al., 2011). The transcriptional reporter of *CKX5* gave a clearer understanding of its cellular expression pattern in the SAM. Its expression is repressed in the CZ of the SAM and the L1 layer of stage-II and older flower primordia (Figure 2.11). Thus, CKX3 and CKX5 are expressed in different cell types of the SAM, but together they deplete CKs throughout the SAM. These findings highlight the dynamic nature of CK biosynthesis and degradation enzymes which are competing to maintain the pool of biologically active CKs in the SAM.

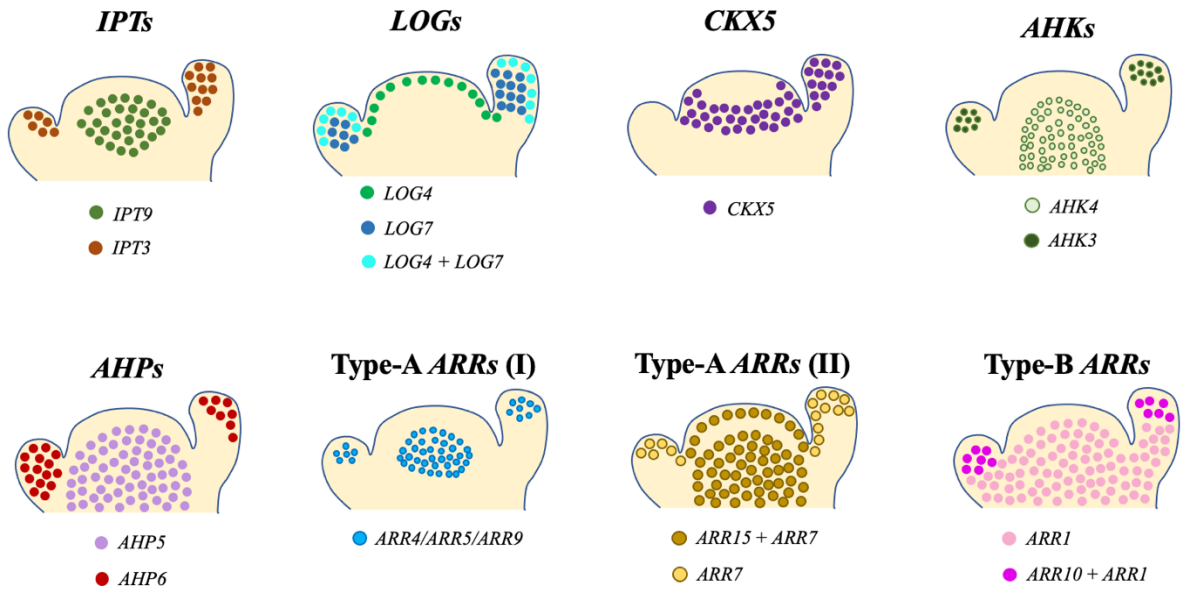

Figure 2.11 : Diagram representing the expression pattern of CK biosynthesis, degradation and signalling genes in the SAM

The CK signalling receptor *AHK4* and phosphotransfer gene *AHP5* have overlapping expression patterns in the SAM. Both are repressed in the L1 layer of the SAM and flower primordia. The receptors AHK3 and AHK4 are highly expressed in the flower meristem but AHP5 expression in the flower primordia is limited. The CK response in the flower primordia is also limited by the pseudo-phosphotransfer protein *AHP6*. So even though there is high CK

biosynthesis in the primordia, the CK response does not increase beyond a threshold because of the presence of these limiting factors.

There are two themes of expression within the type-A ARRs present in the SAM. One group of type-A *ARRs* consisting of *ARR4*, *ARR5* and *ARR9* are expressed in the niche cells such that their expression overlaps with the *TCSn::GFP* expression domain. While *ARR5* and *ARR9* are strongly induced by CK response, *ARR4* is not a reliable CK primary response gene (To et al., 2007). The transcriptional reporter of *ARR4* has an expression domain that is broader than the *TCSn::GFP* domain, this could be due to the contribution of other activators. The second group of type-A *ARRs*, *ARR7* and *ARR15*, are expressed broadly throughout the SAM but they are repressed in the L2 layer. Both these genes are also repressed by WUS and AUXIN RESPONSE FACTOR5 /MONOPTEROS (ARF5/MP) in the SAM (Leibfried et al., 2005; Zhao et al., 2010). They are also activated by the type-B *ARRs* and are therefore considered primary CK response genes (Brenner et al., 2005; To et al., 2007). However, judging by their expression pattern there are other transcription factors that are activating ARR7/ARR15 expression in the L1 layer and PZ of the SAM.

The type-B *ARR* transcription factors that have been studied here are *ARR1* and *ARR10*. While *ARR1* is broadly expressed throughout the shoot, it is absent in the L1 layer and minimally expressed in the L2 layer. Unlike the other cytokinin biosynthesis, degradation and signalling genes the expression of ARR1 extends into all the emerging primordia. Also, *ARR10* is weakly expressed in foci within all primordia and this pattern is not captured by the *TCSn::GFP* reporter. It is possible that the *TCSn* binding sites are activated primarily by *ARR1* and the contribution of *ARR10* in CK response is not captured due to the sensitivity of this reporter. By studying the expression pattern of all these genes, we can get new insights into their function and regulation within the SAM.

CHAPTER 3

A reverse genetics screen to identify novel transcription factors responsible for maintaining cytokinin homeostasis

3.1 Summary

From the knowledge gained by looking at the expression pattern of CK biosynthesis, degradation and signalling genes in chapter-2, I found that the majority of the components involved in CK responses in shoot apical meristem (SAM) show diversity in their expression. I wanted to investigate how upstream factors control their expression in the SAM. Therefore, I have undertaken a yeast-one-hybrid based network biology approach to find the transcriptional regulators that bind to the promoters of these genes. T-DNA insertion mutants for the newly identified transcriptional factors were isolated to analyze the CK response in the SAM. I validated some of the interactions within this network by RT-qPCR experiments. These mutants were also characterized for shoot growth defects as an indication of perturbed CK response. Taken together, my work revealed that upstream regulators induced by hormones and abiotic stress are involved in orchestrating CK responses in the SAM.

3.2 Introduction

The transcriptional reporters of CK biosynthesis, degradation and signalling genes revealed the diversity in the expression pattern of all these genes in the SAM. Any change in the degree of expression of any gene would lead to a subsequent alteration in the CK response. In the shoot CK response positively regulates cell proliferation and influences differentiation (Schaller et al., 2014). Changes in the CK response can affect several shoot developmental processes such as phyllotaxy (Besnard et al., 2014) and seed yield (Bartrina et al., 2011). Many studies show that a change in the CK response can effect bolting time, flowering and overall growth of the plant (Bartrina et al., 2017; Riefler et al., 2006; Tokunaga et al., 2012). Once CK signalling is activated in a particular cell or tissue, the type-B ARRs are primed to bind to their immediate targets which are the early/primary response genes. The type-B ARRs also induce the expression of several other transcription factors that will in turn activate the delayed/secondary

response genes (Brenner et al., 2005). It is due to the combinatorial effect of both the type of response genes that CK signalling in plants has such a diverse effect on the overall development.

While the downstream effect of CK signalling has been well studied, there is a lacuna in our understanding of the upstream factors that influence CK response. The CK biosynthesis, degradation and signalling genes are also regulated by several transcription factors that induce or repress their expression. There have been several reports that suggest that changing the endogenous levels of CK or altering CK response can affect the tolerance of plants toward abiotic and biotic stresses (Cortleven et al., 2019; Kang et al., 2013; Nguyen et al., 2016; Nishiyama et al., 2011, 2013). Based on the type of stress the response can also be enhanced or repressed by exogenous application of CK (A et al., 2019; Kang et al., 2013). Therefore, there must be upstream transcription factors that are responsive to these stresses that can modulate endogenous CK levels and response. These transcription factors can also alter the expression of CK genes in response to other hormone signalling pathways. The crosstalk between several hormone signalling pathways and CK signalling in different tissues of Arabidopsis is quite complex. The transcription factors involved in this crosstalk regulate CK biosynthesis and signalling simultaneously (Eckardt, 2005; Moubayidin et al., 2009). Therefore, transcriptional regulation is the most direct way in which CK response can be modulated in different parts of the plant. These transcription factors can alter the expression of target genes in response to the changes in external and internal stimuli. Also, they can provide cell-type and tissue-specific changes in expression patterns. A reverse genetics approach is required to discover novel interactions between known transcription factors and specific target genes. The forward genetics approach requires the presence of a strong phenotype in the transcription factor mutants or overexpression lines. However, phenotypes in single mutants are rare due to gene redundancy and robustness present within plants. The

Enhanced yeast-one-hybrid (eY1H) assay was developed to test a large-scale amount of interaction among the promoter baits and transcription factor prey proteins using Singer Robot (Deplancke et al., 2004; Gaudinier et al., 2011; Gubelmann et al., 2013). This technique has created avenues in network biology that can help us understand the complex interactions required for a single morphogenic event to occur (Brady et al., 2011; Smit et al., 2020; Tang et al., 2021; Truskina et al., 2021). Therefore, I have used this technique to fish out the transcriptional regulators of CK biosynthesis, degradation and signalling genes within the SAM of *Arabidopsis thaliana*.

3.3 Results

3.3.1 Mapping upstream regulators involved in the regulation of CK signalling

To map the gene regulatory network (GRN) involved in the CK signal homeostasis, I employed a network biology approach to identify the upstream transcription factors that are involved in Cytokinin Gene Regulatory Network (CKGRN) in the shoot apex of *Arabidopsis thaliana*. First, I short-listed genes involved in CK biosynthesis, degradation, signal perception, signal transduction and response based on the shoot cell population gene expression data reported by Yadav et al., (2014). To generate this dataset, stable reporter lines were established for epidermal, subepidermal, stem cells, niche cells, organ boundary regions and organ primordia in *ap;cal1* double mutant background. Fluorescence-activated cell sorter was used to enrich distinct cell populations followed by ATH1 gene chip hybridization to resolve the expression patterns associated with distinct domains and cell layers of SAM. From this dataset transcripts of thirty-five genes, encoding ISOPENTENYL TRANSFERASEs (IPT2, 3 7, 9), LONELY GUYs (LOG1, 2, 3, 4, 5, 6, 7), CYTOKININ OXIDASEs (CKX3, 5, 6), ARABIDOPSIS HISTIDINE KINASEs (AHK, 2, 3, 4, 5), HISTIDINE PHOSPHOTRANSFER PROTEINs (AHP2, 3, 5, 6), Type-A ARRs (ARR 4, 5, 7, 9, 15), and Type-B ARRs (ARR1, 2, 10, 12, 14,

18, 20, 21), whose transcripts displayed ≥ 1.5 fold enrichment in the SAM cell populations were shortlisted to make promoter baits (Figure 3.1). For this, a three kb promoter fragment upstream of ATG including the 5'untranslated region was amplified from the WT L*er* genomic DNA to make the bait constructs.

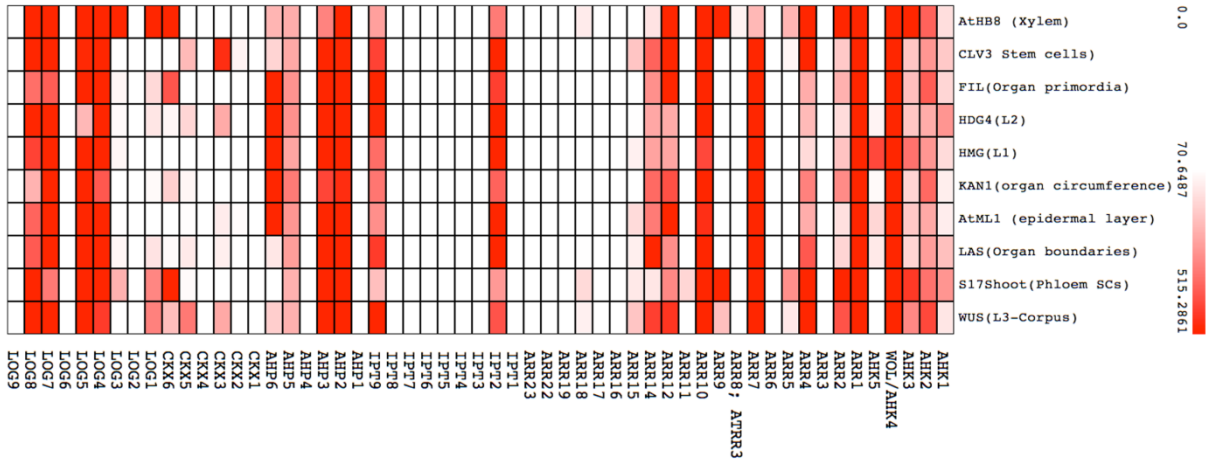

Figure 3.1 : Heat map of Cytokinin biosynthesis, degradation and signalling genes in all shoot-specific cell types

Enhanced yeast-one-hybrid (eY1H) assay was used to test the interaction among the promoter baits and transcription factor prey proteins using Singer Robot (Bhatia et al., 2021; Gaudinier et al., 2011; Gubelmann et al., 2013). Upon checking the individual bait autoactivation status we found that 10 baits had a very high degree of autoactivation. This reduces the sensitivity of the assay, as on high concentrations of 3-aminotriazole the binding of any transcription factor is inhibited. In total 11445 interactions were screened with 327 transcription factor preys and 25 bait promoters, after excluding the baits exhibiting high autoactivation. I have obtained an eY1H protein-DNA network consisting of 49 transcription factors binding to the 23 target gene promoters involving 164 interactions (Figure 3.2). Of these 23 transcription factors are interacting with two or more promoters to control cytokinin levels and cytokinin response, simultaneously. Another 26 transcription factors interact with only a single promoter in the

CKGRN. These transcription factors are differentially expressed in different cell types and domains of the SAM. Among the four *IPT* bait promoters which were selected based on the shoot cell types expression profile, positive interactions for three gene promoters (*IPT2*, *IPT3* and *IPT9*) were obtained. The 3kb promoter fragment was used to fish out interacting transcription factors, but in the case of *IPT7*, I could not find an interacting partner. It is possible that functionally relevant cis-elements are missing from this promoter because the same promoter was unable to drive the expression of the reporter gene when tested *in planta*. Of the seven *LOG* gene baits that were screened, I was able to obtain positive interactions with four promoter baits (*LOG1*, *LOG4*, *LOG5* and *LOG7*). Similarly, for *CKX* gene promoters two (*CKX5* and *CKX6*) were found to be interacting in the CKGRN. There was high autoactivation observed for the *CKX3* and *LOG2* promoter baits. Also, none of the transcription factors was interacting with *LOG3* bait in the eY1H assay.

Three baits belonging to the *AHK* family were screened against the prey library. *AHK3* and *AHK4* showed positive interaction in the eY1H. Interestingly, *AHK2* bait did not show any positive interactions with our collection of transcription factor prey library. The reason for this could be that most of the transcription factors taken in the library are expressed in the upper cell layer of SAM. AHK2 expresses in the rib meristem, and it is possible that there is a poor representation of prey from this tissue. Among the AHPs, there were four promoter baits (*AHP2*, *AHP3*, *AHP5* and *AHP6*) that are interacting with transcription factors in the CKGRN. For this screen, I shortlisted five promoter baits of the type-A *ARRs*, namely *ARR4*, *ARR5*, *ARR7*, *ARR9* and *ARR15*. Baits for all five type-A *ARRs* showed interaction with several binding partners in the eY1H assay. For type-B *ARRs* I screened eight baits but obtained positive interactions with three promoter baits, namely *ARR1*, *ARR10* and *ARR14*. However, baits for *ARR2*, *ARR18*, *ARR20* and *ARR21* exhibited a high autoactivation. Also, *ARR12* was excluded from the CKGRN as it did not interact with any transcription factor.

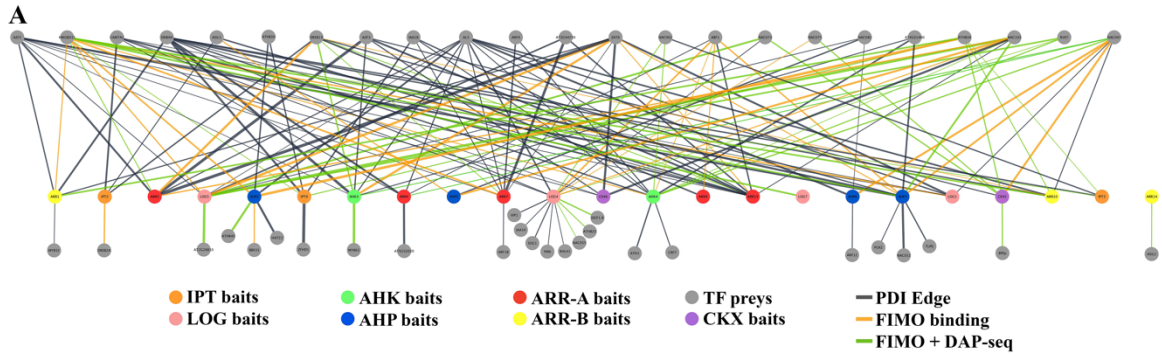

Figure 3.2 : Shoot-specific transcription factors regulate cytokinin biosynthesis, degradation and signalling

(A) The PDI network of 49 TFs preys (grey circles) and 23 promoter baits (coloured circles). Edges are coloured orange to denote binding motifs in FIMO analysis or green to denote binding peaks in DAP-seq database.

A careful analysis of the over-represented nodes revealed that transcription factors that are responsive to phytohormones and environmental stimuli participate in a maximum number of protein-DNA interactions (PDIs) in the CKGRN (Figure 3.3A, B).

Hormone responsive TFs subnetwork

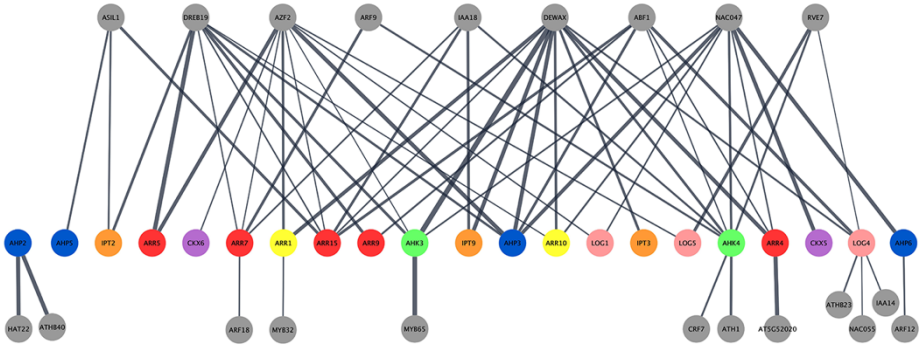

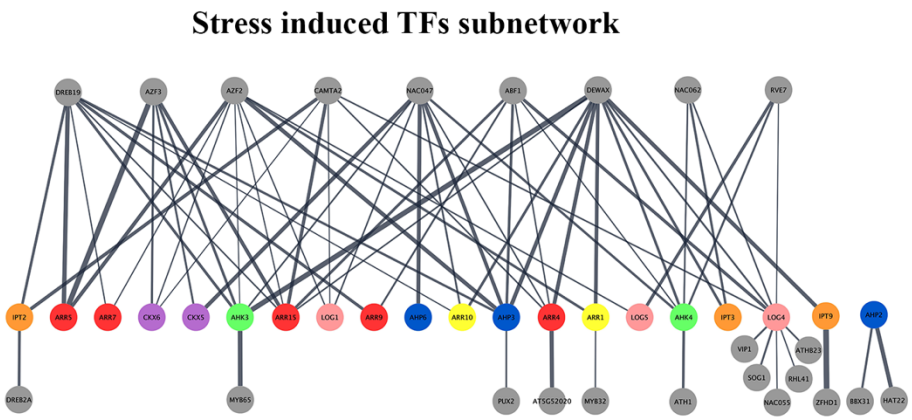

Figure 3.3 : Sub-network of all hormone-responsive and stress-induced transcription factors

Next, I wanted to know the probable cis-elements for upstream regulators so that a meaningful inference can be drawn to assign a putative binding site within the target gene promoter in the CKGRN. To find out the binding sites of the interacting transcription factors in the bait promoters, Find Individual Motif Occurrences (FIMO) analysis was performed using the MEME suite with a p-value $\leq 10^{-4}$ (Grant et al., 2011). I was able to map the binding site for 21 transcription factors within the 3kb promoter region of their respective interacting bait in the CKGRN. These transcription factors account for 64 PDIs in the CKGRN (Figure 3.4, 3.5). In the absence of motif data for 22 transcription factors, we were unable to assign functional binding sites to 69 PDIs (Figure 3.4, 3.5). In parallel, we also parsed the DNA affinity purification sequencing (DAP-seq) database to determine the binding location of the transcription factors. The DAP-seq peaks are used to predict the in-vivo binding site for a transcription factor in the region of interest. There was an overlap between the FIMO binding and DAP-seq peaks for 33 PDIs involving 15 transcription factors (Table ; Figure 3.4, 3.5). For two PDIs there were no binding sites in FIMO, while there was a visible peak in the DAP-

seq database within the promoter region. Specifically, these interactions were between DREB19 and ANAC055 with AHK3 and LOG4, respectively. This could be possible due to the presence of non-canonical binding motifs. We were unable to assign a motif for 68 PDIs because we neither find it in DAP-seq nor in the FIMO dataset (Figure 3.4, 3.5).

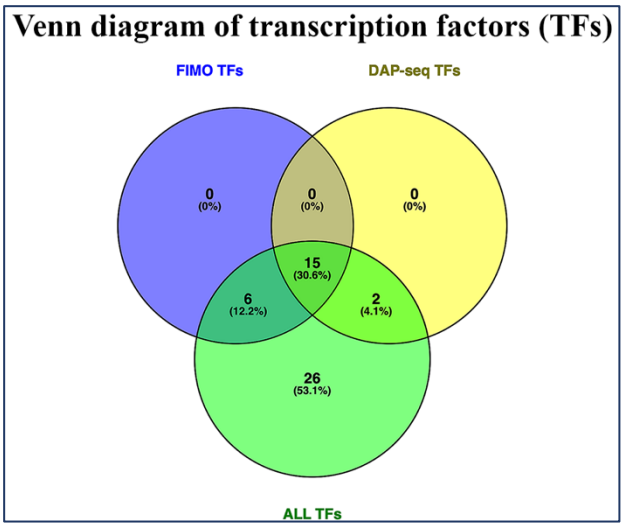

Figure 3.4 : Venn diagram of transcription factors whose binding information was available in FIMO and DAP-seq database

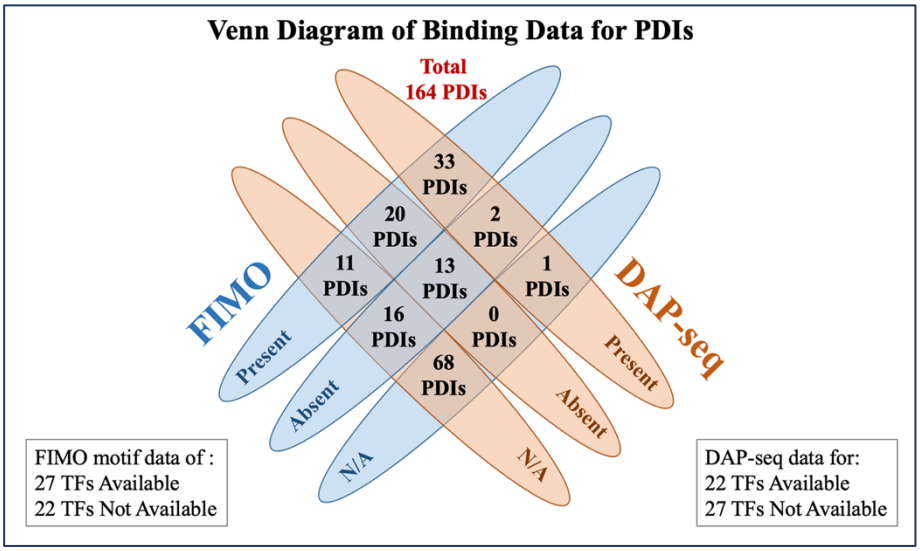

Figure 3.5 : Venn diagram of protein-DNA interactions (PDIs) confirmed by FIMO and DAP-seq database

3.3.2 Isolation T-DNA insertion mutants of prey transcription factor genes

To further validate the CKGRN the T-DNA insertion lines for interacting transcription factors were obtained from the stock centre. The T-DNA insertion in these lines was confirmed by PCR and the insertion site was ascertained by Sanger's sequencing (Figure 3.6). These lines were further used to characterize the *in-planta* effect of an interacting TF on the expression of its target gene using RT-qPCR.

The T-DNA mutant lines of *abf1* (SALK_132819C), *athb23* (SALK_059288), *athb34* (SALK_085482), *azf2* (SALK_132562) and *dreb19* (SALK_083422) were tested for the presence of the transcripts of the respective genes to determine the status of mutant allele by semi-quantitative RT-PCR (Figure 3.6). The *zfhd1* (CS877090) line had an insertion in the promoter in such a position and orientation that there was an increase in its expression when compared with the WT (Figure 3.6F). The T-DNA insertion in the *dreb19* (SALK_083422) mutant line was present in the promoter but this disrupted the natural expression of the gene as seen in semi-quantitative RT-PCR (Figure 3.6E).

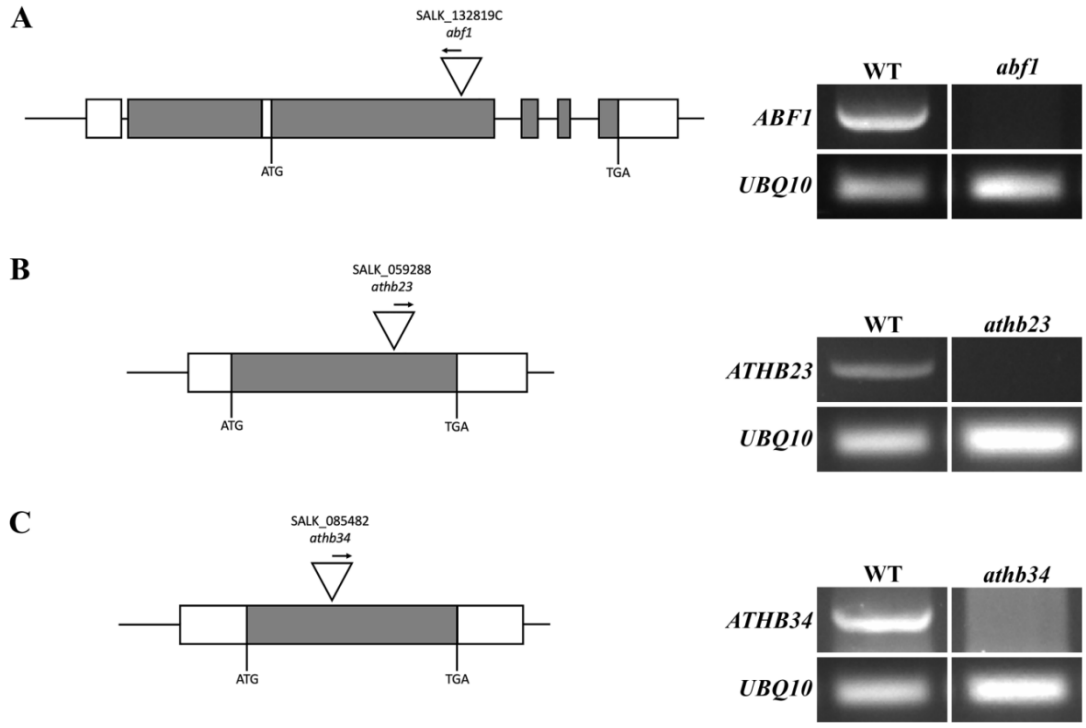

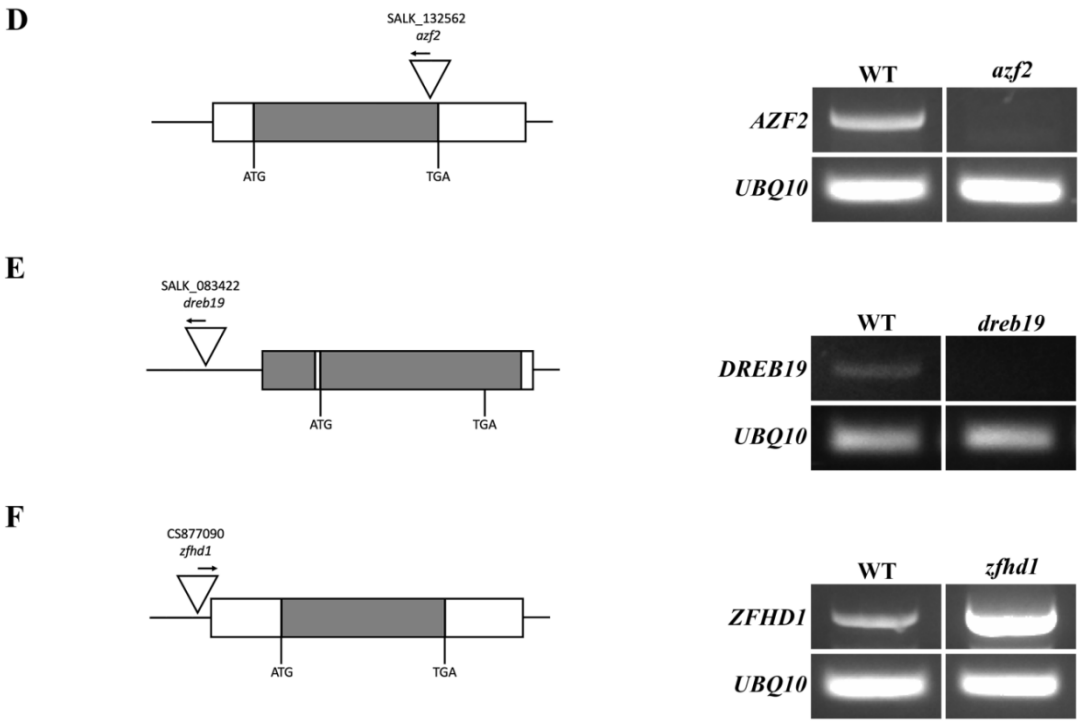

Figure 3.6 : Characterisation of insertional mutants

Schematic of T-DNA insertion within a given gene structure as determined by Sanger's sequencing. Semi-quantitative RT-PCR analysis was performed to determine the transcript levels for the selected transcription factor gene expression in its respective T-DNA mutant. UBQ10 expression was used as reference and loading control.

DEHYDRATION RESPONSE ELEMENT BINDING PROTEIN19 (*DREB19*), an APETALA2-like transcription factor, is induced by heat, salt and drought stress (Krishnaswamy et al., 2011). DREB19 positively regulates *ARR5* and *AHK3* as determined by RT-qPCR of target genes in *dreb19* mutant seedlings. *DREB19* is highly expressed in the L2 layer of the SAM (Yadav et al., 2014), and it negatively regulates *ARR10*, *ARR15* and *IPT9*. Interestingly all three of these genes have a very low expression in the L2 layer as seen in their respective transcriptional reporters.

ZINC-FINGER PROTEIN 2 (*AZF2*), a Cys-2/His-2-type zinc-finger motif-containing transcription factor, is induced by salt, drought and ABA (Sakamoto et al., 2004). In the RT-qPCR assay, I have confirmed that AZF2 negatively regulates *ARR5*, *ARR15*, *AHP3* and *LOG5*. However, in *azf2* mutant seedlings the *AHK3* transcript level increases but not as significantly. AZF2 is a known repressor with an EAR motif, therefore the genes that it represses could be more relevant and studied further.

Another zinc finger homeodomain transcription factor, *ZFHD1/ATHB29*, is induced by salt, dehydration and ABA (L. S. P. Tran et al., 2007). The *zfhd1* mutant has a T-DNA insertion in the promoter (-327bp from ATG) and this led to an increase in *ZFHD1* expression (Figure 3.6F). In *zfhd1* mutant transcript levels of *IPT9* were elevated compared to control as estimated by RT-qPCR analysis (Figure 3.7A). This indicates a positive role played by *ZFHD1/ATHB29* in activating the gene expression of *IPT9* (Figure 3.7B). The orientation of the T-DNA insertion is in the direction of the *ZFHD1/ATHB29* gene and within its promoter. The increase in *ZFHD1/ATHB29* expression could be due to ectopic expression caused by T-DNA or disruption of a repressive binding site within its promoter.

A downstream effector of abscisic acid signalling, *ABSCISIC ACID RESPONSE ELEMENT BINDING-FACTOR1* (*ABF1*) represses *LOG4* (Figure 3.7A, B). The *abf1* mutant has a T-DNA insertion in the first exon that successfully forms a null mutant (Figure 3.6A).

Two closely related homeobox genes, *ATHB23* and *ATHB34* are highly expressed in the inflorescence (Tan & Irish, 2006). ATHB23 positively regulates *LOG4* (Figure 3.7A, B). ATHB34 negatively regulates *ARR10* and *IPT9* (Figure 3.7A, B). In contrast, ATHB34 also induces *ARR1* although this regulation is not robust (Figure 3.7A, B). For a better understanding of the functional relevance of ATHB23 and ATHB34, the phenotype of single and double mutants was studied (Figure 3.12A, B).

ARABIDOPSIS THALIANA HOMEOBOX1 (*ATH1*) is involved in shoot development by inhibiting shoot stem cell proliferation (Ejaz et al., 2021; Gómez-Mena et al., 2005; Proveniers et al., 2007). The expression of *AHK4* increases in the *ath1* mutant (Figure 7A), indicating that *ATH1* negatively regulates *AHK4* (Figure 3.7B). The *woodenleg* mutant has a reduced number of cells in the vasculature due to lower cell divisions from embryonic stages to later stages of development (Scheres et al., 1995). Moreover, the *ath1* mutant is expressed from the embryonic stages and into the reproductive stage SAM (Bhatia et al., 2021; Proveniers et al., 2007). The correlation between previous literature and my findings implies that ATH1 inhibits *AHK4* expression to limit cell divisions in the SAM and shoot stem vasculature.

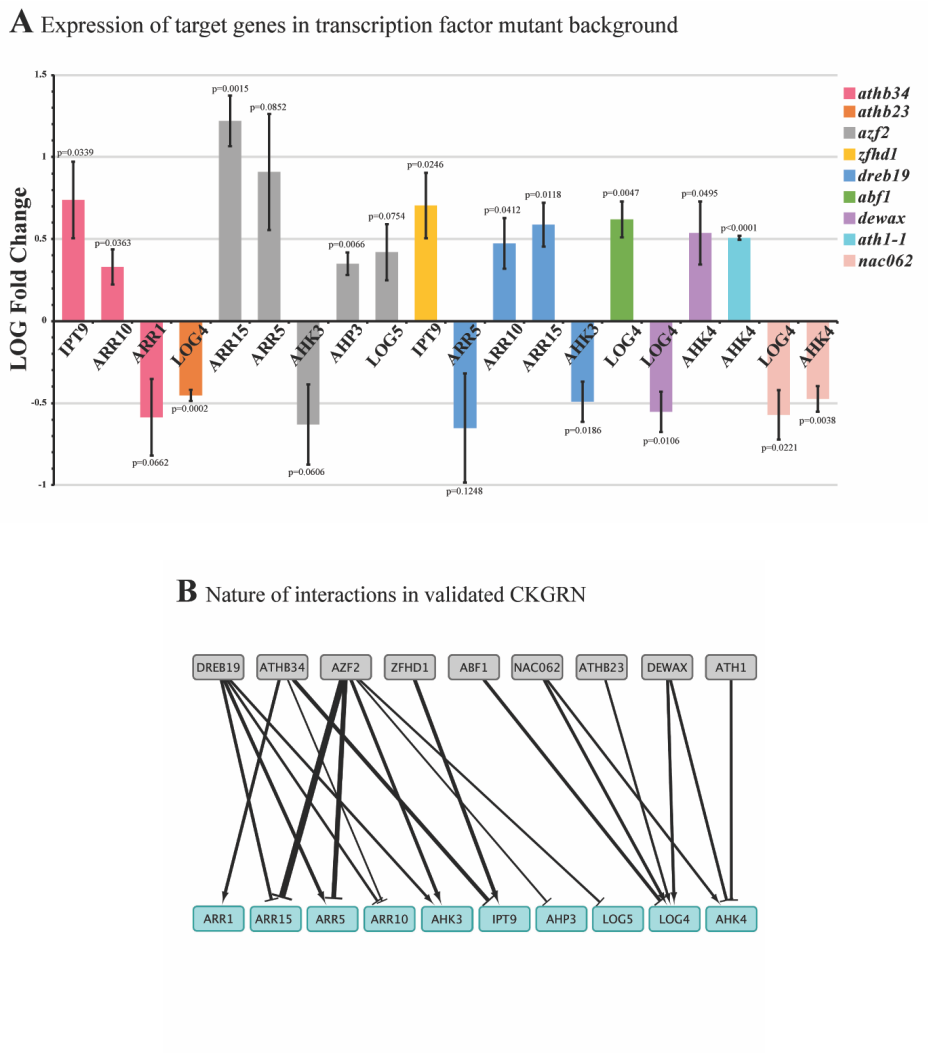

Figure 3.7 : Validation of CKGRN in transcription factor mutants

(A) RT-qPCR validation of target gene expression in 5-day old mutant seedlings. (n=3)

(B) Subnetwork of stress-responsive TFs interactions validated by RT-qPCR. Blue nodes denote target genes and grey nodes are interacting TFs. Width of the edges is denoted by relative expression of target gene in mutant background.

Based on qRT-PCR analysis DEWAX negatively regulates *AHK4*, however, it positively regulates *LOG4* (Figure 3.7A). DEWAX also interacts with the *ARR4* promoter in eY1H, but there was no change in *ARR4* expression level in 5-day old *dewax* mutant seedlings. We followed this by crossing *pARR4::H2B-YFP* reporter line in *dewax* mutant. *pARR4* showed a marked decrease in its expression domain in *dewax* mutant compared to WT (Figure 3.8A, B). The intensity of *pARR4::H2B-YFP* expression was reduced notably in the CZ of *dewax* mutant shoot (Figure 3.8C). Consequently, the size of *dewax* mutant SAM (n=5, 37 ± 0.98) also decreased significantly as compared to WT SAM (n=5, 47 ± 2.3) (Figure 3.8D).

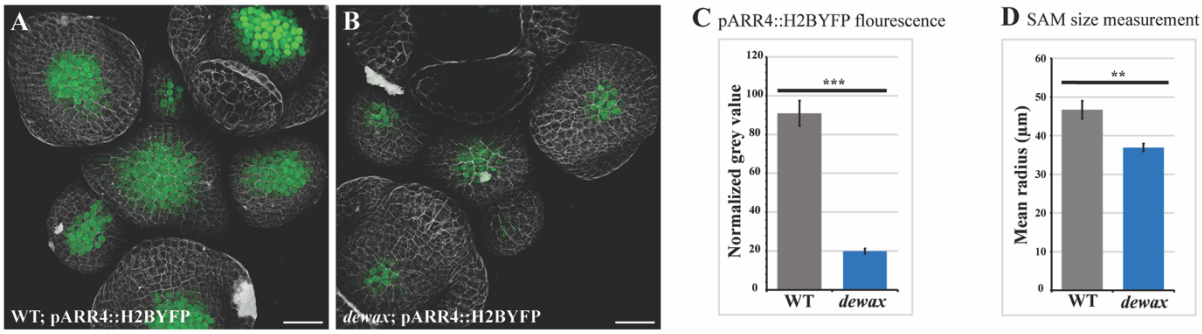

Figure 3.8 : DEWAX regulates *ARR4* expression at night

(A, B) *pARR4::H2BYFP* (green) expression in (A) WT and (B) *dewax* mutant grown in long day (16hr Light/ 8hr Dark) and imaged after 6hrs of dark. Cell wall stained with PI (grey). Scale bar = 25µm.

(C) Normalized grey value of *pARR4::H2BYFP* in WT and *dewax* mutant (n = 7; $p<0.0001$)

(D) Shoot size measurement by estimating SAM mean radius of WT and *dewax* mutant (n=5, Student t-test p-value = 0.0044).

ARR4 is an atypical type-A ARR that is different functionally from *ARR5* as seen by analysing the single mutants for both these *ARRs* (To et al., 2004). Also, ARR4 has a low affinity for binding with the canonical AHPs (Suzuki et al., 1998) and its protein turnover is not stabilized by cytokinin-mediated activation (To et al., 2007). The ARR4 protein accumulates in red light and its stability is promoted by PhyB (Sweere et al., 2001). DEWAX is an AP2/ERF-type transcription factor that is induced in darkness (Go et al., 2014). The regulation in *dewax* mutant indicates that *ARR4* expression is induced at night by DEWAX. Understanding the role of DEWAX would require an in-depth study of ARR4 protein dynamics and the spatiotemporal expression of *LOG4* and *AHK4* in the SAM. However, preliminary results indicate DEWAX positively influences shoot growth by inducing CK response.

The expression of *LOG4* in the shoot is induced by NAC062, ATHB23 and DEWAX. The mutants of all these transcription factors have shoot defects and delayed flowering. Hence by decoding the nature of interactions in our CKGRN we can understand the role of these transcription factors in maintaining the expression domain of each gene.

3.3.3 Testing additive effect of CKGRN interactions in double mutants

3.3.3.1 Homologous transcription factors with overlapping interactions

The AUXIN RESPONSE FACTORs (ARFs), *ARF9* and *ARF18*, are transcription factors involved in auxin signalling response. Both transcription factors are part of the CKGRN, and they are closely related as shown in the phylogenetic tree (Figure 3.9).

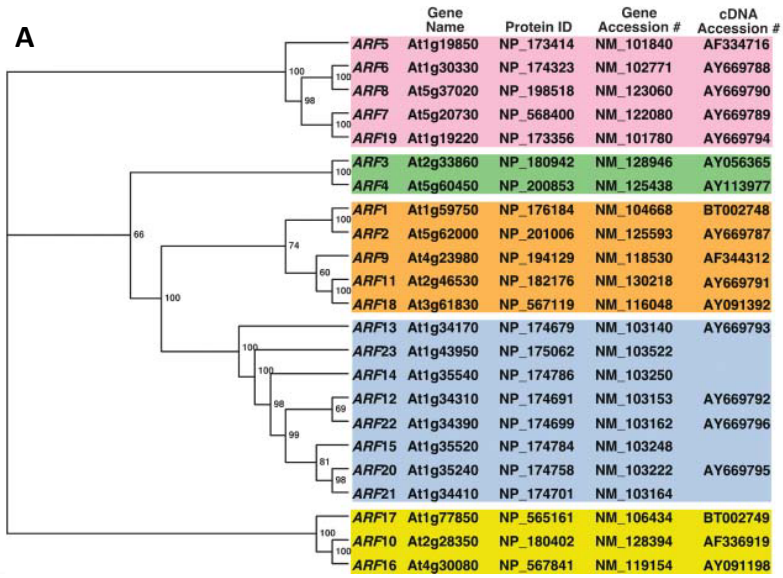

Figure 3.9 : Phylogenetic tree of *ARFs* in *Arabidopsis thaliana* (Okushima et al., 2005)

Phylogenetic analysis of AUXIN RESPONSE FACTORs (ARFs) with the gene names, accession numbers, protein identifier, and the accession numbers.

The Q-rich domain in the ARFs is required to form an activation complex to activate gene expression. The Class I ARFs, like ARF9 and ARF18, lack the Q-rich domain which makes them natural repressors for auxin signalling (Ulmasov et al., 1999). ARF9 binds to the *AHK4* and *ARR7* promoter, ARF18 binds with only the *ARR7* promoter. The single mutants of *ARF9* (CS24609) and *ARF18* (CS467029) were crossed to determine if there is redundancy in their function. The single mutants and different heterozygous/homozygous combinations (*arf9*-/- ; *arf18*+/- or *arf9*+/- ; *arf18*-/-) did not exhibit any phenotype. In the segregating populations, I did not observe any homozygous double mutant upon genotyping ~50 F2 generation plants. Therefore, I decided to check the siliques of the segregating heterozygous plant. In these plants there was embryo lethality observed as 50% of the seeds were ablated (Figure 3.10B), as compared to the WT siliques (Figure 3.10A). Both these transcription factors are interacting with the *ARR7* promoter. Only ARF9 binds with the *AHK4* promoter, indicating possible

repression of *AHK4* in the double mutant. The embryonic lethality in the double mutant could indicate functional redundancy of ARF9 and ARF18 in regulating cytokinin signalling.

Figure 3.10 : Embryonic lethality in *ARF9* and *ARF18* double mutant

Siliques of WT Col (A) and *arf9*-/-;*arf18*+/- mutant (B)

3.3.3.2 Homologous transcription factors with non-overlapping interactions

There were three zinc finger-homeodomain family transcription factors that were interacting with multiple cytokinin biosynthesis, degradation and signalling gene promoters. These are homologous transcription factors *ATHB23*, *ATHB30* and *ATHB34* which are expressed exclusively in the aerial parts of the plant (Figure 3.11) (Tan and Irish, 2006).

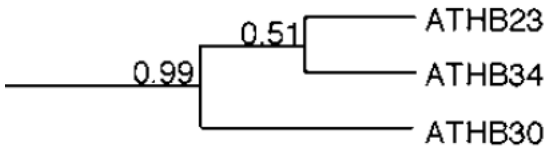

Figure 3.11 : Phylogenetic tree of *ATHB23*, *ATHB30* and *ATHB34* transcription factors

By analysing the expression in the *athb23* mutant background, I was able to determine that ATHB23 positively regulates *LOG4*. ATHB34 interacts with promoters of *IPT3*, *IPT9*, *CKX5*, *ARR1*, *ARR10* and *AHP2*. ATHB30 binds to only *IPT9* and *AHP2* promoters in the CKGRN.

A

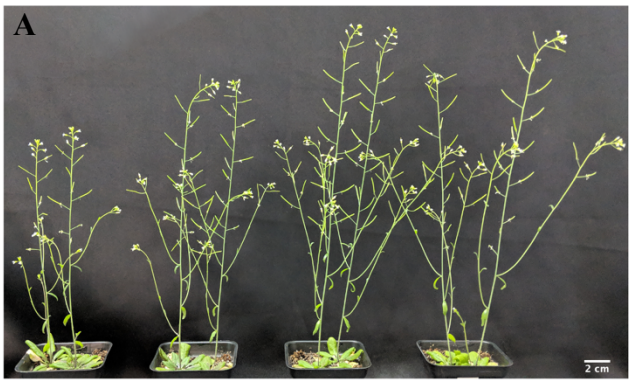

athb23;34 *athb23* *athb34* WT Col

B

	Bolting time (DAG)	Flowering time (DAG)	No. of axillary meristem
WT Col	23.67	27.42	14
athb34	23.33	27.17	14.33
athb23	26***	29.17***	18*
athb23;34	26.5***	30.58***	17.08*

Figure 3.12 : Flowering and shoot growth in *ATHB23* and *ATHB34* mutants

(A) *athb23* and *athb34* single and double mutant plants.

(B) Delayed flowering and growth defects in *athb23* and *athb34* mutants.

The T-DNA insertion line of *ATHB30* could not be isolated due to a lack of a suitable line. I successfully generated *athb23;athb34* double mutant to determine the effect of these transcription factors on the overall growth of the plant.

The *athb23* single mutant has a delayed flowering phenotype, but the same is not observed in *athb34* mutant. In combination, the *athb23;athb34* double mutant has slightly more delayed flowering than the *athb23* single mutant (Figure 3.12A,B). The *athb23* and *athb23;34* have similarly delayed bolting time, however, the flowering time for the double mutant was even later. The number of axillary meristems formed in the *athb23* and *athb23;34* mutants were also higher than the WT (Figure 3.12B). This indicates that in the *ATHB* mutants there is a delay in shoot growth due to the perturbed expression of CK biosynthesis and signalling genes.

3.3.3.3 Non-homologous transcription factors with overlapping interactions

The two transcription factors ATH1 and ABF1 have no homology but they have similar expression patterns in the SAM. Both these transcription factors are expressed in the epidermal

layer of the SAM. Also, both ATH1 and ABF1 inhibit AHK4 in the epidermal layer of the SAM. Therefore, the double mutant *ath1;abf1* was created to see the combinatorial effect. The rosette size of *ath1;abf1* mutant was visibly reduced as compared with WT Col (Figure 3.13A). There was also a decrease in the number of siliques formed in the mature adult 6.90 stage (Figure 3.13B). Therefore, increasing the AHK4 activity by combining *ath1* and *abf1,* also retards the overall growth of the plants.

A

WT Col *ath1;abf1*

B

	Bolting time (DAG)	Flowering time (DAG)	No. of siliques at stage 6.90
WT Col	24.83	28.91	92.18
ath1;abf1	25.92*	31**	68.67***

Figure 3.13 : Phenotype of *ATH1* and *ABF1* double mutant

(A) WT Col and *ath1;abf1* double mutant rosette.

(B) Flowering and yield in WT Col and *ath1;abf1* plants

3.4 Discussion

Cytokinin homeostasis in plants is maintained by the dual regulation of the cytokinin levels and the availability of signalling molecules. Through our network biology approach, we have identified upstream regulators involved in CKGRN. This was achieved with the help of an eY1H screen consisting of an entire array of shoot-enriched transcription factors against the promoters of all relevant cytokinin biosynthesis, degradation and signalling genes.

All the TFs that have been studied in this gene regulatory network have a significant expression in the SAM in normal conditions. While these TFs function as perpetual modulators of cytokinin response, they are also induced by abiotic stresses which will further increase their influence on maintaining cytokinin homeostasis. The preliminary single and double mutant phenotype characterisation indicates defects in CK response in these transcription factor mutants. The RT-qPCR analysis of target gene expression provides some clues about the nature of these interactions. However, further genetics would have to be followed for greater clarity into the role of these transcription factors in the SAM.

DREB19 is differentially expressed in the L2 layer (Yadav et al., 2014), and it negatively regulates *ARR10*, *ARR15* and *IPT9*. Interestingly all three of these genes have a very low expression in the L2 layer as seen in their respective transcriptional reporters (Figure 7A, B). ATHB23 and ATHB34 are homologous transcription factors that are highly expressed throughout the SAM (Perotti et al., 2019; Yadav et al., 2014). Interestingly, both these TFs regulate different cytokinin biosynthesis and signalling genes, however, they are functionally redundant as their overall effect is to induce cytokinin signalling in the shoot.

Another layer of complexity can be seen in the interaction of DEWAX with *LOG4* and *AHK4*. *DEWAX* is expressed in the L1 layer where it induces *LOG4*. Conversely, *AHK4* is absent in the L1 layer where it is repressed by *DEWAX*. Furthermore, LOG4 and AHK4 are controlled by two more L1-specific TFs. *ABF1* negatively regulates *LOG4* in the L1 layer, and *ATH1*

negatively regulates *AHK4* in the L1 layer. Thus, the contrasting expression of *LOG4* and *AHK4* in the L1 layer is a combination of these unique PDIs.

There are 23 TFs that are modulating multiple genes of cytokinin biosynthesis, degradation or signalling simultaneously, whereas 26 TFs are involved in only a single PDI. The single interactors can be just as integral for maintaining cytokinin homeostasis. *ATH1* is one such unique TF that is downregulated in cytokinin deficient plants, and it negatively regulates *AHK4* (Brenner et al., 2005). Moreover, *AHK4* expression increases in a delayed response to cytokinin treatment. Therefore, the increase in *AHK4* expression would require the repression by ATH1 and ABF1 to be reduced.

Cytokinin deficient plants have been studied for their stress tolerance for many abiotic stresses (Cortleven et al., 2019; Nishiyama et al., 2011). The cytokinin signalling factors negatively regulate the stress-responsive genes by ABA-dependent and ABA-independent mechanisms (Nguyen et al., 2016; Nishiyama et al., 2013; L. P. Tran et al., 2007). It has been established that cytokinin response is downregulated when the plants are coping with salt and drought stress, but the effect of temperature stress is not well studied. The transcriptional reporters of the CKGRN target genes can be used as a resource to dissect these interactions. They will be essential in studying the spatiotemporal regulation of the cytokinin genes in various genetic backgrounds and environmental conditions.

CHAPTER 4

NAC062 regulates shoot growth by maintaining cytokinin biosynthesis and signalling in the SAM

4.1 Summary

The eY1H screen revealed that NAC062/NAC WITH TRANSMEMBRANE MOTIF1 (NTM1)-LIKE6 (NTL6) binds to the *LOG4* and *AHK4* gene promoters. In this chapter, I show that the CK signalling output is decreased in the stem cell niche of *nac062*/*ntl6* mutant plant SAM, and as a result size of the shoot is also reduced. NAC062/NTL6 is present throughout the SAM and has a minimal effect on growth even in ambient conditions. Cold stress further stimulates NAC062/NTL6 cleavage from the membrane and thus enters the nucleus where it activates the transcription of *LOG4* and *AHK4*. The ectopic expression of the constitutively active *NAC062/NTL6* resulted in delayed senescence and arrested shoot growth due to increased cytokinin response. In summary, my work reveals an interesting molecular function of NAC062/NTL6 where it delays the growth of shoot apex in *Arabidopsis* by regulating CK signalling in response to cold.

4.2 Introduction

The activity of transcription factors is regulated by several processes and dormant transcription factors can be stimulated by interactions with other factors and posttranslational modifications. The membrane-bound transcription factors (MTFs) are inserted in the plasma membrane, endoplasmic reticulum, outer mitochondrial, outer chloroplast or peroxisomal membranes (Liang et al., 2015). These MTFs are stimulated by several developmental and environmental signals. Upon stimulation, they are activated by proteolytic cleavage by two different mechanisms that are biochemically related. First is the process of intramembrane proteolysis (RIP) which leads to the liberation of active transcription factors by specific membrane-associated proteases (Vik and Rine, 2000). The other process requires Regulated

Ubiquitin/26S proteasome-dependent Processing (RUP) where the MTFs are ubiquitinated and degraded by the 26S proteasome. The proteasomal degradation is controlled in such a manner that it leads to the release of the transcriptionally active form of the protein (Hoppe et al., 2000). Several MTFs activated by RIP were first characterized in yeast and mammalian cells. One such MTF is activating transcription factor 6 (ATF6) and it plays a role in sensing ER stress. The translocation of ATF6 from the ER membrane to Golgi is triggered by changes in membrane fluidity and its cleavage is mediated by a two-step process. It is first cleaved by a serine protease, S1P(site-1 protease) and further by a metalloprotease S2P (site-2 protease) (Shen et al., 2002). With the characterization of mammalian MTFs, there were efforts made to study the role of plant specific MTFs. The ER stress response is triggered in plants by the application of tunicamycin and dithiothreitol (DTT). This concept was used to screen for several plant MTFs that are cleaved in response to changes in membrane fluidity (Iwata and Koizumi, 2005). This led to the discovery of several bZIP and NAC MTFs that are cleaved by a range of proteases using the RIP mechanism (Seo et al., 2008).

Among the other types of abiotic stresses, membrane fluidity can also be disrupted by cold stress. The membrane fluidity change in cold temperatures is linked to cytoskeleton reorganization and alteration of phospholipid content of membranes (Vik and Rine, 2000; Xiong et al., 2002). One such NAC MTF that is induced by changes in membrane fluidity is NAC062/NTL6. The cleavage of NAC062/NTL6 is enhanced by cold, drought, salt and UPR stress. Its cleavage is also promoted by treatment with Abscisic acid (ABA) (Kim et al., 2007; Seo et al., 2010; Yang et al., 2014). The cleavage of NAC062/NTL6 is mediated by metalloproteases as the presence of nuclear form is diminished by treatment with a metalloprotease inhibitor (Seo et al., 2010). The overexpression of the constitutively active form of NAC062/NTL6 leads to growth defects in *Arabidopsis* that resemble the effects of cold

on plant growth. However, the exact mechanism by which the alteration in growth happens is not well understood.

4.3 Results

4.3.1 Membrane-Associated NAC062/NTL6 induces Cytokinin responses in the Shoot Apex

Among the identified interacting partners, NAC062/NTL6 was studied to characterise the physiological effects of its binding with promoters of *LOG4* and *AHK4* in the eY1H assay. The binding was also reconfirmed using a one-to-one Y1H assay independently (Figure 4.1A, B).

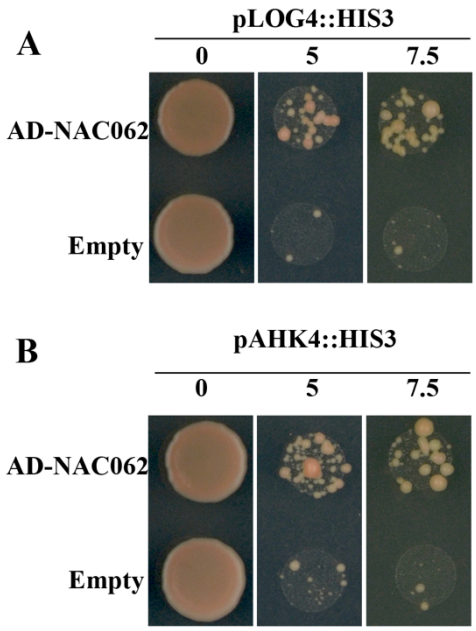

Figure 4.1 : NAC062 binds to CK biosynthesis and signalling genes

(A) Y1H assay of AD-NAC062 prey with pLOG4::HIS3 bait on 5-7.5mM 3AT concentration

(B) Y1H assay of AD-NAC062 prey with pAHK4::HIS3 bait on 5-7.5mM 3AT concentration

To further probe the role of NAC062/NTL6 in CKGRN, a T-DNA insertion line (SALK_103823) was isolated. The T-DNA insertion site was identified to be present in the

NAC062/NTL6 promoter (at -273bp) (Figure 4.1A). Further transcript analysis revealed that *NAC062/NTL6* expression was notably reduced in the insertion mutant line compared to WT. Even though this was not a null mutant, the decrease in the *NAC062* expression in the *nac062-1/ntl6* mutant allele led to a mild phenotype (Figure 4.2). The size of the mutant rosette leaves was smaller compared to WT (Figure 4.2B, C). Although the development of the lateral organs was normal, the overall growth of the mutant plant was delayed including flowering (Figure 4.2B, C). Shoot size was also reduced in the *nac062-1* mutant plants compared to WT (Figure 4.2D, E).

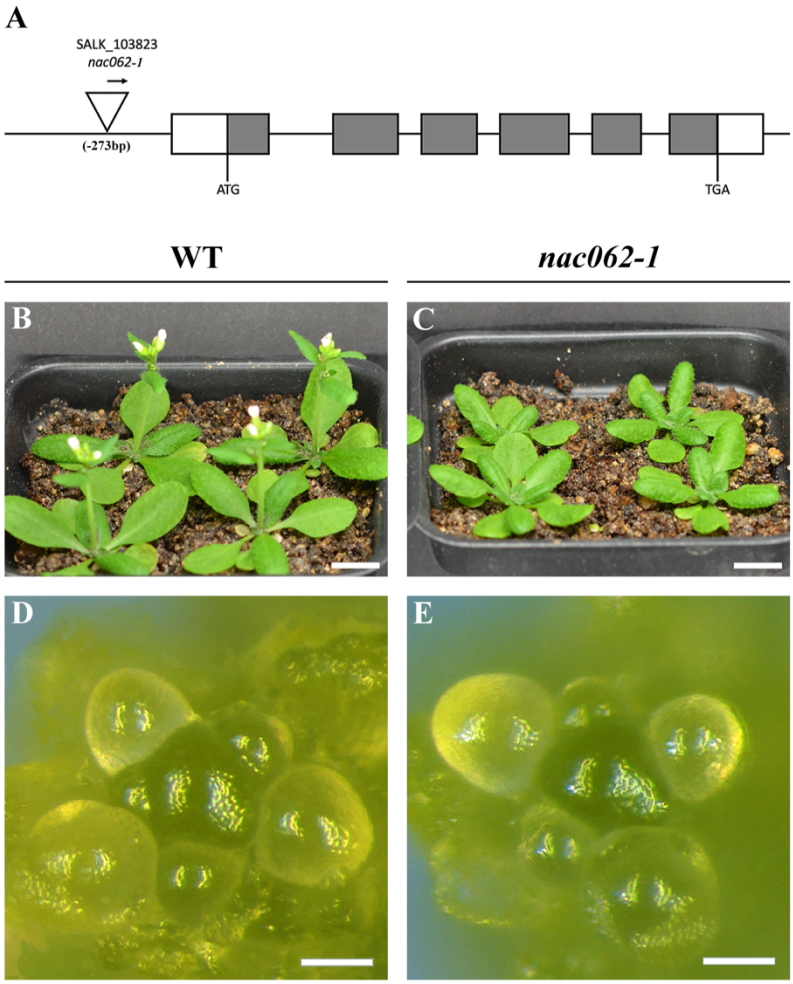

Figure 4.2 : *nac062-1* mutant has a mild phenotype

(A) SALK_103823 (*nac062-1*) T-DNA insertion gene structure.

(B, C) Side view of 25 day old WT and *nac062-1* mutant. Scale bar = 1cm.

(D, E) SAM top view of 25 day old WT and *nac062-1* mutant. Scale bar = 50μm.

To determine how the changes in CKGRN alters CK responses in *nac062-1/ntl6* SAM, the mutant line was crossed with *pTCSn::GFP-ER* reporter line (*TCSn*). Homozygous plants for both *nac062-1/ntl6* and *TCSn* reporter genes were isolated by following segregating progenies. Inflorescence meristem of four week old *nac062-1/ntl6* and WT plants carrying *pTCSn::GFP-ER* reporter were clipped to remove older floral buds. In WT, *pTCSn::GFP-ER* is broadly expressed in the niche/organizing center (OC) of SAM as reported by previous studies (Figure 4.3A, B) (Zürcher et al., 2013). In flower meristem, *pTCSn::GFP-ER* expression is extended up to the subepidermal cell layer (Figure 4.3B). In *nac62-1/ntl6* mutant SAM, the *pTCSn::GFP-ER* expression is reduced significantly in the OC barring one or two cells that still glows with GFP. In *nac062-1/ntl6* floral meristem, there is a significant decrease in *pTCSn::GFP-ER* expression (Figure 4.3C, D) compared to control. This finding suggests that *NAC062/NTL6* is playing a key role in maintaining CK responses within the stem cell niche of the shoot apex.

The logical hypothesis is that the differences observed in *TCSn* expression in WT and *nac062-1/ntl6* mutant SAM is because CK signalling is not sufficiently activated in these plants. To test whether CK responses in *nac062-1* mutant SAM can be recovered by external application of CK. The synthetic CK, 6-Benzylaminopurine (BAP) was applied externally to the inflorescence meristem. BAP has been used in the past for CK treatment since it is resistant to degradation (Galuszka et al., 2007). To study this first the *nac062-1/ntl6; pTCSn::GFP-ER* and WT; *pTCSn::GFP-ER* lines were grown in parallel. Plants were treated with varying concentrations of BAP or mock solution and the SAM was imaged using confocal microscopy. WT plants treated with 10μM BAP showed a strong expression of *TCSn* in the SAM and floral

meristem compared to mock (Figure 4.3E, F, M). Expression of *TCSn* expanded apically towards subepidermis and laterally in the organ boundary region, indicating that external application of BAP can induce robust CK responses in the treated plants (Figure 4.3E, F). In *nac062-1* mutant SAM, 10µM BAP treatment produced a slight upsurge in *pTCSn::GFP-ER* expression compared to mock, but there was no recovery in the OC cells (Figure 4.3G, H). *TCSn* expression in the flower meristem of *nac062-1/ntl6* mutant plant treated with BAP was partially rescued and had a similar expression pattern as the untreated WT control (Figure 4.3A, B, G, H). This finding suggests a critical role of NAC062/NTL6 in CKGRN which influences CK responses, especially in the stem cell niche of the shoot apex. We also applied a higher concentration of BAP (20 µM). In WT, *TCSn* expression expanded laterally towards the organ boundaries and in the subepidermal cell layer (Figure 4.3I, J), but the intensity was the same as seen in the lower concentration (Figure 4.3M). Similarly, the same was noted in *TCSn* expression in the 20 µM BAP treated *nac062-1/ntl6* mutant (Figure 4.3K, L). The intensity of *TCSn::GFP* in WT SAM increases ~2 fold when treated with 10µM BAP compared to mock-treated. When this was increased to 20µM, it did not produce a significant gain in the expression of *TCSn* reporter compared to plants that were treated with 10µM BAP, indicating that CK response is not linear (Figure 4.3M). In contrast to WT (Figure 4.3B), the *TCSn* reporter activity in *nac062-1* mutant plants did not recover in the central zone after 10µM or 20µM BAP treatment, suggesting that the CK receptor is a limiting factor in the mutant (Figure 4.3H, L). Taken together the *TCSn* expression and BAP treatment in WT and *nac062-1/ntl6* mutant, our results revealed that CK responses can be uncoupled in the SAM and flower meristem. NAC062/NTL6 is involved in maintaining CK responses in the stem cell niche to sustain the growth of shoot meristem.

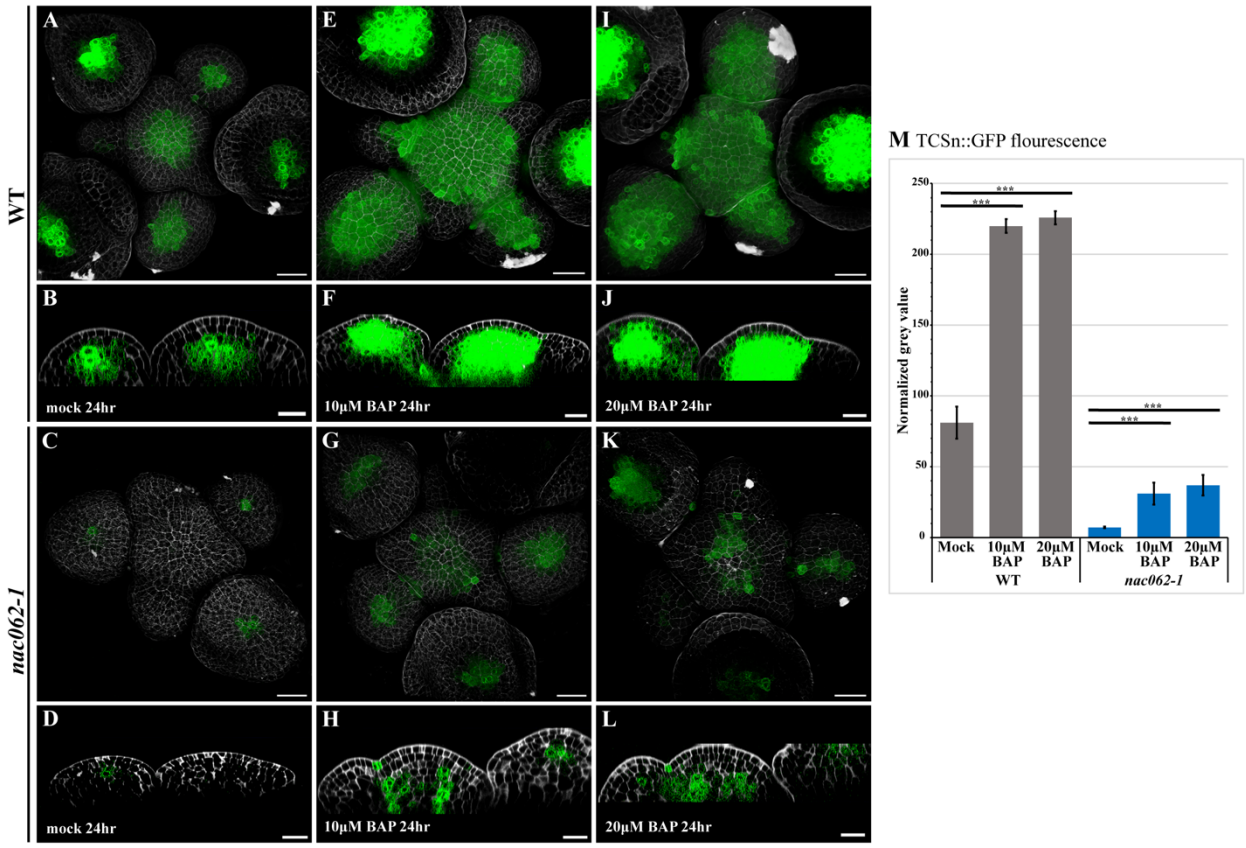

Figure 4.3 : *nac062-1* mutant has defective cytokinin signalling

(A-D) *TCSn::GFP* (green) in SAM of mock-treated WT and *nac062-1* mutant.

(E-L) *TCSn::GFP* (green) in SAM of (E-H) 10µM BAP and (I-L) 20µM BAP treated WT and *nac062-1*. PI (grey); Scale bar = 25µm

(M) Normalized grey value of *TCSn::GFP* in mock and BAP-treated SAM of WT (n=5-6; Student t-test p-value <0.0001) and *nac062-1* mutant (n=5-7; Student t-test p-value =0.0005).

4.3.2 Ectopic expression of NAC062/NTL6 triggers delayed senescence and arrest in plant growth

The activity of all membrane-bound NACs, like NAC062NTL6, is limited by their association with the membrane. To exert their influence on target genes they need to be translocated into the nucleus (Ernst et al., 2004). To study the gain-of-function effect of NAC062/NTL6, a

constitutively active form was engineered where a 140 amino acid long C-terminal region was deleted to create NAC062ΔC (Figure 4.4). In the absence of the C-terminal transmembrane region, NAC062ΔC will enter the nucleus after protein synthesis (Kim et al., 2007).

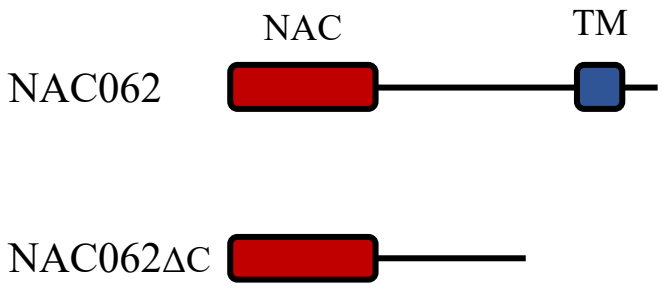

Figure 4.4 : Diagram of NAC062 full length and NAC062ΔC truncated protein

NAC062 protein consisting of NAC domain (petunia NAM and Arabidopsis ATAF1, ATAF2, and CUC2) and a Transmembrane domain (TM).

To test the role of NAC062/NTL6 in CK responses, plants containing *TCSn* reporter were dipped with *35S::NAC062* and *35S::NAC062ΔC* constructs, respectively. Plants carrying *35S::NAC062ΔC* transgene displayed variability in their phenotype in the first generation (T1). Of the 41 seedlings, ~ 27% had a severe phenotype (type-A) such as serrated leaves and inability to form fully developed flowers (Figure 4.5A-C). However, 39% of the T1 plants had a mild phenotype (type-B) and could be propagated further. The remaining 34% T1 plants appeared normal (type-C) like *35S::NAC062* and WT (data not shown). *35S::NAC062ΔC* type-A plants that showed strong phenotype stayed green for a long time and displayed loss of apical dominance with multiple shoots developing over time (Figure 5A, B). In addition, floral organ primordia failed to form distinct petals (Figure 4.5C).

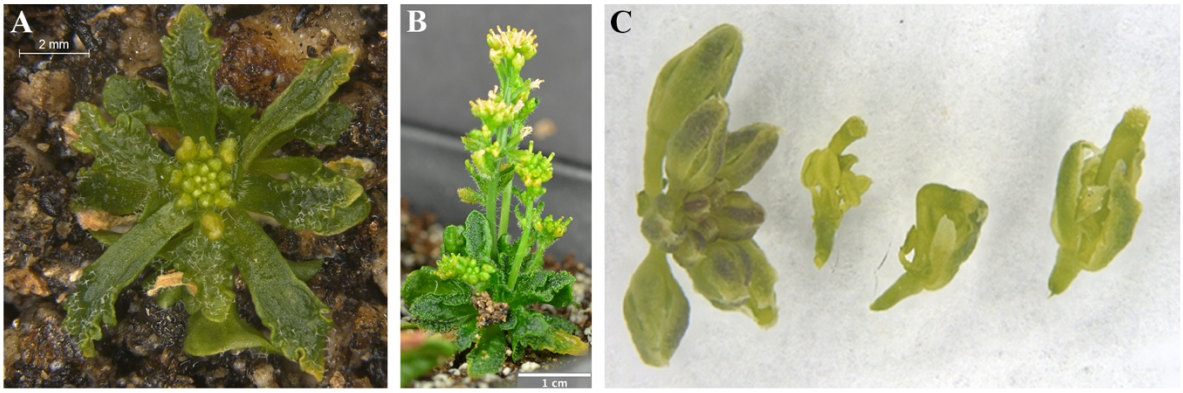

Figure 4.5 : Phenotype of *35S::NAC062ΔC* type-A plants

(A) *35S::NAC062* plants at bolting time. Scale bar = 2mm

(B) *35S::NAC062* flowering plants (~2 months old). Scale bar = 1cm

(B) *35S::NAC062* inflorescence and open flowers.

The heterozygous *35S::NAC062ΔC* type-B plants that exhibited normal height but delayed senescence phenotype in T1 were followed into T2 generation (Figure 4.6A). The type-A like plant phenotype was observed in the homozygous *35S::NAC062ΔC* type-B plants (Figure 4.6A, B). This indicates that a higher dosage of *NAC062ΔC* is detrimental for shoot growth (Figure 4.6A, B).

TCSn expression was also analysed to investigate the effect of *35S::NAC062* and *35S::NAC062ΔC* transgenes on the CK response in SAM. The activity of *TCSn* reporter gene did not change significantly in *35S::NAC062* plants compared to control (Figure 4.6C, D). However, the analysis of *TCSn* reporter in homozygous *35::NAC062ΔC* type-B plants revealed that plants expressing *NAC062ΔC* version displayed robust CK responses in the SAM, suggesting that delayed senescence in these plants is linked to ectopic CK signalling (Figure 4.6E).

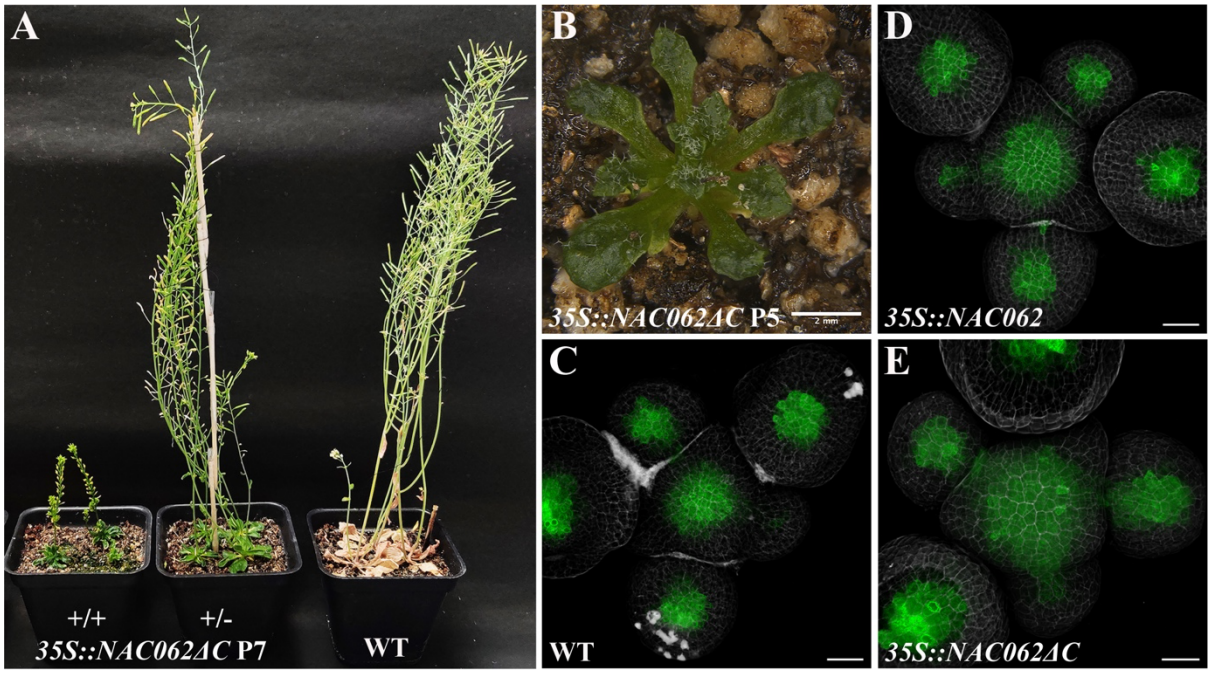

Figure 4.6 : Over-expression of active NAC062 leads to severe growth defects

(A) Homozygous and heterozygous *35S::NAC062*Δ*C* plant line 7 along with WT.

(B) Heterozygous T1 generation *35S::NAC062*Δ*C* plant line 5. Scale bar = 2mm

(C-E) *TCSn::GFP* (green) in SAM of (C) WT, (D) *35S::NAC062* and (E) *35S::NAC062*Δ*C*. Scale bar = 25µm

4.3.3 NAC062/NTL6 positively regulates *LOG4* and *AHK4* in *Arabidopsis* SAM

The mutant and overexpression phenotypes were characterised for the effect of NAC062/NTL6 on CK responses in the shoot apex. Interestingly, the mutant phenotype was mild, however, constitutively active *NAC062ΔC* led to a strong phenotype, which is attributed to its role in CKGRN. To investigate the molecular link between NAC062 and its target genes based on the eY1H data, we conducted an RT-qPCR assay to check the relative expression of *LOG4* and *AHK4* transcript levels in WT and *nac062-1/ntl6* mutant.

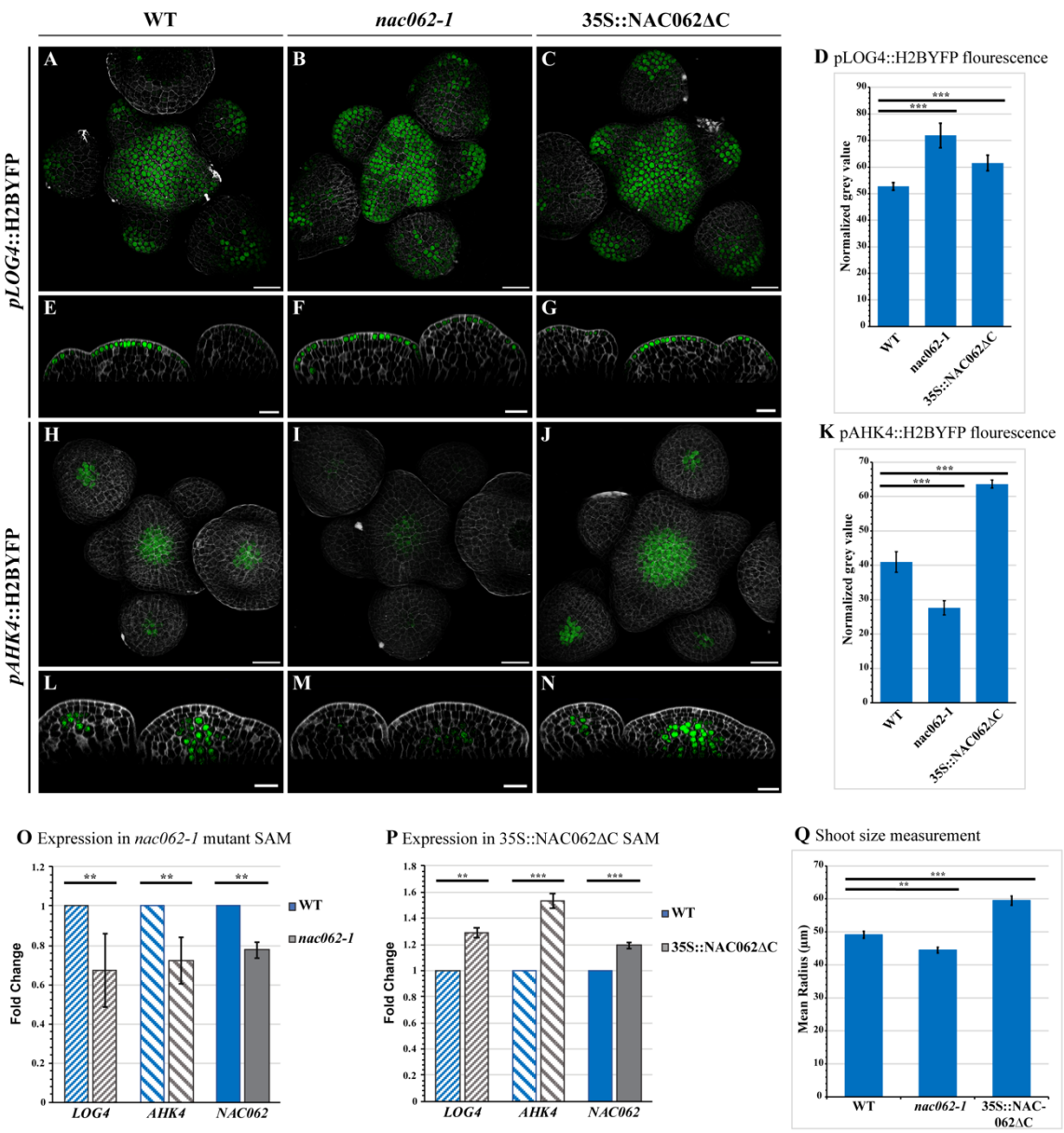

Figure 4.7 : NAC062 induces *AHK4* and *LOG4* expression

(A-C, E-G) *pLOG4::H2BYFP* (green) expression in the SAMs of (A, E) WT, (B, F) *nac062-1* and (C, G) *35S::NAC062ΔC*. Scale bar = 25µm

(H-J, L-N) *pAHK4::H2BYFP* (green) expression in the SAMs of (H, L) WT, (I, M) *nac062-1* and (J, N) *35S::NAC062ΔC*. Scale bar = 25µm

(D) Normalized grey value of *pLOG4::H2BYFP* in SAMs (n=17-20) of WT, *nac062-1* and *35S::NAC062ΔC*. (Student t-test p-value <0.0001)

(K) Normalized grey value of *pAHK4::H2BYFP* in SAMs (n=13-20) of WT, *nac062-1* and *35S::NAC062ΔC*. (Student t-test p-value <0.0001)

(O,P) qRT-PCR relative expression of *LOG4*, *AHK4* and *NAC062* in (O) *nac062-1* and (P) *35S::NAC062ΔC* line as compared with WT. (n=3; Student t-test p-value <0.05)

(Q) Shoot size measurement by estimating SAM mean radius of WT (n=14), *nac062-1* (n=17, Student t-test p-value = 0.0018), *35S::NAC062ΔC*. (n=16, Student t-test p-value <0.0001)

To explore this regulation in the inflorescence meristem, *nac062-1/ntl6* and WT plants were grown in parallel until bolting and finely dissected shoot apices to extract total RNA. We detected a reduction in the transcript levels of *LOG4* and *AHK4* in *nac062-1/ntl6* mutant compared to WT in RT-qPCR (Figure 4.7O). The expression of the target genes was also analysed in the *35S::NAC062ΔC* line. *LOG4* transcript levels increased in proportion to *NAC062ΔC* transcript levels, whereas the *AHK4* levels were elevated ~2 times relative to the change in *NAC062ΔC* transcript levels (Figure 4.7P).

The analysis of gene expression by qRT-PCR assay did not give us an accurate picture regarding the spatiotemporal regulation of *LOG4* and *AHK4* in the SAM. To investigate this, *nac062-1* mutant and *35S::NAC062ΔC* lines were crossed with *pLOG4::H2B-YFP* and *pAHK4::H2B-YFP,* respectively. Both lines were made homozygous for the reporter gene in *nac062-1* mutant and control. Finally, third-generation plants were obtained to check the effect of NAC062/NTL6 on maintaining the spatiotemporal expression pattern of *LOG4* and *AHK4*. *pLOG4::H2B-YFP* expression in the *nac062-1/ntl6* mutant (Figure 4.7B, F) was irregular in the central and peripheral zone epidermal cells of shoot compared to control SAM (Figure 4.7A, E). *pAHK4::H2B-YFP* expression was reduced drastically in the OC and lateral organ

primordia cells (Figure 4I, M), as compared to the WT control (Figure 4.7H, L). The expression of *pLOG4::H2B-YFP* and *pAHK4::H2B-YFP* was also checked in *35S::NAC062ΔC* lines. The expression of *pLOG4::H2B-YFP* increased in the central and primordial cells of *35S::NAC062ΔC* SAM (Figure 4.7C, G). There was an expansion in the *pAHK4* expression domain towards the peripheral zone of the shoot in *35S::NAC062ΔC* (Figure 4.7J, N). However, this expansion was not obvious in the floral meristem. The fluorescence intensity of *pLOG4* increased in the *nac062-1/ntl6* mutant central zone (Figure 4.7D). This shows that expression in some epidermal cells is increasing to compensate for the lack of *pLOG4* activity in other cells. The fluorescence intensity of *pAHK4::H2BYFP* decreases significantly in the *nac062-1/ntl6* mutant plants (Figure 4.7K). Although the change in *NAC062* transcript is similar in the mutant and overexpression lines (±20%), the expression of *pAHK4::H2BYFP* reporter increased by ~60% in *35S::NAC062ΔC* (Figure 4.7K). Similarly, the shoot size in *35S::NAC062ΔC* plants is increased by ~20% (n=13, 59.5 ± 1.4), whereas in the mutant shoot size is decreased by ~10% (n=17, 44.5 ± 0.9), when compared to WT (n=14, 49.1 ± 1.06) (Figure 4.7Q). Thus, NAC062/NTL6 maintains CK responses in the SAM by binding to *LOG4* and *AHK4* promoters and activating their expression in the respective domains (Figure 4.8A-C).

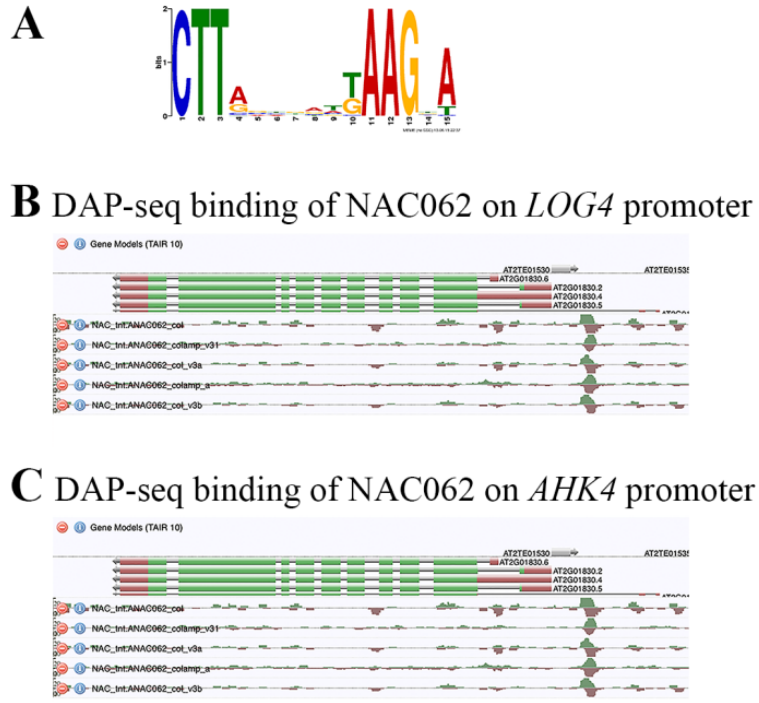

Figure 4.8 : Binding information of NAC062

(A) Binding motif of NAC062.

(B) DAP-seq peaks for NAC062 on *LOG4* gene.

(C) DAP-seq peaks for NAC062 on *AHK4* gene.

4.3.4 *NAC062/NTL6* expression and its cleavage from ER is induced by cold stress

To study the physiological relevance of NAC062/NTL6 on CK signalling, first, I studied the expression of *TCSn::GFP* reporter in WT and *nac062-1/ntl6* mutant background after cold exposure. Plants were grown at 22°C in long-day conditions. For cold treatment, plants were shifted to 4°C once flowering was initiated. The *TCSn* activity increases in the cold-treated SAM after 24 h (Figure 4.9E, F) compared to control (Figure 4.9A, B). Despite 24 h of cold exposure, no change in *TCSn* expression was observed in the *nac062-1* mutant (Figure 4.9C, D, G, H, I).

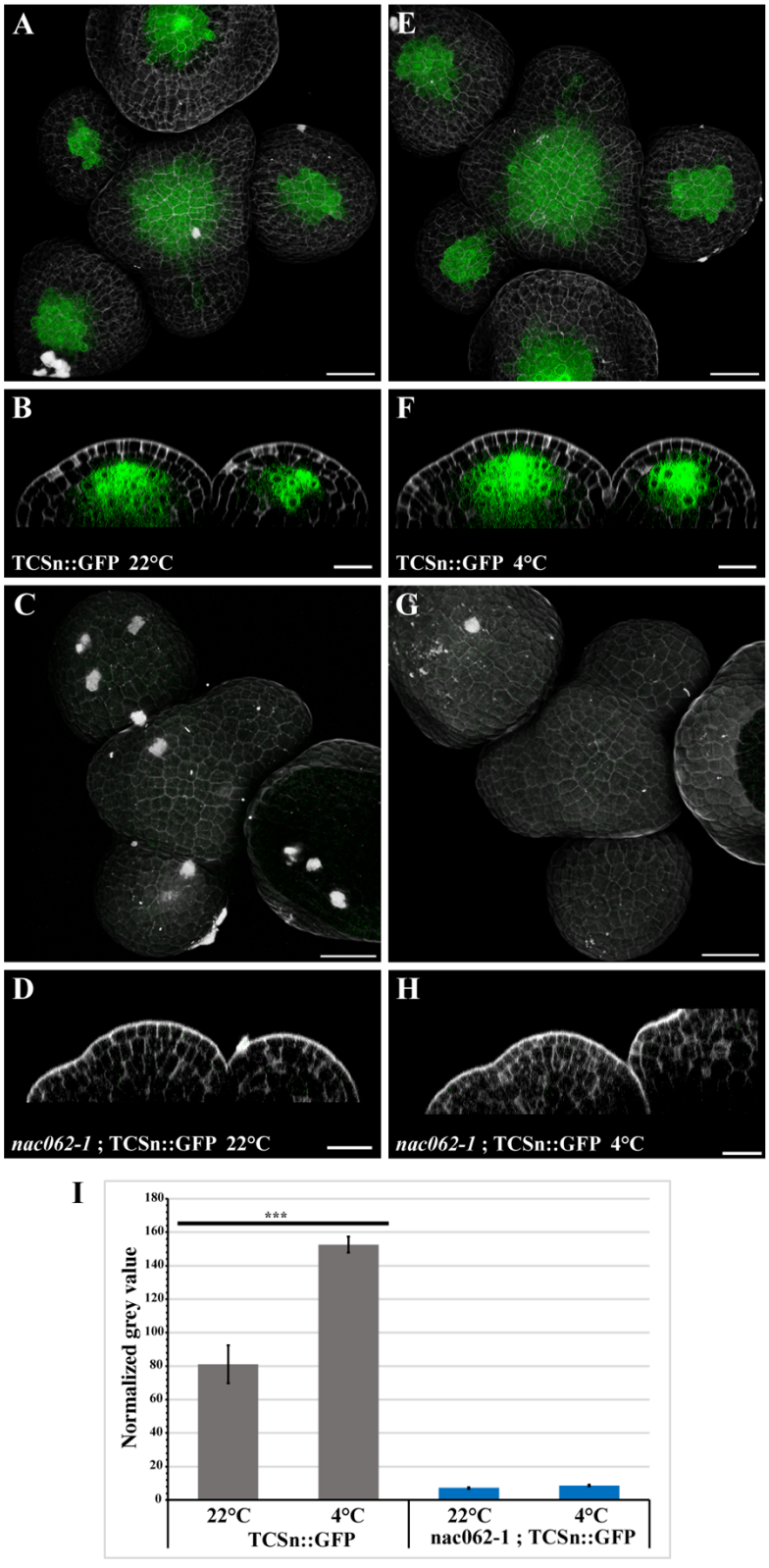

Figure 4.9 : Cold treatment activates cytokinin signalling via *NAC062*

(A,H) *TCSn::GFP* (green) in SAM of WT plants grown in (A,B) 22°C and (E,F) 4°C for 24 h. SAM of *nac062-1; TCSn::GFP* grown in (C,D) 22°C and (G,H) 4°C for 24 h. Scale bar = 25µm

(I) Normalized grey value of *TCSn::GFP* in WT (n=6-8, Student t-test p-value <0.0001) and *nac062-1* background (n=8, Student t-test p-value =0.0589).

The release of NAC062 from ER membrane can be triggered by changes in membrane fluidity during cold stress (Seo et al., 2010) (Figure 4.10A). Previous studies have shown that *NAC062/NTL6* is expressed throughout the plant and its activity depends on proteolytic cleavage of the C-terminal transmembrane domain (Kim et al., 2007; Seo et al., 2010). To test this hypothesis, a translational fusion was created by inserting *eGFP* sequence at N-terminus of NAC062 before the start codon of *NAC062* genomic fragment (Figure 4.10B). In *pNAC062::eGFP-gNAC062* lines, as expected the eGFP-NAC062 fusion protein localizes to ER membrane and some fraction of the activated protein enters the nucleus (Figure 4.10C). When *pNAC062::eGFP-gNAC062* lines were exposed to cold at 4°C for 24 h the eGFP-NAC062 fusion protein starts showing enhanced movement to the cell nucleus becoming apparent in its nuclear localization compared to control (Figure 4.10D). The proteolytic cleavage of NAC062 is activated by changes in membrane fluidity at 4°C for a period of 24 h, after which the membranes are stabilized due to cold acclimation (Seo et al., 2010). However, in subzero temperatures such as -4°C, the eGFP-NAC062 fusion protein exclusively enters the nucleus within 2 h due to disruption of membranes (Figure 4.10E).

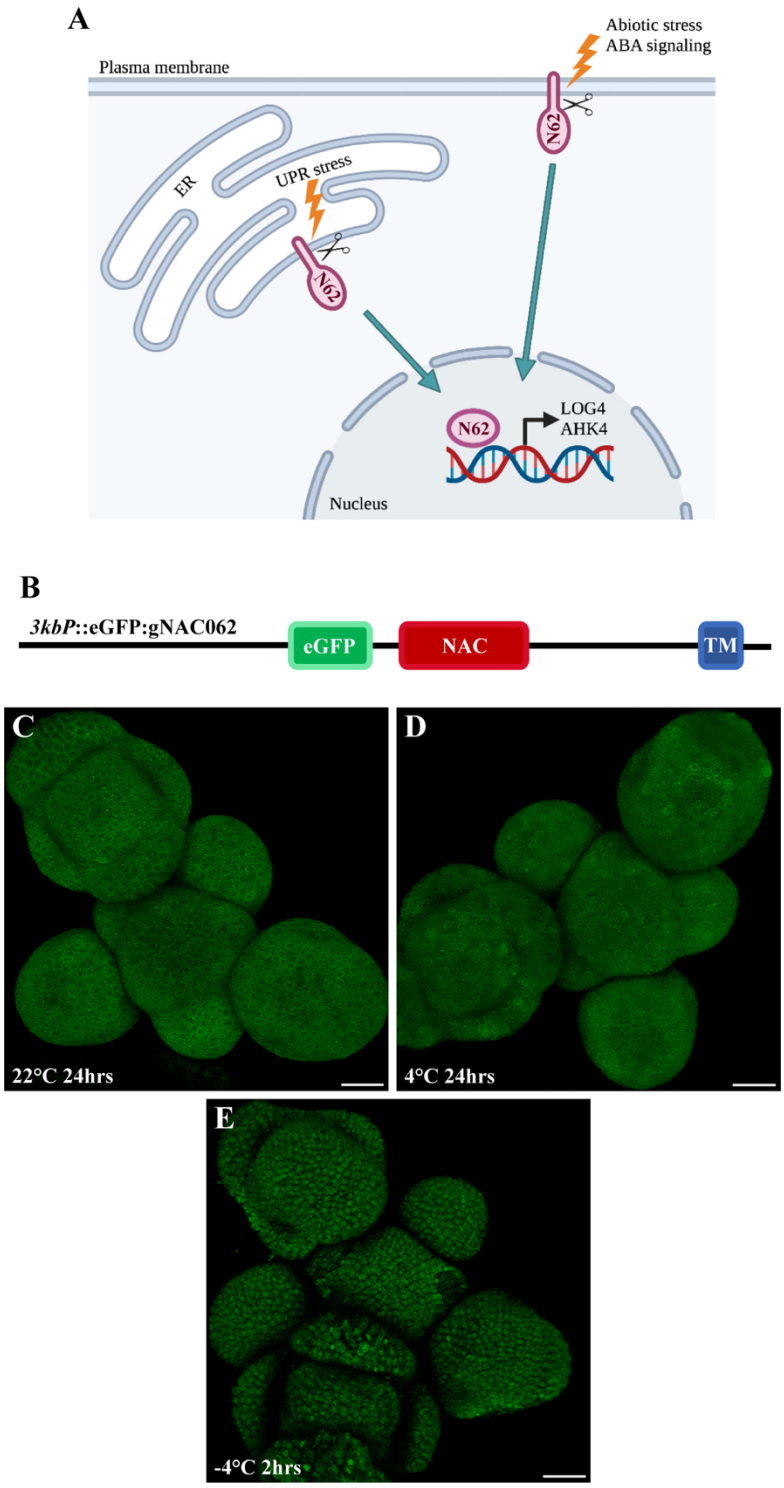

Figure 4.10 : NAC062 expression and activation in the SAM

(A) Model of NAC062 cleavage in response to various environmental factors.

(B) Diagrammatic representation of translational fusion reporter *pNAC062::eGFP:gNAC062*.

(C-E) *3kbP::eGFP:gNAC062* translational fusion reporter, grown in (C) 22°C for 25days and treated in (D) 4°C for 24 h and (E) -4°C for 2 h. Scale bar = 25µm

The *pNAC062::eGFP-gNAC062* was also introduced into the *nac062-1* mutant. The roots of WT and *nac062-1* mutant was imaged to study the protein activation dynamics in the root meristem (Figure 4.11A, B). In the roots, *NAC062* is broadly expressed throughout the meristematic and differentiation zones. The NAC062 protein is both membrane and nuclear localised in the roots of WT and *nac062-1* mutant (Figure 4.11A, B).

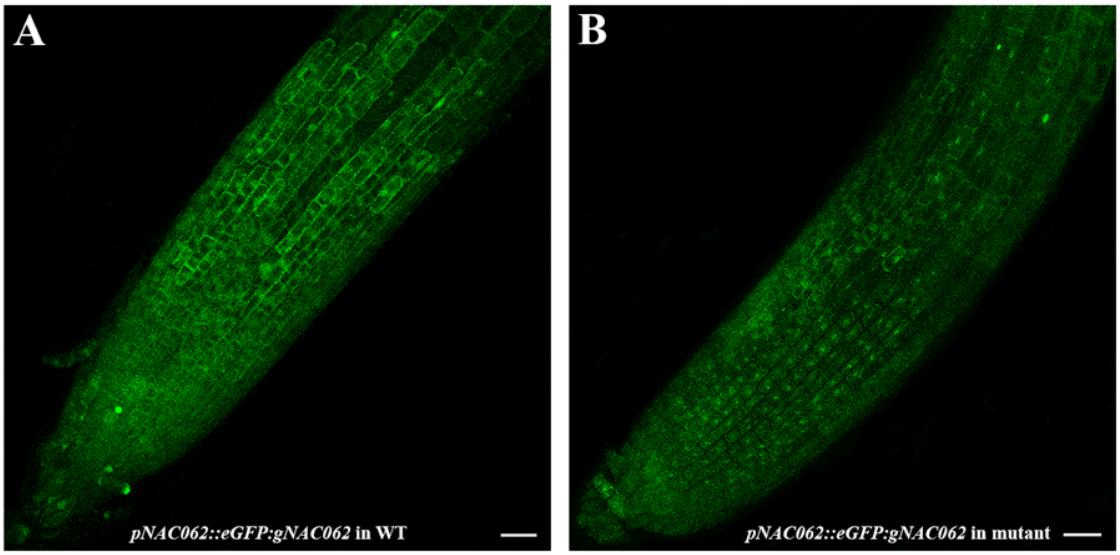

Figure 4.11 : NAC062 expression and activation in the root

(A) *pNAC062::eGFP:gNAC062* translational fusion reporter in WT root. Scale bar = 25µm

(B) *pNAC062::eGFP:gNAC062* translational fusion reporter in *nac062-1* mutant root. Scale bar = 25µm

The plants expressing *NAC062ΔC* transgene did not allow us to evaluate the immediate effect of NAC062ΔC activation on shoot growth and CK responses in SAM. To understand how

homeostasis in CK responses is achieved after initial activation, we developed a two-component based transient system. *NAC062ΔC* was combined with 3X-Operator (*p3XOP::NAC062ΔC*), and this construct was introduced into a *35S::LhG4-GR* line. Application of dexamethasone (Dex) will lead to the nuclear localisation of the LhG4-GR chimeric transcription factor, which binds to *p3XOP* and will induce the expression of *NAC062ΔC*. *p3XOP::NAC062ΔC*; *35S::LhG4-GR* line was crossed with *TCSn::GFP* to monitor the CK signalling upon Dex treatment. Inflorescence meristem of *p3XOP::NAC062ΔC*; *35S::LhG4-GR; TCSn::GFP* was treated with 10µM Dex and imaged after 24 hr with control. There was an increase in the *TCSn::GFP* expression compared to mock (Figure 4.13A, B). To observe the long-term activation of NAC062ΔC, these plants were treated every alternate day (Figure 4.12A). The continuous treatment led to constant activation of *NAC062ΔC* expression in the shoot. There was a severe loss of apical dominance in Dex treated plants by the 7th day (Figure 4.12B). This resembles the condition in *35S::NAC062ΔC* type-A plants that make multiple shoots over time as each emerging shoot is arrested (Figure 4.12C). There was a prominent effect of the treatment by day 5 on Dex-treated plants, such that floral buds failed to open in treated plants (Figure 4.12D, E). *TCSn::GFP* expression expanded in the beginning but got stabilized by day 5 in Dex-treated plants (Figure 4.13C, D). The WT plants are more than a month old by day 7 of initial treatment, thus they form fewer open flowers as part of the natural ageing process (Figure 4.12F). However, this was not the case with Dex treated plants that were arrested in the same stage as Day 0 and fail to form mature siliques (Figure 4.12B, G).

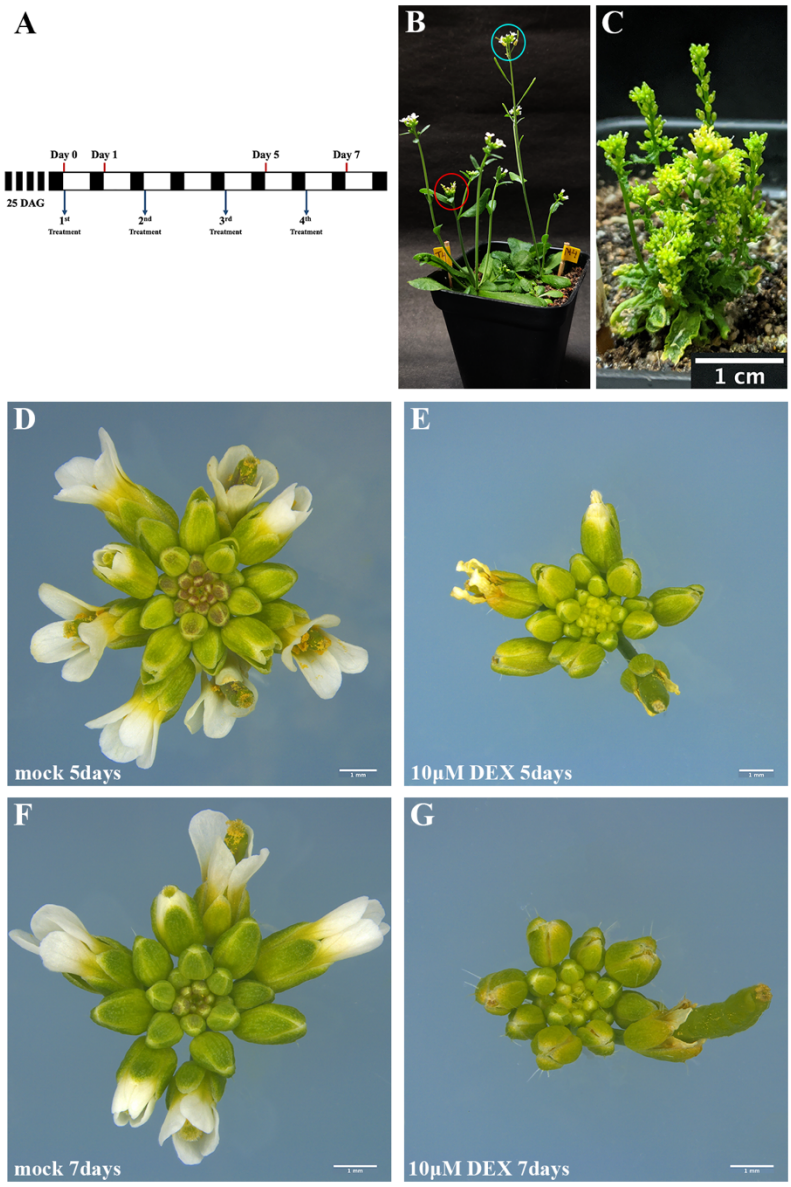

Figure 4.12 : Transient overexpression of *NAC062ΔC* led to the loss of apical dominance

(A) Schematic representing Dex treatment of *35S::LHG4-GR;3XOP::NAC062*ΔC*; TCSn::GFP* 25 day old plants.

(B) *35S::LHG4-GR;3XOP::NAC062*Δ*C* 32 day old plants treated with 10µM Dex (red circle) and DMSO (blue circle) for 7 days.

(C) Image of 2 month old *35S::NAC062*Δ*C* type-A plant. Scale bar = 1cm

(D, F) Top-view of shoots from mock-treated and (E, G) 10µM Dex-treated plants after 5 days (D, E) and 7 days (F, G) respectively. Scale bar = 1mm

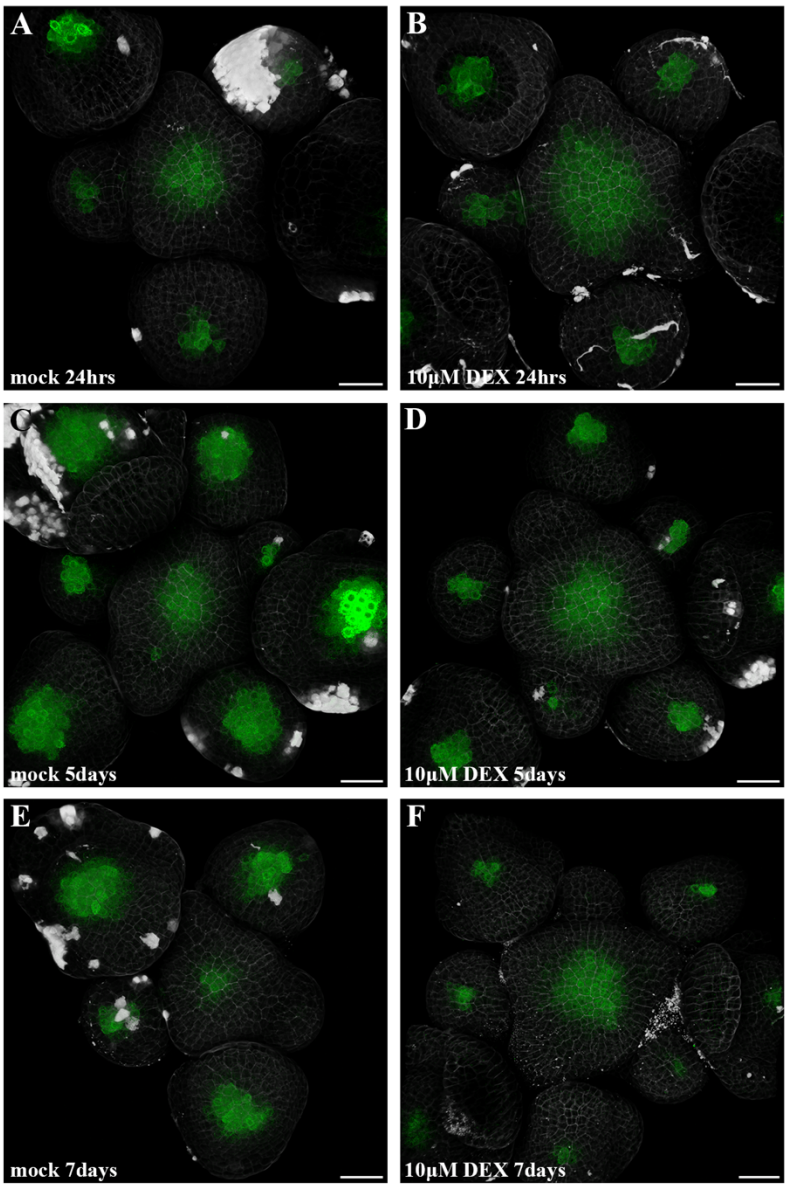

Figure 4.13 : CK response upon transient overexpression of *NAC062ΔC*

(A, B) *TCSn::GFP* in mock-treated (A) and 10μM Dex-treated (B) *35S::LHG4-GR;3XOP::NAC062*ΔC line SAM after 24 h. Scale bar = 25μm

(C, D) *TCSn::GFP* in mock-treated (C) and 10μM Dex-treated (D) *35S::LHG4-GR;3XOP::NAC062*ΔC line SAM after 5days. Scale bar = 25μm

(E, F) *TCSn::GFP* in mock-treated (E) and 10μM Dex-treated (F) *35S::LHG4-GR;3XOP::NAC062*ΔC line SAM after 7days. Scale bar = 25μm

As the SAM ages, the *TCSn::GFP* domain is reduced in the centre while remaining constant in the primordia (Figure 4.13E). In Dex-treated SAM where *NAC062ΔC* is induced, the *TCSn::GFP* expression is maintained in the centre until day 7, but the *TCSn::GFP* expression reduces in the primordia (Figure 4.13F). The transient overexpression and mutant phenotypes are indicative of the role that NAC062/NTL6 plays in decoupling CK response in the SAM and flower primordia.

4.4 Discussion

NAC062/NTL6 is a membrane-associated transcription factor that is released from the membrane due to cleavage by metalloproteases in response to stress. We decided to study the relationship of cold with cytokinin response since the cleavage of NAC062 is related to changes in membrane fluidity, and NAC062 binds to the two important targets, *LOG4* and *AHK4*. We found that NAC062 induces cytokinin response by increasing the expressivity of both *LOG4* and *AHK4*. A similar increase in cytokinin response was observed when WT type plants were shifted to colder temperatures. There was no change in CK response in the *nac062-1* mutant, indicating a direct involvement of NAC062 in inducing the cold-related CK response.

Constitutively active form NAC062ΔC allowed us to study the morphological effect of NAC062 on growth. The 35S::*NAC062ΔC* line had many growth defects that have also been previously reported (Kim et al., 2007; Seo et al., 2010), but the defect in the growth of the inflorescence was not studied. The Dex-inducible *NAC062ΔC* line was used to demonstrate that the multiple shoot phenotype in the 35S::*NAC062ΔC* line was due to the retarded growth of the main shoot. This phenotype is also interesting because one consequence of keeping plants in colder temperatures is that this will slow the plant's growth.

Notably, there is always a minimal amount of the processed NAC062 that is present even in normal conditions and it is constantly inducing basal level of cytokinin response in the shoot.

While NAC062 has a significant expression in the SAM in normal conditions its activity depends upon its processivity. The identity of the metalloproteases responsible for the cleavage of NAC062/NTL6 is not known. In *Arabidopsis,* there are several metalloproteases but a few jump out as probable candidates due to the phenotype in mutant alleles. There is the matrix metalloproteinase (MMP), *At2-MMP*, which is expressed throughout the plant. The mutant *at2-mmp-1* displays a delayed flowering and early senescence phenotype (Golldack et al., 2002). Also, the ATP-dependent zinc metalloprotease, *FTSH2*, is also known as *VARIEGATED 2* (*VAR2*) as its mutant has a unique variegated phenotype of leaves that develop white and yellow spots (Rodermel, 2002). Since there are also several other *NTLs* that are involved in flowering and stress response, the inhibition of their cleavage by blocking the metalloproteases would lead to drastic downstream effects. But each NTL has a unique function and in the case of NAC062 this is mediated partly by regulating CK biosynthesis and response.

CHAPTER 5

Materials and Methods

5.1 Preparing Yeast Competent Cells (Ym4271/Yα1867)

A primary culture was set up by inoculating one yeast colony in 20 mL YAPD media. The culture was incubated overnight at 30°C, until the OD reaches above 2. This primary culture was used to inoculate 200 mL of YAPD, such that the secondary culture has a 0.2 OD (approximately 1:10 dilution). The secondary culture was incubated with shaking at 200 rpm at 30°C for 4-5 h (OD 0.6-1). Cells were pelleted by spinning at 3500 rpm for 15 mins at room temperature. The supernatant was discarded, and the pellet was resuspended in 100 mL of distilled water. The cells were pelleted again at 3500 rpm for 15 mins at room temperature. The supernatant was discarded, and cells were dissolved in SORB. The volume of SORB should be $1/10^{th}$ of the original culture (approximately 22 mL). Finally, the cells were spun down again at 3500 rpm for 15 mins at room temperature. The pelleted cells were dissolved in 1440 µL SORB and 160 µL salmon sperm DNA. Resuspended cells were distributed as 25-50 µL aliquots and stored in -80°C.

5.2 Yeast Transformations (Ym4271/Yα1867)

The aliquots of 20-25 µL yeast competent cells were thawed on ice and 400-500 ng of a plasmid is added to the cells. To these cells 6 times the volume of 40% PEG (150-200 µL) was added and mixed well. This mixture was incubated at 30°C for 30 mins. The heat shock of the cells was performed by incubating the mixture at 42°C for 30 mins. The mixture is then transferred onto ice for 10 mins and then centrifuged at 3500 rpm for 15 mins. The supernatant is discarded, and the pelleted cells are dissolved in 100 µL sterile dH_2O. The cells are plated on selective yeast minimal media plates (-Histidine for baits/ -Tryptophan for preys) and grown for 2-3 days at 30°C.

5.3 Yeast Colony PCR

A single yeast colony is dissolved in 20 µL 0.02N NaOH. To this glass beads are added till the entire solution is covered and incubated at 100°C for 5 mins with 1400 rpm shaking. The mixture is then cooled on ice and 20 µL ddH_2O is added to it. The cells are vortexed shortly and spun at 14000 rpm for 15mins. The supernatant is taken out (approx. 20 µL) and shifted to a fresh MCT. 1-2 µL of the supernatant was used as a template for a total 25 µL colony PCR.

5.4 Yeast Shuttle Prep

A primary culture was inoculated and 1.5 mL of this culture was spun at 5000 rpm for 5 mins. The pellet is dissolved in 400 µL lysis buffer and 400 µL Phenol:Chloroform:Isoamyl alcohol (PCI) is added to it. This was topped up with glass beads till the lower meniscus of the aqueous solution. The cells are lysed by shaking in a thermomixer at 1400 rpm for 2 mins. To this 400 µL ddH_2O was added and vortexed well for at least 2 mins. This mixture was spun for 15 mins at 14 Krpm in 4°C. The upper aqueous layer was shifted to a fresh MCT and 400 µL Chloroform:Isoamyl alcohol (CI) was added to it. This is mixed well by inverting and spun for 15 mins at 14 Krpm in 4°C. The upper aqueous layer was shifted to a fresh MCT and equal volumes Isopropanol was added to it. This was spun for 15 mins at 14 Krpm in 4°C. The supernatant was discarded without disturbing the pellet. To this 400 µL of 70% Ethanol was added and spun for 15 mins at 14 Krpm in room temperature. The pellet was dried at 37°C and dissolved in 20 µL ddH_2O.

5.5 Cloning of Baits for Yeast-one-Hybrid

The cytokinin biosynthesis, signaling and degradation genes that are expressed in the shoot were selected by analyzing transcriptomic data (Yadav et al. 2014). Primers containing attB4/attB1r tails were designed to amplify the 3kb promoter region of respective genes using the DNA isolated from WT *Ler* ecotype plants. Gateway cloning was used to insert the PCR products containing attB4/attB1r sites into the compatible P4P1r vector. For BP clonase reaction, composition of the reaction mixture is as described below:

Composition of BP clonase reaction

Component	Amount
PCR product	100 ng
P4P1r vector	100 ng
BP clonase	0.3 µL
TE pH8.0	To final volume 3 µL

The reaction was incubated at 25°C for 2 h or overnight. This was subsequently transformed into 50 µL ultracompetent DH5α cells and plated fully onto LB agar plates containing Ampicillin. The colonies were screened using PCR with an internal forward primer of the respective promoter and M13R primer. The entry clones were confirmed by plasmid PCR, restriction digestion and sequencing.

The promoters were successfully cloned in the entry clones containing attL4/attR1 sites. They were subcloned by LR reaction into the destination vector pMW2 containing attR4/attL1 sites. Since both entry and destination vectors have the same resistance (AmpR), the entry clones were linearized with a unique restriction endonuclease cutting in the vector backbone to avoid false-positive colonies. The reaction mixture for LR cloning was as shown in the table below.

Composition of the LR clonase reaction

Component	Amount
Linearized entry	100 ng
pMW2 vector	100 ng
LR clonase	0.3 µL
TE pH8.0	To final volume 3 µL

The reaction was incubated at 25°C for 2 hours, subsequently transformed into 50µL ultracompetent DH5α cells and plated fully onto LB agar Ampicillin plates.

This will place the respective promoter upstream of the HIS3 gene in the recombined pMW2 vector. The resulting promoter *HIS3* gene fusions were confirmed by PCR with a promoter-specific internal forward primer and a HIS3-specific reverse primer (Deplancke et al., 2006a). They were further verified by restriction digestion and sequencing.

These pMW2 bait clones contacting *promoter::HIS3* cassette were linearized with a suitable restriction enzyme to facilitate recombination in Yeast strain Ym427. The restriction enzyme was selected such that it does not cut within the particular promoter. A suitable choice can be made from the following restriction enzymes, AflII, BseR1, NsiI, and XhoI. The reaction mixture for the same is as given below:

Composition of the pMW2 linearization reaction

Component	Amount
Promoter – pMW2 vector	3-4 µg
10X restriction Buffer	2.5 µL
Bovine serum albumin (10 mg/mL)	0.25 µL

Restriction Enzyme select one (AflII, BseR1, NsiI, and XhoI)	1 µL
ddH_20	To final volume 25 µL

The linearized vectors were transformed into 100 µL Ym4271 strain of yeast. Transformants were selected on yeast minimal media lacking histidine. Integration of bait DNA within the yeast genome was confirmed by PCR (Deplancke et al., 2006a). Check auto-activation of baits by mating with empty prey vector and selecting on selective media containing 3-amino-1,2,4-triazole (3-AT). The auto-activation level of each bait can vary vastly, as they can grow on 1mM to 50mM 3AT.

5.6 High-throughput Yeast-one-Hybrid Assay

The shoot-specific prey library was compiled by shortlisting transcription factors that had a significant expression in the shoot apical meristem (Yadav et al. 2009). Preys were spotted in 96 format using Singer robot. There were four prey plates with 85-90 preys each. These were further combined in 384 format such that one spot is a unique transcription factor. These were then converted into 1536 format such that each transcription factor prey was spotted in 4 replicates. The prey library was maintained on -Trp selective plates and grown at 30°C for 2 days.

The baits were first grown in liquid -His media at 30°C for 2 days. About 2-3 mL of the culture is flooded onto levelled -His plates and, the excess liquid was removed carefully. For even growth allow the plates to dry completely without disturbance and, leave at 30°C for 2 days.

Next, for the mating of baits and preys, prepare levelled YAPD and -His-Trp plates. Make sure that there is no moisture on the plates. Mating is carried out in 1536 format with the Singer Robot. Pinning requires multiple spotting with no mixing, to get sufficient cells without

intermingling of spots. First, spot bait (lawn) and preys (1536 format) on YAPD plates and grow at 30°C for 1 day. Next, spot the mated yeast in the same 1536 format onto selective -His-Trp plates and grow at 30°C for 2 days.

Prepare -His-Trp plates with increasing concentrations of 3AT based on the previously determined auto-activation levels. Spot the selected diploid yeast in 1536 format on the -His-Trp plus 3AT plates. Grow for 7 days on 30°C and keep the plates fully covered to prevent drying. Take pictures of the plates after 7 days and grow for another 3 days. Take again image of the plates on the 10^{th} day and compare it with image taken on 7^{th} day. In few instances where interactions are weak they may take longer time to appear on 10^{th} day.

5.7 Network analysis

The protein DNA interactions (PDIs) were counted as positive if they showed consistently interaction in 3 independent replicates. The interaction network was constructed by using the Cytoscape software. The binding site analysis for interacting transcription factors in the target gene promoters was performed by Finding Individual Motif Occurrence (FIMO) using the MEME suite as described in Bhatia et al. (2021). The presence of visible binding peaks on the target promoters was confirmed by analysing the Plant Cistrome database available courtesy of SALK (O'Malley et al., 2016).

5.8 Plant material and growth conditions

Arabidopsis thaliana ecotypes Columbia-0 (Col-0) and Landsberg *erecta* (L*er*) were used as the Wild Type strain and were obtained from Arabidopsis Biological Resource Center (ABRC, Ohio University, USA). All T-DNA insertion lines were also obtained from ABRC. Seeds were stratified for 3-4 days at 4°C on Murashige and Skoog (MS) medium (1/2 MS base, Sigma; 0.8% w/v Bacto agar, Himedia; 1% w/v Sucrose; 0.1% w/v MES, Sigma) or soil (3

parts Solerite, KELTECH Energies Ltd. India; 1-part Perlite; 1-part Compost). Plants were grown at 22°C under long-day conditions (16 h of light and 8 h of dark) in the growth chambers (Conviron PGC Flex, Canada) under Philips fluorescent tube lights (120µmol $m^{-2}s^{-1}$). For cold treatment, all plant lines were first grown at 22°C for 25 days (till the first flower opens). For treatment, one batch was shifted to 4°C for 24 h with lights at 75µmol $m^{-2}s^{-1}$. The other was kept at 22°C with lights also at 75µmol $m^{-2}s^{-1}$.

5.9 Seed sterilization

The solution for seed surface sterilisation of seed was prepared with 70% ethanol and 0.03% Triton X-100. Seeds were washed with this solution for 1min, followed by at least 3 washings with sterile ddH_20. Seeds were then directly transferred to the MS media plates and kept for stratification for 4 days.

5.10 Cloning

For eY1H assay, a 3kb promoter fragment including the 5' untranslated region above the start codon was amplified for 35 genes using WT L*er* genomic DNA as a template. To increase the chances of amplification from genomic DNA, slowdown PCR technique was adopted. Primers containing the B4-B1r recombination sites were designed to clone the amplicon in a gateway compatible entry vector. Gateway BP clonase reaction was set up to insert 3kb promoter into P4P1r vector. Next, gateway LR clonase reaction was set up with the confirmed entry clones to transfer the promoter fragment into pMW2 vector. This way the promoter fragment was inserted in front of the *HIS3* reporter gene in pMW2 vector.

The pGreen::H2B-YFP vector was modified by replacing the attL1-ccdB-attL2 cassette with attL1-ccdB-attR4 gateway cassette from pMW2 vector. For this, PCR amplification was used to amplify attL1-ccdB-attR4 cassette. To facilitate the sub cloning of attL1-ccdB-attR4

cassette into pGreen::H2B-YFP vector, *Xho*I and *Spe*I sites were introduced in the overhang region of the forward and reverse primer, respectively. The amplified product was used as insert after digestion. pGreen0229 vector containing attL1-ccdB-attL2::*H2BYFP* was digested with *Xho*I and *Spe*I without disrupting the *H2B-YFP* to make the vector backbone. Further, both insert and vector were ligated to obtain pGreen0229 attL1-ccdB-attR4::*H2BYFP* vector. Gateway LR clonase reaction was setup to shuffle the 3kb promoter from P4P1r entry vector into pGreen 0229 attL1-ccdB-attR4::*H2BYFP* destination vector to make reporter constructs. This binary vector has ampicillin resistance in *E.coli*, while BASTA selection was used to raise T1 transgenic plants.

For *35S::NAC062*Δ*C* construct, *NAC062*Δ*C* (1-329aa) was amplified from WT-L*er* cDNA library and cloned into pENTR/D/TOPO. Gateway LR clonase reaction was performed with the binary destination vector pMDC32. The transient vector system was constructed by cloning gateway cassette, attR1-ccdB-attR2 from the pMDC32 vector by digestion with *Asc*I and *Afl*II, into compatible sites resulting in pCAMBIA2300 R1-R2 vector. The multimerized 3X Lac operator (3XOP) was amplified with primers consisting of *Kpn*I and *Asc*I overhangs. The pCAMBIA2300 R1-R2 binary vector and 3XOP PCR product were sequentially digested with *Asc*I and *Kpn*I, and were ligated to create 3XOP::attR1-ccdB-attR2 pCAMBIA2300. Gateway LR clonase reaction was set up between the 3XOP-pCAMBIA gateway destination vector and the *NAC062*Δ*C* pENTR/D/TOPO vector to create *3XOP::NAC062*Δ*C*-pCAMBIA vector.

A flexible GSA linker (Robinson & Sauer, 1998) including the *Spe*I site was added in the 5' overhang of forward primer, which was used to amplify the entire genomic fragment of *NAC062* from WT Col-0 genomic DNA. The forward primer used to clone this entire *Spe*I-linker-gNAC062 fragment also contains a CACC overhang at extreme 5' end in order to clone into a pENTR/D/TOPO vector. The eGFP CDS was amplified from an eGFP-pENTRY vector such that forward primer contained *Spe*I site and reverse primer contained *Not*I, *Nco*I and *Xma*I

restriction sites. The *Spe*I:linker:gNAC062-pENTRY vector and eGFP PCR product were digested with *Spe*I and *Not*I-HF. These fragments were ligated to obtain an N-terminal eGFP fusion construct (eGFP:linker:gNAC062) in the pENTRY vector backbone. The *NAC062* upstream 3kb promoter was amplified using primers containing *Nco*I and *Xma*I in the overhangs. The 3kb promoter PCR product was inserted into the pENTRY fusion vector with the help of the *Nco*I and *Xma*I sites. The entire translation fusion of *NAC062* (pNAC062::eGFP:linker:gNAC062) was shuffled into a pCAMBIA2300 vector containing compatible attR1-attR2 cassette with the help of LR Clonase.

5.11 Transgenic lines and genotyping

Four-week-old plants were transformed with floral dip method using respective vector constructs (Clough & Bent, 1998). Multiple T1 lines were selected for each construct. For phenotypic analysis and imaging purposes, two representative lines were followed till T3 generation until the transgene became homozygous. Genetic crosses with respective reporter lines were obtained successfully after confirming the expression of reporter. They were made homozygous for both reporter gene and T-DNA insertion by following the progeny till F3 generation.

BASTA selection was performed directly on soil by diluting the Finale solution 1:1000 (Bayer Crop Sciences, Germany). T1 seedlings were selected at 10 DAG by spraying 1:1000 diluted Finale solution. The surviving plants were transferred in fresh pots one week after selection. The pMDC32 vector lines were selected on ½ MS media containing 50µg/mL hygromycin (Sigma). The pCAMBIA2300 vector lines were selected on ½ MS media containing 50µg/mL kanamycin (Sigma). The T-DNA insertion mutant lines were genotyped using the respective border- and gene-specific primers (Supplementary Table S6). The mutant lines were crossed either with promoter::H2B-YFP or TCSn::GFP reporter lines, subsequently, selected by

genotyping and BASTA-resistance in following generations. The *35S::NAC062ΔC* P7 line was crossed with individual lines of *pLOG4::H2BYFP* and *pAHK4::H2BYFP*. The transgenic lines *35S::NAC062ΔC; pLOG4::H2BYFP* and *35S::NAC062ΔC; pAHK4::H2BYFP* were selected with hygromycin and BASTA to obtain homozygote plants.

The *35S::LhG4-GR* driver line was crossed with *TCSn::GFP* and selected with hygromycin and BASTA. The homozygous *35S::LhG4-GR; TCSn::GFP* was crossed with multiple T1 plants of *3XOP::NAC062ΔC*. The *35S::LHG4-GR; TCSn::GFP; 3XOP::NAC062ΔC* plants were made homozygote for all transgenes by selecting with hygromycin, BASTA and kanamycin.

5.12 Dexamethasone treatment of SAM

The inflorescence meristem of 25-day old plants was treated with 10 μM Dex solution containing 0.015% SilwetL-77 and mock solution (DMSO, 0.015% SilwetL-77). The shoots were treated every alternate day for a week. Shoots for each time point were imaged using the Leica M205C stereomicroscope. The same shoots were dissected and imaged using a confocal microscope.

5.13 RT-qPCR for Expression analysis

The shoot of 5-day old seedlings of mutant and WT were collected and processed separately for RNA extraction with ReliaPrep RNA tissue miniprep kit (Promega, USA). For RT-qPCR analysis in the SAM, mature shoots of 25-day old plants were dissected. The cDNA of each sample was synthesized from 3 μg total RNA with the iScript cDNA synthesis kit (BioRad, USA). Each RT-qPCR experiment contained 3 technical replicates for each gene and was performed using BioRad CFX6 machine (BioRad, USA). Expression of the *UBQ10* gene was used as standard. Primer efficiency corrected ratio was calculated using standard curves for

each primer pair. Each genotype was compared with WT across 3 biological replicates and the relative expression ratio was calculated using the Pfaffl method (Pfaffl, 2001). The statistical analysis was performed by using the two-tailed *t*-test.

5.14 Confocal Laser Scanning Microscopy

Mature shoots were dissected to expose the SAM using a stereomicroscope and placed in 2% agar. Dissected shoot apices were stained with 10 µg/mL Propidium Iodide (PI) (Invitrogen). PI allows visualization of cell outline in the stained tissue upon excitation with appropriate laser in confocal microscopy. The SAMs were scanned using an upright confocal microscope with a 63X long-distance water dipping lens (Leica SP8, Germany). Images of 1024x1024 pixels were taken using a step size of 0.7 µm. The emission and excitation spectra were collected according to the tagged fluorescence reporter. H2B-YFP was excited at 488 nm wavelength with argon laser lines at 5-10% laser power, and the emission spectra were collected using a HyD detector adjusted to 524–540 nm bandwidth. GFP was excited at 488 nm, and emission spectra were collected at 500–530 nm. PI was excited using a 561 nm laser line, and emission spectra were filtered with a 600-650 nm adjustable bandpass filter.

5.15 Fluorescence intensity and meristem size measurement

The raw images were loaded onto ImageJ and the z-stack was created for the relevant channel. The region of interest (ROI) in the centre of the shoot was defined and kept constant. The mean grey value was determined for each SAM and the area of ROI was constant for all samples. The mean grey value for each SAM was normalised against the background fluorescence. The shoot size measurement was performed by analysing the PI-stained SAM in ImageJ. The centre of the shoot was determined, and the mean diameter was calculated using the methodology defined by Landrein et al., 2015.

5.16 NAC062 CRISPR design

The CRISPR target sequence was determined using the CHOPCHOP web tool. The target sequence binding was determined in SeqViewer on TAIR website. The off targets were determined with the help of the Cas-OFFinder tool. A BLAST was also performed by varying the PAM sequence (NGG) to check for the off targets. A single gDNA for NAC062 gene was synthesized using a forward primer (5' ATTGAATCCGTTACTATCTCCGT 3') and reverse primer (5' AAACACGGAGATAGTAACGGATT '3). The primers are annealed in an annealing mixture, whose composition is as shown in the table below.

Composition of the annealing mixture

Component	Amount
Forward Primer	1 µL
Reverse Primer	1 µL
10X annealing buffer	5 µL
ddH_20	To final volume 50 µL

The primers were oligomerised by heating the annealing mixture to 95°C and cooling down to 25°C. This annealed oligo mixture was taken further for digestion and ligation in pHEE401E vector. The reaction mixture for the same is as given below:

Composition for the digestion and ligation in pHEE401E

Component	Amount
Oligo/PCR product	1 µL
pHEE401E	200 ng

Ligation buffer	1.5 µL
100X BSA	0.15 µL
BsaI enzyme	1 µL
T4 DNA Ligase	1 µL
ddH_20	To final volume 15 µL

This mixture was kept at 37°C for 3 h and cooled down to 10°C. From this mixture about 5-10 µL was transformed into 50 µL DH5α ultracompetent cells. The insertion of the oligo in the pHEE401E vector was determined by colony PCR and digestions. The WT plants were transformed with NAC062 CRISPR-pHEE401E binary vector using agrobacterium mediated transfection. The T1 generation seeds were selected on MS agar plates containing Hygromycin.

5.17 Primers used in the study

Table 5.1 Primers for promoter cloning

PRIMER NAME	PRIMER SEQUENCE
attB4 SP/ipt2_AT2G27760 /1-3000	GGGGACAACTTTGTATAGAAAAGTTGCTACAGAAGAAAT GGCTCGGTGAAGAA
attB1r ASP /ipt2_AT2G27760/1-3000	GGGGACTGCTTTTTTGTACAAACTTGCCGCCTTCGTCTCT CTCTCTCTCTCT
SP/ipt2_AT2G27760 /2501-3000	CAAACCTGAGTCTCTCTTC

attB4 SP/ipt3_AT3G63110 /1-3000	GGGGACAACTTTGTATAGAAAAGTTGCTGATGGAATGCA CTCCTAATCATAAA
attB1r ASP /ipt3_AT3G63110/1-3000	GGGGACTGCTTTTTTGTACAAACTTGCGATGAAACGCTTT GCAATATAAACTTG
SP/ipt3_AT3G63110 /2501-3000	ATCTATTAAAAACAAATATACT
attB4 SP/ipt6_AT1G25410 /1-3000	GGGGACAACTTTGTATAGAAAAGTTGCTGTTTTTTCTGCA TAGATTTTGTAAA
attB1r ASP /ipt6_AT1G25410/1-3000	GGGGACTGCTTTTTTGTACAAACTTGCTTTCTTTAACAGC TTTCTCTTTAAC
SP/ipt6_AT1G25410 /2501-3000	TCTGAAACTTATACACATTTGT
attB4 SP/ipt7_AT3G23630 /1-3000	GGGGACAACTTTGTATAGAAAAGTTGCTTTTATTTCTGTG AAAAAAGTTTGTGTGTT
attB1r ASP /ipt7_AT3G23630/1-3000	GGGGACTGCTTTTTTGTACAAACTTGCGATGATTGACTTT TTTTGTTGGGACAA
SP/ipt7_AT3G23630 /2501-3000	GAAGTTAGTTAAAAAAATTAGAA

attB4 SP/ipt9_AT5G20040 /1-3000	GGGGACAACTTTGTATAGAAAAGTTGCTTCAACCGATCG GTGTGTGTTGAAAA
attB1r ASP /ipt9_AT5G20040/1-3000	GGGGACTGCTTTTTTGTACAAACTTGCTATAAACGGATA ACGAAGCTTTGAA
SP/ipt9_AT5G20040 /2501-3000	GTTATACGGCTTAATAGAGTC
attB4 SP /log1_AT2G28305/1-3000	GGGGACAACTTTGTATAGAAAAGTTGCTGACTTGATGAC ACTTTGATTTCGCT
attB1r ASP /log1_AT2G28305/1-3000	GGGGACTGCTTTTTTGTACAAACTTGCCTTTCTCTTCACA CAAAGTTTTGTT
SP/log1_AT2G28305 /2501-3000	TATCACAATTTAAATTTT
attB4 SP /log2_AT2G35990/1-3000	GGGGACAACTTTGTATAGAAAAGTTGCTTTCCAAGGCCA AAACCTTGTTATTT
attB1r ASP /log2_AT2G35990/1-3000	GGGGACTGCTTTTTTGTACAAACTTGCTATCTCTCTCTCT TTCTGTCTTTTT
SP/log2_AT2G35990 /2401-3000	ATATTTGCTGTTATAATA

attB4 SP /log3_AT2G37210/1-3000	GGGGACAACTTTGTATAGAAAAGTTGCTTAAACAATTTTTTAAAAAAGTTGAAGGTG
attB1r ASP /log3_AT2G37210/1-3000	GGGGACTGCTTTTTTGTACAAACTTGCGTGATTCTAAATTTTGGGCGGAAAG
SP/log3_AT2G37210 /2501-3000	AAATTTCTTTTTTCCCCC
attB4 SP /log4_AT3G53450/1-3000	GGGGACAACTTTGTATAGAAAAGTTGCTTTGGGGCCCTTGTTAGTACTACAGC
attB1r ASP /log4_AT3G53450/1-3000	GGGGACTGCTTTTTTGTACAAACTTGCTGGTTACGATGAGAGCTCAAGCTAT
SP/log4_AT3G53450 /2501-3000	ATAGAAAGTTATAGAAAT
attB4 SP /LOG5_AT4G35190/ 1-3000	GGGGACAACTTTGTATAGAAAAGTTGCTAGATATACTTTAACATTTTTGTTGT
SP/LOG5_AT4G351 90/2501-3000	AGGTCTTATGACATCATCAC
attB1r ASP /LOG5_AT4G35190/ 1-3000	GGGGACTGCTTTTTTGTACAAACTTGCTTTCTTAGCCAAATCAGTTTACTTT

attB4 SP /log6_AT5G03270/1-3000	GGGGACAACTTTGTATAGAAAAGTTGCTAACCGTTCCGGTACTGTTTAAGCCC
attB1r ASP /log6_AT5G03270/1-3000	GGGGACTGCTTTTTTGTACAAACTTGCTGTTTCGGCTAACTTGTCAAAGTCG
SP/log6_AT5G03270 /2401-3000	TGCGGAAATTTAGTATAAA
attB4 SP /LOG7_AT5G11950/ 1-3000	GGGGACAACTTTGTATAGAAAAGTTGCTAAAAAAAAATCTATGATATGAGTTT
attB1r ASP /LOG7_AT5G11950/ 1-3000	GGGGACTGCTTTTTTGTACAAACTTGCATTTCTCTCTCTTTCTCTTTGTTAC
SP/LOG7_AT5G119 50/2501-2950	ATTAGAAGATCATATTAT
attB4 SP /LOG8_AT5G11950/ 1-3000	GGGGACAACTTTGTATAGAAAAGTTGCTTCCGAGTCCAAAGCCTTCTATGCTT
attB1r ASP /LOG8_AT5G11950/ 1-3000	GGGGACTGCTTTTTTGTACAAACTTGCTAATGGATAAAAATCTACAAATCAAGG
SP/LOG8_AT5G119 50/2501-3000	GGTTGAGTATGTGATGAAAA

attB4 SP /ARR1_AT3G16857/ 1-3000	GGGGACAACTTTGTATAGAAAAGTTGCTAAACAGATACT TCCAATGCAAAATA
attB1r ASP /ARR1_AT3G16857/ 1-3000	GGGGACTGCTTTTTTGTACAAACTTGCACCTCTCTCTATG TAGCTCGAACCC
SP/ARR1_AT3G168 57/2501-3000	CTTGTAAGAAATTGAGAATAAA
attB4 SP /ARR2_AT4G16110/ 1-3000	GGGGACAACTTTGTATAGAAAAGTTGCTATGAAAGAAAG GTCGAAACCCGTAA
attB1r ASP /ARR2_AT4G16110/ 1-3000	GGGGACTGCTTTTTTGTACAAACTTGCCTCTCTCGTCCAG AAAACGAACGAT
SP/ARR2_AT4G161 10/2501-3000	TTTGGTAATTTAGCATTTAG
attB4 SP /ARR4_AT1G10470/ 1-3000	GGGGACAACTTTGTATAGAAAAGTTGCTATAAAAAAATA GGCTTGAATCGCAG
attB1r ASP /ARR4_AT1G10470/ 1-3000	GGGGACTGCTTTTTTGTACAAACTTGCAGACGAGCTTAT AGTAACTGTGAGGA
SP/ARR4_AT1G104 70/2501-3000	GTAATGACGAGATTTTGACT

attB4 SP /ARR5_AT3G48100/ 1-3000	GGGGACAACTTTGTATAGAAAAGTTGCTAAACAAAAGA GAAGGCAGAAAGAAT
attB1r ASP /ARR5_AT3G48100/ 1-3000	GGGGACTGCTTTTTTGTACAAACTTGCATCAAGAAGAGT AGGATCGTGACTC
SP/ARR5_AT3G481 00/2501-3000	ATCAAGAAAGTATCGAAAAT
attB4 SP/ARR7/1- 3000	GGGGACAACTTTGTATAGAAAAGTTGCTTCAGATAGATT AAAACCAGTTATTT
attB1r ASP/ARR7/1- 3000	GGGGACTGCTTTTTTGTACAAACTTGCTGTCAAACTCAGA ATAAAAAAGAGA
SP/ARR7/2501-3000	AAATGCAAAGTAGTAGCC
attB4 SP /ARR9_AT3G57040/ 1-3000	GGGGACAACTTTGTATAGAAAAGTTGCTGAAAGAGAGA GGAGGGGCCATATTG
attB1r ASP /ARR9_AT3G57040/ 1-3000	GGGGACTGCTTTTTTGTACAAACTTGCTGCAGAAACTTG AAGATAACAAATA
SP/ARR9_AT3G570 40/2501-3000	TCAAGCGGCTGTGGTAGT
attB4 SP/ ARR10_AT4G31920 /1-3000	GGGGACAACTTTGTATAGAAAAGTTGCTGATAGGATTGA GCTCATTCAATGGT

attB1r ASP/ ARR10_AT4G31920 /1-3000	GGGGACTGCTTTTTTGTACAAACTTGCCGCCGTCAAAGA TTATGAATTGAAG
SP/ARR10_AT4G31 920/2501-3000	ATCTCTAAATTAATTACA
attB4 SP/ ARR12_AT2G25180 /1-3000	GGGGACAACTTTGTATAGAAAAGTTGCTAAAGAAAGAGT TTTGATGCACGCTC
attB1r ASP/ ARR12_AT2G25180 /1-3000	GGGGACTGCTTTTTTGTACAAACTTGCCGTTTTTCAACAG ACCCAGAAACGAA
SP/ARR12_AT2G25 180/2501-3000	ATATTAGTCATTTCGGTTCA
attB4 SP/ ARR13_AT2G27070 /1-3000	GGGGACAACTTTGTATAGAAAAGTTGCTTGGAATTGTTT TTTTAACATCTGCT
attB1r ASP/ ARR13_AT2G27070 /1-3000	GGGGACTGCTTTTTTGTACAAACTTGCTCTAATAATCTTT GTAAAGAGTTTT
SP/ARR13_AT2G27 070/2451-3000	TTTATTTAGAATTTCTAC
attB4 SP/ ARR14_AT2G01760 /1-3000	GGGGACAACTTTGTATAGAAAAGTTGCTCTCCAGAATAA AAACCAAGAGCTAA

attB1r ASP/ ARR14_AT2G01760 /1-3000	GGGGACTGCTTTTTTGTACAAACTTGCTAAGCTTTGGTGT GAGTATTGAAAA
SP/ARR14_AT2G01 760/2501-3000	TACATTTCATCTTCATCTTCA
attB4 SP/ ARR15_AT1G74890 /1-3000	GGGGACAACTTTGTATAGAAAAGTTGCTCTCTGATTCAA TATCTACTGGAGAA
attB1r ASP/ ARR15_AT1G74890 /1-3000	GGGGACTGCTTTTTTGTACAAACTTGCTGTTTTCTCTCGG GAAAGTAAACAA
SP/ARR15_AT1G74 890/2501-3000	AAAGAATGAAAAGAAACCA
attB4 SP/ ARR18_AT5G58080 /1-3000	GGGGACAACTTTGTATAGAAAAGTTGCTACCCACTTCCA CCGGACATAGTTGT
attB1r ASP/ ARR18_AT5G58080 /1-3000	GGGGACTGCTTTTTTGTACAAACTTGCTCCTACAGGAAA CTTGTCATGCCTT
SP/ARR18_AT5G58 080/2501-3000	TATGGAAAATAGGAAATGC
attB4 SP/ ARR20_AT3G62670 /1-3000	GGGGACAACTTTGTATAGAAAAGTTGCTTAATTGATTTG GTTTAGCCAAATAG

attB1r ASP/ ARR20_AT3G62670 /1-3000	GGGGACTGCTTTTTTGTACAAACTTGCGGCCTCTTCTCCG CTCTCATATTTC
SP/ARR20_AT3G62 670/2501-3000	ATCCATATATATGCATACCTAGT
attB4 SP/ ARR21_AT5G07210 /1-3000	GGGGACAACTTTGTATAGAAAAGTTGCTATGTTTTTATTA TACATTTTTTTT
attB1r ASP/ ARR21_AT5G07210 /1-3000	GGGGACTGCTTTTTTGTACAAACTTGCTCTAATAATCTTT GCAAAGAGTTTTT
SP/ARR21_AT5G07 210/2501-3000	ATCCAACAAAGATGTAGATAA
attB4 SP/ CKX3_AT5G56970/ 1-3000	GGGGACAACTTTGTATAGAAAAGTTGCTAAAAAGAAAA ACAATCGAGTGAAGA
attB1r ASP/ CKX3_AT5G56970/ 1-3000	GGGGACTGCTTTTTTGTACAAACTTGCTTTTTTTGAGAAA TAAGTCTTTTTA
SP/CKX3_AT5G569 70/2501-3000	ACAGTTACAACTATTGCTTTT
attB4 SP/CKX5_ AT1G75450/1-3000	GGGGACAACTTTGTATAGAAAAGTTGCTATTTTGTTCTCC TTCGTGCAGACAT
attB1r ASP/CKX5_ AT1G75450/1-3000	GGGGACTGCTTTTTTGTACAAACTTGCCAAAGAATACTC AAGAAACAAGAAT

SP/CKX5_ AT1G75450/2501-3000	TATGCAAGTAGTATAGTT
attB4 SP/ CKX6_AT3G63440/ 1-3000	GGGGACAACTTTGTATAGAAAAGTTGCTACCAAGACCAA CGCTCAAGGAACAG
attB1r ASP/ CKX6_AT3G63440/ 1-3000	GGGGACTGCTTTTTTGTACAAACTTGCAAGGCCTCTTGAT TTCTGAGAGACAA
SP/CKX6_AT3G634 40/2501-3000	ATCCTTTTTGCGCTTCAT
attB4 SP/ AHP2_AT3G29350/ 1-3000	GGGGACAACTTTGTATAGAAAAGTTGCTTTGAGAAGATT TTGACACATAACAG
attB1r ASP/ AHP2_AT3G29350/ 1-3000	GGGGACTGCTTTTTTGTACAAACTTGCGAGAAGAGTGAA GCGGAGATTGGGA
SP/AHP2_AT3G293 50/2451-3000	AATTATAAATTTCGTGAAACC
attB4 SP/ AHP3_AT5G39340/ 1-3000	GGGGACAACTTTGTATAGAAAAGTTGCTTAATAATATTT CCCACACATATTTT
attB1r ASP/ AHP3_AT5G39340/ 1-3000	GGGGACTGCTTTTTTGTACAAACTTGCGGCTCTCTCTACT CGTCGTGAAGGC

SP/AHP3_AT5G393 40/2501-3000	AAATCTGCCACTATAAGTTG
attB4 SP/ AHP5_AT1G03430/ 1-3000	GGGGACAACTTTGTATAGAAAAGTTGCTAGAAACATCAA CCCAGCATTGGTCA
attB1r ASP/ AHP5_AT1G03430/ 1-3000	GGGGACTGCTTTTTTGTACAAACTTGCAGCTAAAGTTTAC CAAGAACCAGAC
SP/AHP5_AT1G034 30/2501-3000	CAATTGGGACTGGACCTTTTT
attB4 SP/ AHP6_AT1G80100/ 1-3000	GGGGACAACTTTGTATAGAAAAGTTGCTTATATACCCAT ATTTCAGTCATTAA
attB1r ASP/ AHP6_AT1G80100/ 1-3000	GGGGACTGCTTTTTTGTACAAACTTGCCCACAACGGCAC ACCCGTCTTGTCC
SP/AHP6_AT1G801 00/2501-3000	AAAGTTGTTGATTTAATTTAAG
attB4 SP/ AHK1_AT2G17820/ 1-3000	GGGGACAACTTTGTATAGAAAAGTTGCTAATTAAAAAGA TATATAGAATTATG
attB1r ASP/ AHK1_AT2G17820/ 1-3000	GGGGACTGCTTTTTTGTACAAACTTGCCTTGTTTCAGATG ATCCCAAATCAT

SP/AHK1_AT2G178 20/2501-3000	AAACCGTACAACTATATTTGT
attB4 SP/ AHK2_AT5G35750/ 1-3000	GGGGACAACTTTGTATAGAAAAGTTGCTCCTTTACATTA ACTACTAAATCTTG
attB1r ASP/ AHK2_AT5G35750/ 1-3000	GGGGACTGCTTTTTTGTACAAACTTGCTTCGACTCCTAAT CTCAGATTCAGCT
SP/AHK2_AT5G357 50/2501-3000	AAAACAATAATAATAATCAAAAG
attB4 SP/ AHK3_AT1G27320/ 1-3000	GGGGACAACTTTGTATAGAAAAGTTGCTCGTGATTCACA ACACAAGAGATGCA
attB1r ASP/ AHK3_AT1G27320/ 1-3000	GGGGACTGCTTTTTTGTACAAACTTGCCCACCACTTGAAT ACACGATCAACC
SP/AHK3_AT1G273 20/2501-3000	TCGTTGCTTTATTCGCTC
attB4 SP/ AHK4_AT2G01830/ 1-3000	GGGGACAACTTTGTATAGAAAAGTTGCTTCCTTTGTGTAC CCCCTTTTCCCCC
attB1r ASP/ AHK4_AT2G01830/ 1-3000	GGGGACTGCTTTTTTGTACAAACTTGCCACTTCAAATGTA GGTATTCCATTT

SP/AHK4_AT2G018 30/2501-3000	GATGCGGTTCGGTGCGGATCTT
attB4 SP/ AHK5_AT5G10720/ 1-3000	GGGGACAACTTTGTATAGAAAAGTTGCTTCCATCTAACC ATCTTAATAAGTTA
attB1r ASP/ AHK5_AT5G10720/ 1-3000	GGGGACTGCTTTTTTGTACAAACTTGCTGATCAAGGTTTC TCTTCATACAAC
SP/AHK5_AT5G107 20/2501-3000	CTGATGTCAAGAATAAATCACC

Table 5.2 Primers for T-DNA confirmation

AGI/GENE NAME	**T-DNA ID**	**PRIMER TYPE**	**PRIMER SEQUENCE**
AT1G49720/ABF1	SALK_ 132819	LP	CCGGTAAGGGTTCTTCTCAAG
		RP	AGAGGCAACAGACTTTAGGGG
AT2G38340/DREB19	SALK_ 144950	LP	TTGGGTGACAATCCACCTTAC
		RP	TTGTCGAACACCTCTAAACCG
AT5G39760/ATHB23	SALK_ 059288	LP	AATCTTTTTGTTTCTTCATCCG
		RP	CTCTCAAATGTGCTGCTTGTG
AT1G69600/ZFHD1	CS877090	LP	AAATGCAGGGGTGATACAGTG
		RP	TTGGATCTTGATCTGACGGTC
AT3G19580/AZF2	SALK_ 132562	LP	TTGTTGCTAACAAGCATGTGC
		RP	GCCAGAATCAAAGAACCTTCC

AT3G49530/NAC062	SALK_ 103823	LP	TCCCATTTGCAAATATCGATC
		RP	AGTATTCAAATTGGGGATGGC
AT3G28920/ATHB34	SALK_ 085482	LP	CTTCTTCACGACGAAGACGAC
		RP	GCAACATTCATCAACCAGAGC
AT5G61590/DEWAX	SALK_ 015182	LP	CAGCTTAGGATTCGAACCATG
		RP	GAAAACGCAGAAGTTCCATTG
AT4G32980/ATH1	CS303729	PH81	ACGTCTAGCTTTATTTCGGTGTG T

Table 5.3 Primers for RT-qPCR

AGI	**Primer name**	**Primer Sequence**
AT2G27760	IPT2-RT-FP/249	CAATATGTTTGCGAGGC
	IPT2-RT-RP/249	CGTTAATGTGTTTTGATGGG
AT3G63110	IPT3-RT-FP/233	GTACTTATTGGTGATGGTGA
	IPT3-RT-RP/233	CCAAATATAGCATTCCACTC
AT5G20040	IPT9-RT-FP/194	GTATCTGCGATGGTTTATG
	IPT9-RT-RP/194	TACGGCGTAGTCTGTACC
AT2G28305	LOG1-RT-FP/167	TCAAGAAACTTGAGGATTATG
	LOG1-RT-RP/167	CCAATTTGGAGAGATCATTC
AT3G53450	LOG4-RT-FP/233	TACATGATAAACCGGTGG
	LOG4-RT-RP/233	TTCAGAAGAGTAGTCAATCC
AT4G35190	LOG5-RT-FP/168	CCAAAAACTTGAGGCATAC
	LOG5-RT-RP/168	CCATAAGACCCTCTAAAAGTC
AT5G11950	LOG7-RT-FP/305	CGACAACTCGAGGAATATG

	LOG7-RT-RP/305	ATACGCGGTTAGCAGTTAC
AT3G16857	ARR1-RT-FP/233	CAAGTCACCTCCAGAAATAC
	ARR1-RT-RP/233	TGACTTAGAGACCATCGC
AT1G10470	ARR4-RT-FP/172	ACCAGAATCGACAGATGC
	ARR4-RT-RP/172	GAGGAAGCGAAGAGTTAA
AT3G48100	ARR5-RT-FP/205	CCTCGTATCGATAGATGTC
	ARR5-RT-RP/205	GTGGAATCTGATAAACTCAG
AT1G19050	ARR7-RT-FP/203	CTCGTATACAAGAATGTCTC
	ARR7-RT-RP/203	GTCCTTGATAGAAGTATCATC
AT3G57040	ARR9-RT-FP/199	CAAGAATCAGCAGATGTTTAG
	ARR9-RT-RP/199	GTTGAATCTTTAATCTCTGGATC
AT4G31920	ARR10-RT-FP/252	CCTTAATGACACAGGAACAG
	ARR10-RT-RP/252	GGATCTTCCTAAGTTGCTC
AT2G25180	ARR12-RT-FP/216	CACGATGAAGCAGGAAC
	ARR12-RT-RP/216	AATGGAGTCCTAAATTGCTAG
AT2G01760	ARR14-RT-FP/225	GGCTAGTCATTTACAGAAGTTC
	ARR14-RT-RP/225	ATCTACCAAGATTGTCATTAGG
AT1G74890	ARR15-RT-FP/286	ACCTCGTATAGAACAATGTATG
	ARR15-RT-RP/286	AATCATTTAACCCCTAGACTC
AT5G58080	ARR18-RT-FP/180	CCAGTCATTTGCAGAAGTAC
	ARR18-RT-RP/180	AACGCGATAAGAGTCCTG
AT1G75450	CKX5-RT-FP/301	GAACAAAGACAAATGGGAC
	CKX5-RT-RP/301	TGACCAGTAGCGAGTATG
AT3G63440	CKX6-RT-FP/206	CAGTGAACAAATCAAAGTGG

	CKX6-RT-RP/206	CGTGTAATGTGGCAGATAC
AT5G35750	AHK2-RT-FP/217	CGATATTAGCAATGACAGCAG
	AHK2-RT-RP/217	ATGTTCAAGATATACTACCCGATG
AT1G27320	AHK3-RT-FP/299	ACTAACGGGTATCTCGGGG
	AHK3-RT-RP/299	GCAACAAGTAACGCAATCAC
AT2G01830	AHK4-RT-FP/208	CCACAGATGGACGGATTTG
	AHK4-RT-RP/208	TGGCAACGGATTTATAGAGATTC
AT5G39340	AHP3-RT-FP/164	TGTGGCTGAGGTTGTTACTC
	AHP3-RT-RP/164	CTTTGACTCTCTTGGCACC
AT1G03430	AHP5-RT-FP/208	CGTGAAGGGTGTCTAAGGTG
	AHP5-RT-RP/208	CTACAGAGGAGTTTCGGTTTC
AT1G80100	AHP6-RT-FP/111	AAAGATTGAAGCGGAAAACGG
	AHP6-RT-RP/111	GTGGAAAAGAGAGGCTAGGAG
AT4G05320	UBQ10-RT-FP/165	TTCTAAATCTCGTCTCTGTTATGC
	UBQ10-RT-RP/165	GAAGAAGTTCGACTTGTCATTAG
AT3G49530	NAC062-RT-FP/108	GCGCAGGGAAATGGTCCAAG
	NAC062-RT-RP/108	AACCGTGTCCTCAGCCTCTC

Table 5.4 Primers for cloning cDNA in pENTRY

PRIMER NAME	**PRIMER SEQUENCE**
SP/ANAC062 CDS/1410	CACCATGAATCAGAATCTTCATGTATTATC
ASP/ANAC062 CDS	TCAGGACACTGCAGATGCTC
ASP/ ANAC062 Nterm	AAACTATGGTGCTACAACATCAAAA

SP/ATHB23 CDS/1005	CACCATGATGGATATGACTCCTACAATAAC
ASP/ATHB23 CDS	TCACGACGACGATGATCCGTTAAC
SP/ATHB34 CDS/939	CACCATGCTTGAAGTTAGATCAATGGATA
ASP/ATHB34 CDS/939	TCACGACGAAGACGACGAG
SP/ZAT6_CDS/1-717	CACCATGGCACTTGAAACTCTTACTT
ASP/ZAT6_CDS/1-717	TTAGGGTTTCTCCGGGAAGTCA
SP/AZF2_CDS/1-822	CACCATGGCCCTCGAAGCGATG
ASP/AZF2_CDS/1-822	TTAGATTTTTAAAGATAAATCTTCTTTCTTGATG
SP/AZF3_CDS/1-582	CACCATGGCGCTTGAAGCTCTTAA
ASP/AZF3_CDS/1-582	TTACTTCAGGCGAGGCTTCTTAGTC
SP/ARR10_CDS /1-1659	CACCATGACTATGGAGCAAGAAATTGAAG
ASP/ARR10_CDS /1-1659	TCAAGCTGACAAAGAAAAGGGAAAA
SP/ARR10_CDS /1160-1659	AGATCAGCAAGCGTCTAG
SP/ARR12_CDS /1-1791	CACCATGACTGTTGAACAAAATTTAGAAGC
ASP/ARR12_CDS /1-1791	TCATATGCATGTTCTGAGTGAACTA
SP/ARR12_CDS /1292-1791	GTTTGGAGCATTGGTCAA
SP/ARR14_CDS /1-1149	CACCATGCCGATCAACGATCAGTTTCCTA
ASP/ARR14_CDS /1-1149	CTATCTTTGTCTTGAAGATCTTTCC

Table 5.5 Primers for making gateway vectors

PRIMER NAME	**PRIMER SEQUENCE**
SP/pMW2/143-2316	CACCCTCGAGCAACTTTGTATAGAAAAGTTGAACG
ASP/pMW2/143-2316	TGGACTAGTAGCCTGCTTTTTTGTACAAAGTTGG

SP/pMW2/HindIII	CACCAAGCTTCAACTTTGTATAGAAAAGTTGAACG
ASP/pMW2/BclI	TGGTGATCAAGCCTGCTTTTTTGTACAAAGTTGG
ASP/pMW2/2101-2489	GGGCTTTCTGCTCTGTC
SP/pMDC32/HindIII	GAGTAAGCTTGGTCAACATGGTGGAGCACGACAC
ASP/pMDC32/SphI	ACCTGCATGCAGTAACATAGATGACACCGCGCGC
Luciferase_RP	TCTGTGATTTGTATTCAGCCCATATCG
SP/6XOPpzp222 MK/KpnI	AAAGGTACCGAATTCGAGCTCAAGAAATC
ASP/6XOPpzp222 MK/ AscI	AAAGGCGCGCCTCTAGAGGATCCCCGGGTA
SP/minLUC/XmaI SpeI	AAACCCGGGACTAGTGCAAGACCCTTCCTCTATATAAG G
ASP/minLUC/PstI	AAACTGCAGGATCTAGTAACATAGATGACACCGCGC
SP/pMW2/KpnI	AAAGGTACCCAACTTTGTATAGAAAAGTTGAACG

Table 5.6 Vector constructs made for this study

Construct name	**Selection marker**
pIPT2-P4P1r	Ampicillin
pIPT3-P4P1r	Ampicillin
pIPT6-P4P1r	Ampicillin
pIPT7-P4P1r	Ampicillin

pIPT9-P4P1r	Ampicillin
pLOG1-P4P1r	Ampicillin
pLOG2-P4P1r	Ampicillin
pLOG3-P4P1r	Ampicillin
pLOG4-P4P1r	Ampicillin
pLOG5-P4P1r	Ampicillin
pLOG6-P4P1r	Ampicillin
pLOG7-P4P1r	Ampicillin
pLOG8-P4P1r	Ampicillin
pARR1-P4P1r	Ampicillin
pARR2-P4P1r	Ampicillin
pARR4-P4P1r	Ampicillin
pARR5-P4P1r	Ampicillin
pARR7-P4P1r	Ampicillin
pARR9-P4P1r	Ampicillin
pARR10-P4P1r	Ampicillin
pARR12-P4P1r	Ampicillin
pARR13-P4P1r	Ampicillin
pARR14-P4P1r	Ampicillin
pARR15-P4P1r	Ampicillin
pARR18-P4P1r	Ampicillin
pARR20-P4P1r	Ampicillin
pARR21-P4P1r	Ampicillin
pCKX3-P4P1r	Ampicillin

pCKX5-P4P1r	Ampicillin
pCKX6-P4P1r	Ampicillin
pAHP2-P4P1r	Ampicillin
pAHP3-P4P1r	Ampicillin
pAHP5-P4P1r	Ampicillin
pAHP6-P4P1r	Ampicillin
pAHK1-P4P1r	Ampicillin
pAHK2-P4P1r	Ampicillin
pAHK3-P4P1r	Ampicillin
pAHK4-P4P1r	Ampicillin
pAHK5-P4P1r	Ampicillin
pIPT2-pMW2	Ampicillin
pIPT3-pMW2	Ampicillin
pIPT6-pMW2	Ampicillin
pIPT7-pMW2	Ampicillin
pIPT9-pMW2	Ampicillin
pLOG1-pMW2	Ampicillin
pLOG2-pMW2	Ampicillin
pLOG3-pMW2	Ampicillin
pLOG4-pMW2	Ampicillin
pLOG5-pMW2	Ampicillin
pLOG6-pMW2	Ampicillin
pLOG7-pMW2	Ampicillin
pLOG8-pMW2	Ampicillin

pARR1-pMW2	Ampicillin
pARR2-pMW2	Ampicillin
pARR4-pMW2	Ampicillin
pARR5-pMW2	Ampicillin
pARR7-pMW2	Ampicillin
pARR9-pMW2	Ampicillin
pARR10-pMW2	Ampicillin
pARR12-pMW2	Ampicillin
pARR13-pMW2	Ampicillin
pARR14-pMW2	Ampicillin
pARR15-pMW2	Ampicillin
pARR18-pMW2	Ampicillin
pARR20-pMW2	Ampicillin
pARR21-pMW2	Ampicillin
pCKX3-pMW2	Ampicillin
pCKX5-pMW2	Ampicillin
pCKX6-pMW2	Ampicillin
pAHP2-pMW2	Ampicillin
pAHP3-pMW2	Ampicillin
pAHP5-pMW2	Ampicillin
pAHP6-pMW2	Ampicillin
pAHK1-pMW2	Ampicillin
pAHK2-pMW2	Ampicillin
pAHK3-pMW2	Ampicillin

pAHK4-pMW2	Ampicillin
pAHK5-pMW2	Ampicillin
pIPT2::H2BYFP-pGreen	Kanamycin
pIPT3::H2BYFP-pGreen	Kanamycin
pIPT6::H2BYFP-pGreen	Kanamycin
pIPT7::H2BYFP-pGreen	Kanamycin
pIPT9::H2BYFP-pGreen	Kanamycin
pLOG1::H2BYFP-pGreen	Kanamycin
pLOG2::H2BYFP-pGreen	Kanamycin
pLOG3::H2BYFP-pGreen	Kanamycin
pLOG4::H2BYFP-pGreen	Kanamycin
pLOG5::H2BYFP-pGreen	Kanamycin
pLOG6::H2BYFP-pGreen	Kanamycin
pLOG7::H2BYFP-pGreen	Kanamycin
pLOG8::H2BYFP-pGreen	Kanamycin
pARR1::H2BYFP-pGreen	Kanamycin
pARR2::H2BYFP-pGreen	Kanamycin
pARR4::H2BYFP-pGreen	Kanamycin
pARR5::H2BYFP-pGreen	Kanamycin
pARR7::H2BYFP-pGreen	Kanamycin
pARR9::H2BYFP-pGreen	Kanamycin
pARR10::H2BYFP-pGreen	Kanamycin
pARR12::H2BYFP-pGreen	Kanamycin
pARR13::H2BYFP-pGreen	Kanamycin

pARR14::H2BYFP-pGreen	Kanamycin
pARR15::H2BYFP-pGreen	Kanamycin
pARR18::H2BYFP-pGreen	Kanamycin
pARR20::H2BYFP-pGreen	Kanamycin
pARR21::H2BYFP-pGreen	Kanamycin
pCKX3::H2BYFP-pGreen	Kanamycin
pCKX5::H2BYFP-pGreen	Kanamycin
pCKX6::H2BYFP-pGreen	Kanamycin
pAHP2::H2BYFP-pGreen	Kanamycin
pAHP3::H2BYFP-pGreen	Kanamycin
pAHP5::H2BYFP-pGreen	Kanamycin
pAHP6::H2BYFP-pGreen	Kanamycin
pAHK1::H2BYFP-pGreen	Kanamycin
pAHK2::H2BYFP-pGreen	Kanamycin
pAHK3::H2BYFP-pGreen	Kanamycin
pAHK4-::H2BYFP-pGreen	Kanamycin
pAHK5::H2BYFP-pGreen	Kanamycin
ARR1-pENTRY	Kanamycin
ARR12-pENTRY	Kanamycin
ARR10-pENTRY	Kanamycin
ARR14-pENTRY	Kanamycin
ARR12-pDEST-AD-2μ	Kanamycin
ARR10-pDEST-AD-2μ	Kanamycin
ARR14-pDEST-AD-2μ	Kanamycin

LOG1-pENTRY	Kanamycin
LOG3-pENTRY	Kanamycin
LOG4-pENTRY	Kanamycin
LOG5-pENTRY	Kanamycin
LOG7-pENTRY	Kanamycin
LOG8-pENTRY	Kanamycin
ARR4-pENTRY	Kanamycin
ARR4-pMDC32	Kanamycin
AZF2-pENTRY	Kanamycin
AZF3-pENTRY	Kanamycin
ZAT6-pENTRY	Kanamycin
AZF2-pMDC32	Kanamycin
AZF3-pMDC32	Kanamycin
ZAT6-pMDC32	Kanamycin
attL1-attR4::H2BYFP-pGreen	Kanamycin
LOG1-pMDC32	Kanamycin
ATHB23-pENTRY	Kanamycin
ATHB34-pENTRY	Kanamycin
ATHB23-pMDC32	Kanamycin
ATHB34-pMDC32	Kanamycin
3XOP::attR1-attR2-pCAMBIA2300	Kanamycin
attL1-attR4::LUC-pUC19	Ampicillin
35S::attR1-attR2-pUC19	Ampicillin
NAC062-pENTRY	Kanamycin

NAC062ΔC-pENTRY	Kanamycin
35S::H2BYFP-pUC19	Ampicillin
35S::eGFP-pUC19	Ampicillin
35S::AZF2-pUC19	Ampicillin
35S::AZF3-pUC19	Ampicillin
NAC062-pMDC32	Kanamycin
NAC062ΔC-pMDC32	Kanamycin
3XOP::NAC062-pCAMBIA2300	Kanamycin
3XOP::NAC062ΔC-pCAMBIA2300	Kanamycin
attR1-attR2-pCAMBIA2300	Kanamycin
35S::WUS-pUC19	Ampicillin
pTAR2::LUC-pUC19	Ampicillin
3XOP::eGFP-pCAMBIA2300	Kanamycin
SpeI:linker:gNAC062-pENTRY	Kanamycin
eGFP:linker:gNAC062-pENTRY	Kanamycin
pNAC062:eGFP:linker:gNAC062-pENTRY	Kanamycin
mCherry:linker:gNAC062-pENTRY	Kanamycin
pNAC062:mCherry:linker:gNAC062-pENTRY	Kanamycin
pIPT3::LUC-pUC19	Ampicillin
pLOG4::LUC-pUC19	Ampicillin
pAHK4::LUC-pUC19	Ampicillin
35S::NAC062-pUC19	Ampicillin
35S::NAC062ΔC-pUC19	Ampicillin
NAC062 CRISPR-pHEE401E	Kanamycin

pNAC062:eGFP:linker:gNAC062-pCAMBIA2300	Kanamycin
pNAC062:mCherry:linker:gNAC062-pCAMBIA2300	Kanamycin

Table 5.7 Transgenic lines made in this study

Transgenic lines	Selected & positive T1 lines	Selection marker
35S::NAC062		Hygromycin
35S::NAC062ΔC		Hygromycin
35S::ZAT6		Hygromycin
35S::ATHB23		Hygromycin
35S::ATHB34		Hygromycin
35S::AZF2		Hygromycin
35S:AZF3		Hygromycin
pARR1::H2BYFP	10	BASTA
pAHP6::H2BYFP	10	BASTA
pLOG4::H2BYFP	10	BASTA
pARR4::H2BYFP	6	BASTA
pLOG7::H2BYFP	35	BASTA
pAHP5::H2BYFP	36	BASTA
pIPT2::H2BYFP	10	BASTA
pAHK4::H2BYFP	12	BASTA

pARR9::H2BYFP	33	BASTA
pCKX5::H2BYFP	25	BASTA
pARR10::H2BYFP	24	BASTA
pARR5::H2BYFP	31	BASTA
pIPT3::H2BYFP	10	BASTA
pARR7::H2BYFP	7	BASTA
pARR15::H2BYFP	12	BASTA
pAHK2::H2BYFP	24	BASTA
pAHK3::H2BYFP	6	BASTA
pIPT9::H2BYFP	11	BASTA

Table 5.8 Crosses followed for this study

Transgenic lines/Crosses	Selection marker
35S::NAC062	Hygromycin
35S::NAC062ΔC	Hygromycin
35S::ZAT6	Hygromycin
35S::ATHB23	Hygromycin
35S::ATHB34	Hygromycin
35S::AZF2	Hygromycin
35S:AZF3	Hygromycin
arr4;TCSn::GFP	BASTA
log1;log7	
log3;log4	
log1;log3;log4;log7	

asil1;asil2	
athb29;TCSn::GFP	BASTA
arf9;arf18	
azf2; TCSn::GFP	BASTA
athb23; TCSn::GFP	BASTA
athb34; TCSn::GFP	BASTA
dewax; TCSn::GFP	BASTA
ath1;abf1	
athb23;athb34	
athb23;athb34;TCSn::GFP	BASTA
athb23;pLOG4::H2BYFP	BASTA
dewax;pARR4::H2BYFP	BASTA
abf1;pLOG4::H2BYFP	BASTA
abf1;pARR4::H2BYFP	BASTA
35S::LhG4-GR; 3XOP::NAC062	Hygromycin, Kanamycin
35S::LhG4-GR; 3XOP::NAC062ΔC	Hygromycin, Kanamycin
35S::LhG4-GR; 3XOP::NAC062; TCSn::GFP	Hygromycin, Kanamycin, BASTA
35S::LhG4-GR; 3XOP::NAC062; TCSn::GFP	Hygromycin, Kanamycin, BASTA
nac062-1;pLOG4::H2BYFP	BASTA
nac062-1;pAHK4::H2BYFP	BASTA
nac062-1;pIPT3::H2BYFP	BASTA
35S:NAC062ΔC; pLOG4::H2BYFP	BASTA
35S:NAC062ΔC; pAHK4::H2BYFP	BASTA
35S:NAC062ΔC; pIPT3::H2BYFP	BASTA

Appendix

Table S1 List of baits with autoactivation and interactions

Gene Name	Baits tested prior to eY1H assay for autoactivation,	Interacting with preys
AHK2	High	No
AHK3	Low	Yes
AHK4	Low	Yes
AHK5	Low	Yes
AHP2	Low	Yes
AHP3	Low	Yes
AHP5	Low	Yes
AHP6	Low	Yes
ARR1	Low	Yes
ARR2	High	No
ARR4	Low	Yes
ARR5	Low	Yes
ARR7	Low	Yes
ARR9	Low	Yes
ARR10	Low	Yes
ARR12	Low	No
ARR14	Low	Yes
ARR15	Low	Yes
ARR18	High	No
ARR20	High	No

ARR21	High	No
CKX3	High	No
CKX5	Low	Yes
CKX6	Low	Yes
IPT2	Low	Yes
IPT3	Low	Yes
IPT7	High	No
IPT9	Low	Yes
LOG1	Low	Yes
LOG2	High	No
LOG3	Low	No
LOG4	Low	Yes
LOG5	Low	Yes
LOG6	Low	Yes
LOG7	Low	Yes

Table S2 List of PDIs in network and binding information

BAIT	**PREY**	**Prey AGI**	**FIMO**	**DAP-SEQ**
AHK3	DREB19	AT2G38340	NO	YES, Near ATG
AHK3	ANAC047	AT3G04070	YES	YES, 5'UTR
AHK3	MYB65	AT3G11440	N/A	YES, Near ATG
AHK3	AZF2	AT3G19580	N/A	N/A
AHK3	AL3	AT3G42790	N/A	N/A
AHK3	AT4G01460	AT4G01460	N/A	N/A

AHK3	ZAT6	AT5G04340	YES	N/A
AHK3	AZF3	AT5G43170	N/A	N/A
AHK3	DEWAX	AT5G61590	N/A	N/A
AHK4	HMGBD15	AT1G04880	YES	NO
AHK4	EPR1	AT1G18330	YES	YES, -500 & -2500
AHK4	CRF7	AT1G22985	NO	N/A
AHK4	ABF1	AT1G49720	YES	N/A
AHK4	IAA18	AT1G51950	N/A	N/A
AHK4	ANAC047	AT3G04070	YES	YES, 5'UTR
AHK4	AL3	AT3G42790	N/A	N/A
AHK4	ANAC062	AT3G49530	YES	YES, -830, -1400 & -1920
AHK4	AT4G01460	AT4G01460	N/A	N/A
AHK4	ARF9	AT4G23980	N/A	N/A
AHK4	ATH1	AT4G32980	N/A	N/A
AHK4	DEWAX	AT5G61590	N/A	N/A
AHK4	ANAC103	AT5G64060	YES	YES, EXON
AHK5	HMGBD15	AT1G04880	YES	NO
AHK5	ASIL1	AT1G54060	NO	N/A
AHK5	ANAC047	AT3G04070	YES	NO
AHK5	AL3	AT3G42790	N/A	N/A
AHK5	ANAC082	AT5G09330	N/A	N/A
AHK5	ANAC103	AT5G64060	YES	NO
AHP2	HMGBD15	AT1G04880	YES	NO

AHP2	BBX31	AT3G21890	YES	NO
AHP2	AtHB34	AT3G28920	YES	NO
AHP2	AL3	AT3G42790	N/A	N/A
AHP2	ATHB40	AT4G36740	YES	YES, 3'UTR & -710 & -1390
AHP2	HAT22	AT4G37790	NO	NO, NO PEAKS IN OTHER TARGETS
AHP2	ATHB30	AT5G15210	N/A	N/A
AHP3	HMGBD15	AT1G04880	YES	YES, -950
AHP3	TLP6	AT1G47270	N/A	N/A
AHP3	ABF1	AT1G49720	YES	N/A
AHP3	ANAC032	AT1G77450	N/A	N/A
AHP3	PUX2	AT2G01650	N/A	N/A
AHP3	DREB19	AT2G38340	NO	NO
AHP3	ANAC047	AT3G04070	YES	NO
AHP3	AZF2	AT3G19580	N/A	N/A
AHP3	AL3	AT3G42790	N/A	N/A
AHP3	AT4G01460	AT4G01460	N/A	N/A
AHP3	ZAT6	AT5G04340	YES	N/A
AHP3	DEWAX	AT5G61590	N/A	N/A
AHP3	ANAC103	AT5G64060	YES	YES, -3000
AHP5	ASIL1	AT1G54060	YES	N/A
AHP5	ANAC082	AT5G09330	N/A	N/A
AHP5	ANAC103	AT5G64060	YES	NO

AHP6	ARF12	AT1G34310	N/A	N/A
AHP6	ANAC047	AT3G04070	YES	NO
AHP6	AL3	AT3G42790	N/A	N/A
AHP6	ANAC082	AT5G09330	N/A	N/A
ARR1	HMGBD15	AT1G04880	YES	NO
ARR1	AZF2	AT3G19580	N/A	N/A
ARR1	AtHB34	AT3G28920	YES	YES, -790
ARR1	MYB32	AT4G34990	N/A	N/A
ARR1	ZAT6	AT5G04340	NO	N/A
ARR1	DEWAX	AT5G61590	N/A	N/A
ARR1	DEWAX	AT5G61590	N/A	N/A
ARR10	HMGBD15	AT1G04880	YES	YES, -2140
ARR10	DREB19	AT2G38340	YES	NO
ARR10	ANAC047	AT3G04070	NO	NO
ARR10	AtHB34	AT3G28920	YES	YES, -620
ARR10	AL3	AT3G42790	N/A	N/A
ARR10	DEWAX	AT5G61590	N/A	N/A
ARR14	ASIL2	AT3G14180	YES	YES, -310
ARR15	ABF1	AT1G49720	NO	N/A
ARR15	IAA18	AT1G51950	N/A	N/A
ARR15	ASIL1	AT1G54060	NO	N/A
ARR15	DREB19	AT2G38340	YES	YES, -1280
ARR15	AT2G44730	AT2G44730	N/A	N/A
ARR15	AZF2	AT3G19580	N/A	N/A

ARR15	AL3	AT3G42790	N/A	N/A
ARR15	ZAT6	AT5G04340	YES	N/A
ARR15	AZF3	AT5G43170	N/A	N/A
ARR15	DEWAX	AT5G61590	N/A	N/A
ARR15	ANAC103	AT5G64060	NO	NO
ARR15	CAMTA2	AT5G64220	NO	N/A
ARR4	ABF1	AT1G49720	NO	N/A
ARR4	ANAC047	AT3G04070	YES	YES, 3'UTR
ARR4	AL3	AT3G42790	N/A	N/A
ARR4	AT5G52020/RAP210	AT5G52020	NO	NO
ARR4	DEWAX	AT5G61590	N/A	N/A
ARR4	CAMTA2	AT5G64220	NO	N/A
ARR5	HMGBD15	AT1G04880	YES	YES, -1860
ARR5	DREB19	AT2G38340	YES	NO
ARR5	AZF2	AT3G19580	N/A	N/A
ARR5	AL3	AT3G42790	N/A	N/A
ARR5	ZAT6	AT5G04340	NO	N/A
ARR5	AZF3	AT5G43170	N/A	N/A
ARR5	ANAC103	AT5G64060	YES	NO
ARR7	HMGBD15	AT1G04880	YES	NO
ARR7	IAA18	AT1G51950	N/A	N/A
ARR7	DREB19	AT2G38340	YES	YES, 5'UTR
ARR7	AT2G44730	AT2G44730	N/A	N/A

ARR7	AZF2	AT3G19580	N/A	N/A
ARR7	AL3	AT3G42790	N/A	N/A
ARR7	ARF18	AT3G61830	N/A	N/A
ARR7	ARF9	AT4G23980	N/A	N/A
ARR7	ZAT6	AT5G04340	NO	N/A
ARR9	ABF1	AT1G49720	YES	N/A
ARR9	DREB19	AT2G38340	NO	NO
CKX5	BPEP	AT1G59640	YES	YES, -970
CKX5	ANAC047	AT3G04070	YES	NO
CKX5	AtHB34	AT3G28920	YES	YES, -1260, -2120 & -2620
CKX5	ANAC073	AT4G28500	YES	YES, -560 & -1540
CKX5	ANAC075	AT4G29230	YES	YES, -1520
CKX5	AZF3	AT5G43170	N/A	N/A
CKX6	AZF2	AT3G19580	N/A	N/A
CKX6	ZAT6	AT5G04340	NO	N/A
CKX6	AZF3	AT5G43170	N/A	N/A
CKX6	ANAC103	AT5G64060	NO	NO
CKX6	CAMTA2	AT5G64220	NO	N/A
IPT2	ASIL1	AT1G54060	NO	N/A
IPT2	DREB19	AT2G38340	NO	NO
IPT2	DREB2A	AT5G05410	YES	NO
IPT2	CAMTA2	AT5G64220	YES	N/A
IPT3	HMGBD15	AT1G04880	YES	YES, 3'UTR

IPT3	AtHB34	AT3G28920	YES	YES, -210 & -1560
IPT3	ANAC062	AT3G49530	NO	NO
IPT3	DEWAX	AT5G61590	N/A	N/A
IPT9	HMGBD15	AT1G04880	YES	YES, -1200
IPT9	IAA18	AT1G51950	N/A	N/A
IPT9	ZFHD1	AT1G69600	N/A	N/A
IPT9	AtHB34	AT3G28920	YES	YES, -240
IPT9	ATHB30	AT5G15210	N/A	N/A
IPT9	DEWAX	AT5G61590	N/A	N/A
LOG1	HMGBD15	AT1G04880	YES	NO
LOG1	ANAC047	AT3G04070	NO	NO
LOG1	AZF2	AT3G19580	N/A	N/A
LOG1	AL3	AT3G42790	N/A	N/A
LOG1	ZAT6	AT5G04340	NO	N/A
LOG1	CAMTA2	AT5G64220	NO	N/A
LOG4	EPR1	AT1G18330	YES	YES, -800
LOG4	ANAC008	AT1G25580	N/A	N/A
LOG4	VIP1	AT1G43700	NO	NO
LOG4	ABF1	AT1G49720	YES	N/A
LOG4	DOF/1G64620	AT1G64620	YES	YES, -950
LOG4	PERIANTHA	AT1G68640	N/A	N/A
LOG4	ANAC055	AT3G15500	NO	YES, -990
LOG4	AL3	AT3G42790	N/A	N/A
LOG4	ANAC062	AT3G49530	YES	YES, -850 & -1640

LOG4	IAA14	AT4G14550	N/A	N/A
LOG4	ANAC073	AT4G28500	NO	NO
LOG4	ANAC075	AT4G29230	NO	NO
LOG4	ATHB23	AT5G39760	YES	YES, -2240
LOG4	ZAT12/RHL41	AT5G59820	NO	N/A
LOG4	DEWAX	AT5G61590	N/A	N/A
LOG4	ANAC103	AT5G64060	YES	NO
LOG4	CAMTA2	AT5G64220	YES	N/A
LOG5	HMGBD15	AT1G04880	YES	NO
LOG5	EPR1	AT1G18330	YES	YES, -1740
LOG5	DOF/2G28810	AT2G28810	YES	YES, 5'UTR &-1820
LOG5	AT2G44730	AT2G44730	N/A	N/A
LOG5	AZF2	AT3G19580	N/A	N/A
LOG5	AL3	AT3G42790	N/A	N/A
LOG5	ANAC073	AT4G28500	YES	YES, 5'UTR & -1240
LOG5	ZAT6	AT5G04340	YES	N/A
LOG5	ANAC082	AT5G09330	N/A	N/A
LOG5	ANAC103	AT5G64060	YES	YES, 5'UTR
LOG7	HMGBD15	AT1G04880	YES	YES, -400

Table S3 Fluorescence intensity measurements

TCSn::GFP fluorescence intensity in WT vs nac062 mutant			
		Normalized grey value	Normalized grey value (SE)
TCSn::GFP	Mock	81.12083333	11.27482937

	10µM BAP	219.9932	4.900548422
	20µM BAP	225.848	4.686786394
nac062 **; TCSn::GFP**	Mock	7.188857143	0.489513044
	10µM BAP	30.983	7.806932214
	20µM BAP	36.8982	7.18708117
			Student t-test , p-value
	TCSGFP mock VS TCSGFP 10BA		less than 0.0001
	TCSGFP mock VS TCSGFP 20BA		less than 0.0001
	nac062;TCSGFP mock VS nac062;TCSGFP 10BA		equals 0.0070
	nac062;TCSGFP mock VS nac062;TCSGFP 20BA		equals 0.0005

TCSn::GFP fluorescence intensity in RT vs cold treated WT/nac062 mutant			
		Normalized grey value	Normalized grey value (SE)
TCSn::GFP	22°C	81.12083333	11.27482937
	4°C	152.512125	4.810060385
	22°C	7.188857143	0.489513044

nac062 **; TCSn::GFP**	4°C	8.61	0.478082629
			Student t-test , p-value
	TCSGFP 22oC VS 4oC		less than 0.0001
	nac062 ; TCSGFP 22oC VS 4oC		equals 0.0589

pAHK4::H2BYFP fluorescence intensity in WT vs nac062 and 35S::NAC062ΔC			
		Normalized grey value	Normalized grey value (SE)
pAHK4-H2BYFP	WT	40.94123077	3.032605147
	nac062	27.62528571	2.085453732
	35S::NAC062ΔC	63.60144444	1.189561312
			Student t-test , p-value
	WT;pAHK4 VS nac062;pAHK4		less than 0.0001
	WT;pAHK4 VS 35S::NAC062ΔC;pAHK4		less than 0.0001

pLOG4::H2BYFP flourescence intensity in WT vs nac062 and 35S::NAC062ΔC			
		Normalized grey value	Normalized grey value (SE)
pLOG4-H2BYFP PL4-3	WT	52.73671429	1.40653384
	nac062	71.89058824	4.606124952

	35S::NAC062ΔC	61.5595	2.947015482
			Student t-test , p-value
	pLOG4-H2BYFP PL4-3 in WT VS nac062		less than 0.0001
	pLOG4-H2BYFP PL4-3 in WT VS 35S::NAC062ΔC		less than 0.0001

Table S4 Shoot size measurements

Shoot size measurement WT VS nac062 mutant and 35S::NAC062ΔC						
Sample name	I1 length	I2 length	Ig	Mean	Standard Dev	SE
nac062;TCSn-GFP PL1	45.614	47.264	46.439	44.4781176	3.549011119	0.86076163
nac062;TCSn-GFP PL2	42.129	47.745	44.937			
nac062;TCSn-GFP PL3	43.341	47.789	45.565			
nac062;TCSn-GFP PL4	41.671	44.515	43.093			
nac062;TCSn-GFP PL5	38.033	48.39	43.2115			

nac062;TCSn-GFP PL6	44.011	55.27	49.6405			
nac062;TCSn-GFP PL7	44.655	46.564	45.6095			
nac062;TCSn-GFP PL8	42.733	53.44	48.0865			
nac062;TCSn-GFP PL9	41.938	50.055	45.9965			
nac062;TCSn-GFP PL10	42.314	52.564	47.439			
nac062;TCSn-GFP PL11	45.925	49.726	47.8255			
nac062;TCSn-GFP PL12	46.014	47.319	46.6665			
nac062;TCSn-GFP PL13	33.16	44.733	38.9465			
nac062;TCSn-GFP PL14	38.837	49.173	44.005			
nac062;TCSn-GFP PL15	37.661	44.753	41.207			
nac062;TCSn-GFP PL16	32.656	38.948	35.802			
nac062;TCSn-GFP PL17	38.563	44.753	41.658			

Sample name	I1 length	I2 length	Ig	Mean	Standard Dev	SE
35S-NAC062 Nterm PL1	44.48	58.33	51.405	59.4542692	5.027219102	1.39429971
35S-NAC062 Nterm PL2	60.691	65.225	62.958			
35S-NAC062 Nterm PL5	43.287	58.838	51.0625			
35S-NAC062 Nterm PL6	57.433	61.5	59.4665			
35S-NAC062 Nterm PL7	59.545	64.155	61.85			
35S-NAC062 Nterm PL8	55.282	64.685	59.9835			
35S-NAC062 Nterm PL9	63.581	69.383	66.482			
35S-NAC062 Nterm PL10	53.299	64.163	58.731			
35S-NAC062 Nterm PL11	59.522	60.138	59.83			
35S-NAC062 Nterm PL12	44.486	56.009	56.009			

35S-NAC062 Nterm PL14	52.444	59.292	59.292			
35S-NAC062 Nterm PL15	67.296	68.567	68.567			
35S-NAC062 Nterm PL16	57.611	57.269	57.269			
Sample name	I1 length	I2 length	Ig	Mean	Standard Dev	SE
WT TCSn-GFP pl1	44.376	49.776	47.076	49.09825	3.952975504	1.05647714
WT TCSn-GFP pl2	43.195	50.761	46.978			
WT TCSn-GFP pl3	38.359	49.11	43.7345			
WT TCSn-GFP pl4	49.907	56.669	53.288			
WT TCSn-GFP pl5	42.194	45.99	44.092			
WT TCSn-GFP pl6	48.193	49.118	48.6555			

WT TCSn-GFP pl7	55.452	57.639	56.5455			
WT TCSn-GFP pl8	42.004	52.436	47.22			
WT TCSn-GFP pl9	40.289	52.281	46.285			
WT TCSn-GFP pl10	45.343	54.052	49.6975			
WT TCSn-GFP pl11	45.411	55.527	50.469			
WT TCSn-GFP pl12	48.731	56.445	52.588			
WT TCSn-GFP pl13	43.437	48.546	45.9915			
WT TCSn-GFP pl4	51.323	58.187	54.755			
		Student t-test , p-value				
WT VS nac062		equals 0.0018				
WT VS 35S::NAC062ΔC		less than 0.0001				

Shoot size measurement WT VS dewax mutant						
Sample name	I1 length	I2 length	Ig	Mean	Standard Dev	SE
WT PL1	44.364	52.68	48.522	46.7157	5.127148374	2.29293046
WT PL2	39.478	45.302	42.39			
WT PL3	51.944	56.86	54.402			
WT PL4	41.913	50.988	46.4505			
WT PL5	40.016	43.612	41.814			
	I1 length	I2 length	Ig	Mean	Standard Dev	SE
dewax mutant PL1	34.725	39.438	37.0815	36.9473	2.18818848	0.97858764
dewax mutant PL2	33.796	40.677	37.2365			

dewax mutant PL3	31.377	37.498	34.4375			
dewax mutant PL4	37.439	43.141	40.29			
dewax mutant PL5	31.541	39.841	35.691			
		Student t-test , p-value				
WT VS dewax mutant		equals 0.0044				

Table S5 RT-qPCR data and analysis using Pfaffl method

1st Replicate (calculation of efficiency corrected ratio)					
ARR5 in dreb19/M VS WT	delta Cq	Efficiency (E)	E^deltaCq	ratio	LOG fold change
target	0.37640175	2.0170229	1.30224797	0.9762456	-0.034683949
ref	0.42766	1.96156632	1.33393478		
2nd Replicate (calculation of efficiency corrected ratio)					
ARR5 in dreb19/M VS WT	delta Cq	Efficiency (E)	E^deltaCq	ratio	LOG fold change
target	-0.4528042	2.0170229	0.7278228	0.60424646	-0.72679099
ref	0.27618153	1.96156632	1.20451314		

3rd Replicate (calculation of efficiency corrected ratio)					
ARR5 in dreb19/M VS WT	delta Cq	Efficiency (E)	E^deltaCq	ratio	LOG fold change
target	-2.6321246	2.0170229	0.15774774	0.43786867	-1.191429854
ref	-1.515298	1.96156632	0.36026267		
1st Replicate (calculation of efficiency corrected ratio)					
ARR10 in dreb19/M VS WT	delta Cq	Efficiency (E)	E^deltaCq	ratio	LOG fold change
target	1.1407379	2.08429371	2.31125853	1.73266231	0.792990508
ref	0.42766	1.96156632	1.33393478		
2nd Replicate (calculation of efficiency corrected ratio)					
ARR10 in dreb19/M(2) VS WT	delta Cq	Efficiency (E)	E^deltaCq	ratio	LOG fold change
target	0.54256942	2.08429371	1.48955778	1.23664718	0.306433951
ref	0.27618153	1.96156632	1.20451314		
3rd Replicate (calculation of efficiency corrected ratio)					
ARR10 in dreb19/M(3) VS WT	delta Cq	Efficiency (E)	E^deltaCq	ratio	LOG fold change
target	-1.0858089	2.08429371	0.45047591	1.25040963	0.322400798
ref	-1.515298	1.96156632	0.36026267		
1st Replicate (calculation of efficiency corrected ratio)					
ARR15 in dreb19/M VS WT	delta Cq	Efficiency (E)	E^deltaCq	ratio	LOG fold change
target	1.0795157	2.11334671	2.24290577	1.68142086	0.749680875
ref	0.42766	1.96156632	1.33393478		
2nd Replicate (calculation of efficiency corrected ratio)					

ARR10 in dreb19/M(2) VS WT	delta Cq	Efficiency (E)	E^deltaCq	ratio	LOG fold change
target	0.54256942	2.08429371	1.48955778	1.23664718	0.306433951
ref	0.27618153	1.96156632	1.20451314		
3rd Replicate (calculation of efficiency corrected ratio)					
ARR15 in dreb19/M(3) VS WT	delta Cq	Efficiency (E)	E^deltaCq	ratio	LOG fold change
target	-0.7250275	2.11334671	0.58128254	1.61349648	0.690190429
ref	-1.515298	1.96156632	0.36026267		
1st Replicate (calculation of efficiency corrected ratio)					
AHK3 in dreb19/M VS WT	delta Cq	Efficiency (E)	E^deltaCq	ratio	LOG fold change
target	-0.3006704	1.94096826	0.81922156	0.61413914	-0.703362546
ref	0.42766	1.96156632	1.33393478		
2nd Replicate (calculation of efficiency corrected ratio)					
AHK3 in dreb19/M(2) VS WT	delta Cq	Efficiency (E)	E^deltaCq	ratio	LOG fold change
target	-0.2539027	1.94096826	0.84502845	0.70155187	-0.511378319
ref	0.27618153	1.96156632	1.20451314		
3rd Replicate (calculation of efficiency corrected ratio)					
AHK3 in dreb19/M(2) VS WT	delta Cq	Efficiency (E)	E^deltaCq	ratio	LOG fold change
target	-1.8112268	1.94096826	0.30083843	0.83505302	-0.260060293
ref	-1.515298	1.96156632	0.36026267		

1st Replicate (calculation of efficiency corrected ratio)					
IPT9 in athb34/M VS WT	delta Cq	Efficiency (E)	E^deltaCq	ratio	LOG fold change
target	2.19561263	2.022876943	4.69667404	1.87372477	0.905909051
ref	1.3639116	1.961566321	2.50659762		
2nd Replicate (calculation of efficiency corrected ratio)					
IPT9 in athb34/M(2) VS WT	delta Cq	Efficiency (E)	E^deltaCq	ratio	LOG fold change
target	1.14920579	2.022876943	2.24709731	2.04440188	1.031678825
ref	0.14031164	1.961566321	1.09914656		
3rd Replicate (calculation of efficiency corrected ratio)					
IPT9 in athb34/M(3) VS WT	delta Cq	Efficiency (E)	E^deltaCq	ratio	LOG fold change
target	0.29626136	2.022876943	1.23210276	1.21266997	0.278186966
ref	0.02359616	1.961566321	1.0160248		
1st Replicate (calculation of efficiency corrected ratio)					
ARR10 in athb34/M VS WT	delta Cq	Efficiency (E)	E^deltaCq	ratio	LOG fold change
target	1.34641408	2.084293711	2.68813316	1.3232045	0.404036042
ref	1.05201865	1.961566321	2.03153266		
2nd Replicate (calculation of efficiency corrected ratio)					
ARR10 in athb34/M(2) VS WT	delta Cq	Efficiency (E)	E^deltaCq	ratio	LOG fold change
target	0.57012659	2.084293711	1.5200118	1.38290183	0.46769875
ref	0.14031164	1.961566321	1.09914656		

3rd Replicate (calculation of efficiency corrected ratio)					
ARR10 in athb34/M(3) VS WT	delta Cq	Efficiency (E)	E^deltaCq	ratio	LOG fold change
target	0.13517661	2.084293711	1.10437301	1.08695478	0.120291918
ref	0.02359616	1.961566321	1.0160248		
1st Replicate (calculation of efficiency corrected ratio)					
ARR1 in athb34/M VS WT	delta Cq	Efficiency (E)	E^deltaCq	ratio	LOG fold change
target	0.28052843	1.923422838	1.20140947	0.59138083	-0.757840625
ref	1.05201865	1.961566321	2.03153266		
2nd Replicate (calculation of efficiency corrected ratio)					
ARR1 in athb34/M(2) VS WT	delta Cq	Efficiency (E)	E^deltaCq	ratio	LOG fold change
target	0.01317904	1.923422838	1.00865776	0.91767358	-0.123947027
ref	0.14031164	1.961566321	1.09914656		
3rd Replicate (calculation of efficiency corrected ratio)					
ARR1 in athb34/M(3) VS WT	delta Cq	Efficiency (E)	E^deltaCq	ratio	LOG fold change
target	-0.906135	1.923422838	0.55282784	0.54410861	-0.87803343
ref	0.02359616	1.961566321	1.0160248		

1st Replicate (calculation of efficiency corrected ratio)					
LOG4 in athb23/M VS WT	delta Cq	Efficiency (E)	E^deltaCq	ratio	LOG fold change
target	0.87384228	1.961566321	1.80172651	0.75040406	-0.414260469
ref	1.31174962	1.94979773	2.40100849		
2nd Replicate (calculation of efficiency corrected ratio)					

LOG4 in athb23/M(2) VS WT	delta Cq	Efficiency (E)	E^deltaCq	ratio	LOG fold change
target	-0.1063788	1.961566321	0.93083613	0.74629472	-0.422182625
ref	0.33091835	1.94979773	1.24727687		
3rd Replicate (calculation of efficiency corrected ratio)					
LOG4 in athb23/M(3) VS WT	delta Cq	Efficiency (E)	E^deltaCq	ratio	LOG fold change
target	0.00133288	1.961566321	1.00089842	0.6971952	-0.520365464
ref	0.54152162	1.94979773	1.43560716		

1st Replicate (calculation of efficiency corrected ratio)					
LOG5 in azf2/M VS WT	delta Cq	Efficiency (E)	E^deltaCq	ratio	LOG fold change
target	1.05616024	1.941561814	2.01527289	1.53496255	0.618203458
ref	0.40408362	1.961566321	1.31291339		
2nd Replicate (calculation of efficiency corrected ratio)					
LOG5 in azf2/M(2) VS WT	delta Cq	Efficiency (E)	E^deltaCq	ratio	LOG fold change
target	0.76926475	1.941561814	1.66596003	1.48638638	0.571809187
ref	0.16928351	1.961566321	1.12081223		
3rd Replicate (calculation of efficiency corrected ratio)					
LOG5 in azf2/M(3) VS WT	delta Cq	Efficiency (E)	E^deltaCq	ratio	LOG fold change
target	-0.1425268	1.941561814	0.90976814	1.04899971	0.069014284
ref	-0.2113603	1.961566321	0.86727206		
1st Replicate (calculation of efficiency corrected ratio)					
ARR15 in azf2/M VS WT	delta Cq	Efficiency (E)	E^deltaCq	ratio	LOG fold change

target	1.6439655	2.113346713	3.42169035	2.83770932	1.504726817
ref	0.27775792	1.961566321	1.20579311		
2nd Replicate (calculation of efficiency corrected ratio)					
ARR15 in azf2/M(2) VS WT	delta Cq	Efficiency (E)	E^deltaCq	ratio	LOG fold change
target	1.26512092	2.113346713	2.57707643	2.29929363	1.201190718
ref	0.16928351	1.961566321	1.12081223		
3rd Replicate (calculation of efficiency corrected ratio)					
ARR15 in azf2/M(3) VS WT	delta Cq	Efficiency (E)	E^deltaCq	ratio	LOG fold change
target	0.69575099	2.113346713	1.68305661	1.94063281	0.956527173
ref	-0.2113603	1.961566321	0.86727206		
1st Replicate (calculation of efficiency corrected ratio)					
ARR5 in azf2/M VS WT	delta Cq	Efficiency (E)	E^deltaCq	ratio	LOG fold change
target	1.30685563	2.017022902	2.50157232	2.07462814	1.052852766
ref	0.27775792	1.961566321	1.20579311		
2nd Replicate (calculation of efficiency corrected ratio)					
ARR5 in azf2/M(2) VS WT	delta Cq	Efficiency (E)	E^deltaCq	ratio	LOG fold change
target	0.31724505	2.017022902	1.24930363	1.11464132	0.156579545
ref	0.16928351	1.961566321	1.12081223		
3rd Replicate (calculation of efficiency corrected ratio)					
ARR5 in azf2/M(3) VS WT	delta Cq	Efficiency (E)	E^deltaCq	ratio	LOG fold change
target	1.2972777	2.017022902	2.48481789	2.86509622	1.518583591
ref	-0.2113603	1.961566321	0.86727206		

1st Replicate (calculation of efficiency corrected ratio)					
AHK3 in azf2(M) VS WT	delta Cq	Efficiency (E)	E^deltaCq	ratio	LOG fold change
target	-1.109777	1.940968258	0.47903117	0.5085729	-0.97547351
ref	-0.0888215	1.961566321	0.9419125		
2nd Replicate (calculation of efficiency corrected ratio)					
AHK3 in azf2/M(2) VS WT	delta Cq	Efficiency (E)	E^deltaCq	ratio	LOG fold change
target	-0.6193238	1.940968258	0.66316763	0.59168486	-0.757099115
ref	0.16928351	1.961566321	1.12081223		
3rd Replicate (calculation of efficiency corrected ratio)					
AHK3 in azf2/M(3) VS WT	delta Cq	Efficiency (E)	E^deltaCq	ratio	LOG fold change
target	-0.3825059	1.940968258	0.77594556	0.89469684	-0.160529179
ref	-0.2113603	1.961566321	0.86727206		
1st Replicate (calculation of efficiency corrected ratio)					
AHP3 in azf2(M) VS WT	delta Cq	Efficiency (E)	E^deltaCq	ratio	LOG fold change
target	0.32030181	1.940931185	1.23665959	1.31292406	0.392783475
ref	-0.0888215	1.961566321	0.9419125		
2nd Replicate (calculation of efficiency corrected ratio)					
AHP3 in azf2/M(2) VS WT	delta Cq	Efficiency (E)	E^deltaCq	ratio	LOG fold change
target	0.39951272	1.940931185	1.30335798	1.16286916	0.21768878
ref	0.16928351	1.961566321	1.12081223		
3rd Replicate (calculation of efficiency corrected ratio)					

AHP3 in azf2/M(3) VS WT	delta Cq	Efficiency (E)	E^deltaCq	ratio	LOG fold change
target	0.2453488	1.940931185	1.17669238	1.35677424	0.440180684
ref	-0.2113603	1.961566321	0.86727206		

1st Replicate (calculation of efficiency corrected ratio)					
IPT9 in zfhd1/M VS WT	delta Cq	Efficiency (E)	E^deltaCq	ratio	LOG fold change
target	1.53965197	2.022876943	2.9586016	1.60462173	0.682233243
ref	0.90810354	1.961566321	1.84380003		
2nd Replicate (calculation of efficiency corrected ratio)					
IPT9 in zfhd1/M(2) VS WT	delta Cq	Efficiency (E)	E^deltaCq	ratio	LOG fold change
target	0.7052388	2.022876943	1.64354477	2.08849423	1.062463154
ref	-0.3556072	1.961566321	0.78695203		
3rd Replicate (calculation of efficiency corrected ratio)					
IPT9 in zfhd1/M(3) VS WT	delta Cq	Efficiency (E)	E^deltaCq	ratio	LOG fold change
target	0.42242333	2.022876943	1.3466311	1.29161628	0.369177525
ref	0.06191027	1.961566321	1.04259378		

1st Replicate (calculation of efficiency corrected ratio)					
LOG4 in abf1/M vs WT	delta Cq	Efficiency (E)	E^deltaCq	ratio	LOG fold change
target	0.76050694	1.94979773	1.66164817	1.36231601	0.446061392
ref	0.29480633	1.961566321	1.219723		
2nd Replicate (calculation of efficiency corrected ratio)					
LOG4 in abf1/M(2) vs WT	delta Cq	Efficiency (E)	E^deltaCq	ratio	LOG fold change

target	0.4067282	1.94979773	1.31203957	1.50520641	0.589961338
ref(UBQ10)	-0.2038569	1.961566321	0.87166754		
3rd Replicate (calculation of efficiency corrected ratio)					
LOG4 in abf1/M(3) vs WT	delta Cq	Efficiency (E)	E^deltaCq	ratio	LOG fold change
target	0.65732488	1.94979773	1.55101984	1.76577641	0.820302671
ref(UBQ10)	-0.1924736	1.961566321	0.87837839		

1st Replicate (calculation of efficiency corrected ratio)					
AHK4 in ath1/M vs WT	delta Cq	Efficiency (E)	E^deltaCq	ratio	LOG fold change
target	0.66816358	1.845255508	1.50580685	1.40995463	0.495648743
ref(UBQ10)	0.09762077	1.961566321	1.06798249		
2nd Replicate (calculation of efficiency corrected ratio)					
AHK4 in ath1M vs WT	delta Cq	Efficiency (E)	E^deltaCq	ratio	LOG fold change
target	0.60504254	1.94979773	1.49780756	1.39496244	0.480226277
ref(UBQ10)	0.10558164	1.961566321	1.07372609		
3rd Replicate (calculation of efficiency corrected ratio)					
AHK4 in ath1/M vs WT	delta Cq	Efficiency (E)	E^deltaCq	ratio	LOG fold change
target	0.55831017	1.845255508	1.40780355	1.43281481	0.518852156
ref(UBQ10)	-0.0261378	1.961566321	0.98254397		

1st Replicate (calculation of efficiency corrected ratio)					
LOG4 in dewax/M VS WT-N	delta Cq	Efficiency (E)	E^deltaCq	ratio	LOG fold change
target	-0.0124244	1.94979773	0.99173821	0.79996861	-0.3219847
ref	0.31894443	1.961566321	1.2397214		

2nd Replicate (calculation of efficiency corrected ratio)					
LOG4 in dewax/M VS WT-N	delta Cq	Efficiency (E)	E^deltaCq	ratio	LOG fold change
target	-1.6873795	1.94979773	0.32409891	0.60003706	-0.736876494
ref	-0.9142097	1.961566321	0.5401315		
3rd Replicate (calculation of efficiency corrected ratio)					
LOG4 in dewax/M VS WT-N	delta Cq	Efficiency (E)	E^deltaCq	ratio	LOG fold change
target	-1.3233867	1.94979773	0.41326789	0.65946733	-0.600626896
ref (UBQ10)	-0.6936416	1.961566321	0.62666924		
1st Replicate (calculation of efficiency corrected ratio)					
AHK4 in dewax/M VS WT-N	delta Cq	Efficiency (E)	E^deltaCq	ratio	LOG fold change
target	0.85252694	1.845255508	1.68585548	1.3598664	0.443464924
ref	0.31894443	1.961566321	1.2397214		
2nd Replicate (calculation of efficiency corrected ratio)					
AHK4 in dewax/M VS WT-N	delta Cq	Efficiency (E)	E^deltaCq	ratio	LOG fold change
target	0.02164523	1.845255508	1.01334856	1.87611455	0.907747919
ref	-0.9142097	1.961566321	0.5401315		
3rd Replicate (calculation of efficiency corrected ratio)					
AHK4 in dewax/M VS WT-N	delta Cq	Efficiency (E)	E^deltaCq	ratio	LOG fold change
target	-0.4684743	1.845255508	0.75051497	1.19762534	0.260176656
ref (UBQ10)	-0.6936416	1.961566321	0.62666924		

1st Replicate (calculation of efficiency corrected ratio)					
LOG4 in nac062/M VS WT	delta Cq	Efficiency (E)	E^deltaCq	ratio	LOG fold change
target	-0.6281448	1.94979773	0.65742252	0.78328268	-0.352395037
ref	-0.2599903	1.961566321	0.83931707		
2nd Replicate (calculation of efficiency corrected ratio)					
LOG4 in nac062/M VS WT	delta Cq	Efficiency (E)	E^deltaCq	ratio	LOG fold change
target	-0.1698528	1.94979773	0.89278004	0.68516559	-0.545475404
ref	0.39284947	1.961566321	1.30301355		
3rd Replicate (calculation of efficiency corrected ratio)					
LOG4 in nac062/M VS WT	delta Cq	Efficiency (E)	E^deltaCq	ratio	LOG fold change
target	-0.4684598	1.94979773	0.73139425	0.51766934	-0.949897212
ref (UBQ10)	0.51297867	1.961566321	1.41285988		
1st Replicate (calculation of efficiency corrected ratio)					
AHK4 in nac062/M VS WT	delta Cq	Efficiency (E)	E^deltaCq	ratio	LOG fold change
target	-0.530462	1.845255508	0.7225487	0.86087693	-0.216121093
ref	-0.2599903	1.961566321	0.83931707		
2nd Replicate (calculation of efficiency corrected ratio)					
AHK4 in nac062/M VS WT	delta Cq	Efficiency (E)	E^deltaCq	ratio	LOG fold change
target	-0.1827936	1.845255508	0.8940598	0.68614774	-0.543408842
ref	0.39284947	1.961566321	1.30301355		

3rd Replicate (calculation of efficiency corrected ratio)					
AHK4 in nac062/M VS WT	delta Cq	Efficiency (E)	E^deltaCq	ratio	LOG fold change
target	-0.1484472	1.845255508	0.91307125	0.64625747	-0.629819049
ref (UBQ10)	0.51297867	1.961566321	1.41285988		

1st Replicate (calculation of efficiency corrected ratio)					
LOG4 in 35S-N62ΔC VS WT	delta Cq	Efficiency (E)	E^deltaCq	ratio	LOG fold change
target	0.07318013	1.94979773	1.05007779	1.31281647	0.392665244
ref	-0.3314475	1.96156632	0.79986641		
2nd Replicate (calculation of efficiency corrected ratio)					
LOG4 in 35S-N62ΔC VS WT	delta Cq	Efficiency (E)	E^deltaCq	ratio	LOG fold change
target	-0.3789853	1.94979773	0.77642271	1.30155626	0.380237678
ref	-0.7667889	1.96156632	0.59653411		
3rd Replicate (calculation of efficiency corrected ratio)					
LOG4 in 35S-N62ΔC VS WT	delta Cq	Efficiency (E)	E^deltaCq	ratio	LOG fold change
target	-0.1087713	1.94979773	0.92994543	1.18065451	0.239586855
ref (UBQ10)	-0.3542868	1.96156632	0.78765246		
4th Replicate (calculation of efficiency corrected ratio)					
LOG4 in 35S-N62ΔC VS WT	delta Cq	Efficiency (E)	E^deltaCq	ratio	LOG fold change
target	-0.2724053	1.94979773	0.83369138	1.3663631	0.450340922
ref (UBQ10)	-0.733283	1.96156632	0.61015361		

1st Replicate (calculation of efficiency corrected ratio)					
AHK4 in 35S-N62ΔC VS WT	delta Cq	Efficiency (E)	E^deltaCq	ratio	LOG fold change
target	0.1878068	1.84525551	1.12193378	1.40265145	0.488156551
ref	-0.3314475	1.96156632	0.79986641		
2nd Replicate (calculation of efficiency corrected ratio)					
AHK4 in 35S-N62ΔC VS WT	delta Cq	Efficiency (E)	E^deltaCq	ratio	LOG fold change
target	-0.0699818	1.84525551	0.95803394	1.60600026	0.68347213
ref	-0.7667889	1.96156632	0.59653411		
3rd Replicate (calculation of efficiency corrected ratio)					
AHK4 in 35S-N62ΔC VS WT	delta Cq	Efficiency (E)	E^deltaCq	ratio	LOG fold change
target	0.24732505	1.84525551	1.16359659	1.47729697	0.562959867
ref (UBQ10)	-0.3542868	1.96156632	0.78765246		
4th Replicate (calculation of efficiency corrected ratio)					
AHK4 in 35S-N62ΔC VS WT	delta Cq	Efficiency (E)	E^deltaCq	ratio	LOG fold change
target	-0.0003184	1.84525551	0.99980495	1.63861187	0.712474172
ref (UBQ10)	-0.733283	1.96156632	0.61015361		
NAC062 in 35S-N62ΔC VS WT	delta Cq	Efficiency (E)	E^deltaCq	ratio	LOG fold change
target	-0.0202092	1.94979773	0.98659645	1.23345153	0.302701025
ref	-0.3314475	1.96156632	0.79986641		
2nd Replicate (calculation of efficiency corrected ratio)					
NAC062 in 35S-N62ΔC VS WT	delta Cq	Efficiency (E)	E^deltaCq	ratio	LOG fold change
target	-0.5699746	1.94979773	0.68346036	1.14571882	0.196253029
ref	-0.7667889	1.96156632	0.59653411		

3rd Replicate (calculation of efficiency corrected ratio)					
NAC062 in 35S-N62ΔC VS WT	delta Cq	Efficiency (E)	E^deltaCq	ratio	LOG fold change
target	-0.0495983	1.94979773	0.96742436	1.22823759	0.296589663
ref (UBQ10)	-0.3542868	1.96156632	0.78765246		
4th Replicate (calculation of efficiency corrected ratio)					
NAC062 in 35S-N62ΔC VS WT	delta Cq	Efficiency (E)	E^deltaCq	ratio	LOG fold change
target	-0.5189117	1.94979773	0.70716546	1.15899577	0.212875303
ref (UBQ10)	-0.733283	1.96156632	0.61015361		

Bibliography

A, C., JE, L., M, F., D, P., S, B., & T, S. (2019). Cytokinin action in response to abiotic and biotic stresses in plants. *Plant, Cell & Environment*, *42*(3), 998–1018. https://doi.org/10.1111/PCE.13494

Abe, M., Takahashi, T., & Komeda, Y. (2001). Identification of a cis-regulatory element for L1 layer-specific gene expression, which is targeted by an L1-specific homeodomain protein. *The Plant journal : for cell and molecular biology*, *26*(5), 487–494. https://doi.org/10.1046/j.1365-313x.2001.01047.x

Aggarwal, P., Yadav, R. K., & Reddy, G. V. (2010). Identification of novel markers for stem-cell niche of Arabidopsis shoot apex. *Gene Expression Patterns : GEP*, *10*(6), 259–264. https://doi.org/10.1016/j.gep.2010.05.004

Appleby, J. L., Parkinson, J. S., & Bourret, R. B. (1996). Signal transduction via the multi-step phosphorelay: not necessarily a road less traveled. *Cell*, *86*(6), 845–848. https://doi.org/10.1016/s0092-8674(00)80158-0

Bartrina, I., Jensen, H., Novák, O., Strnad, M., Werner, T., & Schmülling, T. (2017). Gain-of-function mutants of the cytokinin receptors AHK2 and AHK3 regulate plant organ size, flowering time and plant longevity. *Plant Physiology*, *173*(3), 1783–1797. https://doi.org/10.1104/pp.16.01903

Bartrina, I., Otto, E., Strnad, M., Werner, T., & Schmülling, T. (2011). Cytokinin regulates the activity of reproductive meristems, flower organ size, ovule formation, and thus seed yield in Arabidopsis thaliana. *The Plant Cell*, *23*(1), 69–80. https://doi.org/10.1105/tpc.110.079079

Barton M. K. (2010). Twenty years on: the inner workings of the shoot apical meristem, a developmental dynamo. *Developmental biology*, *341*(1), 95–113. https://doi.org/10.1016/j.ydbio.2009.11.029

T. Berleth, G. Jurgens; The role of the monopteros gene in organising the basal body region of the Arabidopsis embryo. *Development* 1 June 1993; 118 (2): 575–587. doi: https://doi.org/10.1242/dev.118.2.575

Besnard, F., Refahi, Y., Morin, V., Marteaux, B., Brunoud, G., Chambrier, P., Rozier, F., Mirabet, V., Legrand, J., Lainé, S., Thévenon, E., Farcot, E., Cellier, C., Das, P., Bishopp, A., Dumas, R., Parcy, F., Helariutta, Y., Boudaoud, A., … Vernoux, T. (2014). Cytokinin signalling inhibitory fields provide robustness to phyllotaxis. *Nature*, *505*(7483), 417–421. https://doi.org/10.1038/nature12791

Bhatia, N., Bozorg, B., Larsson, A., Ohno, C., Jönsson, H., & Heisler, M. G. (2016). Auxin Acts through MONOPTEROS to Regulate Plant Cell Polarity and Pattern Phyllotaxis. *Current biology : CB*, *26*(23), 3202–3208. https://doi.org/10.1016/j.cub.2016.09.044

Bhatia, S., Kumar, H., Mahajan, M., Yadav, S., Saini, P., Yadav, S., Sahu, S. K., Sundaram, J. K., & Yadav, R. K. (2021). A cellular expression map of epidermal and subepidermal cell layer-enriched transcription factor genes integrated with the regulatory network in Arabidopsis shoot apical meristem. *Plant Direct*, *5*(3), e00306. https://doi.org/10.1002/pld3.306

Brady, S. M., Zhang, L., Megraw, M., Martinez, N. J., Jiang, E., Yi, C. S., Liu, W., Zeng, A., Taylor-Teeples, M., Kim, D., Ahnert, S., Ohler, U., Ware, D., Walhout, A. J. M., & Benfey, P. N. (2011). A stele-enriched gene regulatory network in the Arabidopsis root. *Molecular Systems Biology*, *7*(459), 1–9. https://doi.org/10.1038/msb.2010.114

Brand, U., Fletcher, J. C., Hobe, M., Meyerowitz, E. M., & Simon, R. (2000). Dependence of stem cell fate in Arabidopsis on a feedback loop regulated by CLV3 activity. *Science (New York, N.Y.)*, *289*(5479), 617–619. https://doi.org/10.1126/science.289.5479.617

Brandstatter, I., & Kieber, J. J. (1998). Two Genes with Similarity to Bacterial Response Regulators Are Rapidly and Specifically Induced by Cytokinin in Arabidopsis. In *The Plant Cell* (Vol. 10). www.plantcell.org

Brenner, W. G., Romanov, G. a., Köllmer, I., Bürkle, L., & Schmülling, T. (2005). Immediate-early and delayed cytokinin response genes of Arabidopsis thaliana identified by genome-wide expression profiling reveal novel cytokinin-sensitive processes and suggest cytokinin action through transcriptional cascades. *Plant Journal*, *44*(2), 314–333. https://doi.org/10.1111/j.1365-313X.2005.02530.x

Caesar, K., Thamm, A. M., Witthöft, J., Elgass, K., Huppenberger, P., Grefen, C., Horak, J., & Harter, K. (2011). Evidence for the localization of the Arabidopsis cytokinin receptors AHK3 and AHK4 in the endoplasmic reticulum. *Journal of experimental botany*, *62*(15), 5571–5580. https://doi.org/10.1093/jxb/err238

Carrel, A. 1912. On the permanent life of tissues outside of the organism. J. Exp. Med. 15: 516-528.

Caggiano, M. P., Yu, X., Bhatia, N., Larsson, A., Ram, H., Ohno, C. K., Sappl, P., Meyerowitz, E. M., Jönsson, H., & Heisler, M. G. (2017). Cell type boundaries organize plant development. *eLife*, *6*, e27421. https://doi.org/10.7554/eLife.27421

Chickarmane, V. S., Gordon, S. P., Tarr, P. T., Heisler, M. G., & Meyerowitz, E. M. (2012). Cytokinin signaling as a positional cue for patterning the apical-basal axis of the growing Arabidopsis shoot meristem. *Proceedings of the National Academy of Sciences*, *109*(10), 4002–4007. https://doi.org/10.1073/pnas.1200636109

Clark, S. E., Running, M. P., & Meyerowitz, E. M. (1993). CLAVATA1, a regulator of meristem and flower development in Arabidopsis. *Development (Cambridge, England)*, *119*(2), 397–418. https://doi.org/10.1242/dev.119.2.397

Clark, S.E., Running, M.P., and Meyerowitz, E.M. (1995). *CLAVATA3* is a specific regulator of shoot and floral meristem development affecting the same processes as *CLAVATA1*. Development *121*, 2057–2067.

Clough, S. J., & Bent, A. F. (1998). Floral dip: a simplified method for Agrobacterium-mediated transformation of Arabidopsis thaliana. In *The Plant Journal* (Issue 6). www.stanford.edu/cgi-bin/biosci_arabidopsis

D'Agostino, I. B., Deruère, J., & Kieber, J. J. (2000). Characterization of the response of the Arabidopsis response regulator gene family to cytokinin. *Plant Physiology*, *124*(4), 1706–1717. https://doi.org/10.1104/pp.124.4.1706

Deplancke, B., Dupuy, D., Vidal, M., & Walhout, A. J. M. (2004). *A Gateway-Compatible Yeast One-Hybrid System*. *508*, 2093–2101. https://doi.org/10.1101/gr.2445504.14

Dewitte W, Scofield S, Alcasabas AA, Maughan SC, Menges M, Braun N, Collins C, Nieuwland J, Prinsen E, Sundaresan V, Murray JA. Arabidopsis CYCD3 D-type cyclins link cell proliferation and endocycles and are rate-limiting for cytokinin responses. Proc Natl Acad Sci U S A. 2007 Sep 4;104(36):14537-42. doi: 10.1073/pnas.0704166104. Epub 2007 Aug 28. PMID: 17726100; PMCID: PMC1964848.

Ejaz, M., Bencivenga, S., Tavares, R., Bush, M., & Sablowski, R. (2021). ARABIDOPSIS THALIANA HOMEOBOX GENE 1 controls plant architecture by locally restricting environmental responses. *Proceedings of the National Academy of Sciences of the United States of America*, *118*(17). https://doi.org/10.1073/pnas.2018615118

Emery, J. F., Floyd, S. K., Alvarez, J., Eshed, Y., Hawker, N. P., Izhaki, A., Baum, S. F., & Bowman, J. L. (2003). Radial patterning of Arabidopsis shoots by class III HD-ZIP and KANADI genes. *Current Biology*, *13*, 1768-1774. https://doi.org/10.1016/j.cub.2003.09.035

Ernst, H. A., Olsen, A. N., Skriver, K., Larsen, S., & lo Leggio, L. (2004). Structure of the conserved domain of ANAC, a member of the NAC family of transcription factors. *EMBO Reports*, *5*(3), 297–303. https://doi.org/10.1038/sj.embor.7400093

Eshed, Y., Izhaki, A., Baum, S. F., Floyd, S. K., & Bowman, J. L. (2004). Asymmetric leaf development and blade expansion in Arabidopsis are mediated by KANADI and YABBY activities. *Development (Cambridge, England)*, *131*(12), 2997–3006. https://doi.org/10.1242/dev.01186

Ferreira, F. J., & Kieber, J. J. (2005). Cytokinin signaling. *Current Opinion in Plant Biology*, *8*(5), 518–525. https://doi.org/10.1016/j.pbi.2005.07.013

Gaudinier, A., Zhang, L., Reece-Hoyes, J. S., Taylor-Teeples, M., Pu, L., Liu, Z., Breton, G., Pruneda-Paz, J. L., Kim, D., Kay, S. A., Walhout, A. J. M., Ware, D., & Brady, S. M. (2011). Enhanced Y1H assays for Arabidopsis. *Nature Methods*, *8*(12), 1053–1056. https://doi.org/10.1038/nmeth.1750

Gautheret, R. J. 1939. Sur la possibilité de réaliser la culture indéfinie des tissus de tubercules de Carotte. C. R. Ac. Sc. 208: 118-130.

Go, Y. S., Kim, H., Kim, H. J., & Suh, M. C. (2014). Arabidopsis cuticular wax biosynthesis is negatively regulated by the DEWAX gene encoding an AP2/ERF-type transcription factor. *Plant Cell*, *26*(4), 1666–1680. https://doi.org/10.1105/tpc.114.123307

Golldack, D., Popova, O. v., & Dietz, K. J. (2002). Mutation of the matrix metalloproteinase At2-MMP inhibits growth and causes late flowering and early senescence in Arabidopsis. *Journal of Biological Chemistry*, *277*(7), 5541–5547. https://doi.org/10.1074/jbc.M106197200

Gómez-Mena, C., de Folter, S., Costa, M. M. R., Angenent, G. C., & Sablowski, R. (2005). Transcriptional program controlled by the floral homeotic gene AGAMOUS during early organogenesis. *Development*, *132*(3), 429–438. https://doi.org/10.1242/dev.01600

Gordon, S. P., Chickarmane, V. S., Ohno, C., & Meyerowitz, E. M. (2009). Multiple feedback loops through cytokinin signaling control stem cell number within the Arabidopsis shoot meristem. *Proceedings of the National Academy of Sciences of the United States of America*, *106*(38), 16529–16534. https://doi.org/10.1073/pnas.0908122106

Golovko, A., Sitbon, F., Tillberg, E., & Nicander, B. (2002). Identification of a tRNA isopentenyltransferase gene from Arabidopsis thaliana. *Plant molecular biology*, *49*(2), 161–169. https://doi.org/10.1023/a:1014958816241

Grant, C. E., Bailey, T. L., & Noble, W. S. (2011). FIMO: Scanning for occurrences of a given motif. *Bioinformatics*, *27*(7), 1017–1018. https://doi.org/10.1093/bioinformatics/btr064

Gubelmann, C., Waszak, S. M., Isakova, A., Holcombe, W., Hens, K., Iagovitina, A., Feuz, J. D., Raghav, S. K., Simicevic, J., & Deplancke, B. (2013). A yeast one-hybrid and microfluidics-based pipeline to map mammalian gene regulatory networks. *Molecular Systems Biology*, *9*(682). https://doi.org/10.1038/msb.2013.38

Haberlandt, G. 1902. Kulturversuche mit isolierten Pflanzenzellen. Sitz. Akad. Wiss. Wien 111: 69-92

Hardtke, C. S., & Berleth, T. (1998). The Arabidopsis gene MONOPTEROS encodes a transcription factor mediating embryo axis formation and vascular development. *The EMBO journal*, *17*(5), 1405–1411. https://doi.org/10.1093/emboj/17.5.1405

Hardtke, C. S., Ckurshumova, W., Vidaurre, D. P., Singh, S. A., Stamatiou, G., Tiwari, S. B., Hagen, G., Guilfoyle, T. J., & Berleth, T. (2004). Overlapping and non-redundant functions of the Arabidopsis auxin response factors MONOPTEROS and NONPHOTOTROPIC HYPOCOTYL 4.

Higuchi, M., Pischke, M. S., Mähönen, A. P., Miyawaki, K., Hashimoto, Y., Seki, M., Kobayashi, M., Shinozaki, K., Kato, T., Tabata, S., Helariutta, Y., Sussman, M. R., & Kakimoto, T. (2004). In planta functions of the Arabidopsis cytokinin receptor family. *Proceedings of the National Academy of Sciences of the United States of America*, *101*(23), 8821–8826. https://doi.org/10.1073/pnas.0402887101

Hothorn, M., Dabi, T., & Chory, J. (2011). Structural basis for cytokinin recognition by Arabidopsis thaliana histidine kinase 4. *Nature chemical biology*, *7*(11), 766–768. https://doi.org/10.1038/nchembio.667

Hua, J., & Meyerowitz, E. M. (1998). Ethylene responses are negatively regulated by a receptor gene family in Arabidopsis thaliana. *Cell*, *94*(2), 261–271. https://doi.org/10.1016/s0092-8674(00)81425-7

Hutchison, C. E., Li, J., Argueso, C., Gonzalez, M., Lee, E., Lewis, M. W., Maxwell, B. B., Perdue, T. D., Schaller, G. E., Alonso, J. M., Ecker, J. R., & Kieber, J. J. (2006). The Arabidopsis histidine phosphotransfer proteins are redundant positive regulators of cytokinin signaling. *Plant Cell*, *18*(11), 3073–3087. https://doi.org/10.1105/tpc.106.045674

Hwang, I., & Sheen, J. (2001). Two-component circuitry in Arabidopsis cytokinin signal transduction. *Nature*, *413*(6854), 383–389. https://doi.org/10.1038/35096500

Inoue, T., Higuchi, M., Hashimoto, Y., Seki, M., Kobayashi, M., Kato, T., Tabata, S., Shinozaki, K., & Kakimoto, T. (2001). *Identification of CRE1 as a cytokinin receptor from Arabidopsis*. *409*(February), 48–51.

Imamura, A., Hanaki, N., Nakamura, A., Suzuki, T., Taniguchi, M., Kiba, T., Ueguchi, C., Sugiyama, T., & Mizuno, T. (1999). Compilation and characterization of Arabidopsis thaliana response regulators implicated in His-Asp phosphorelay signal transduction.

Plant & Cell Physiology, *40*(7), 733–742. https://doi.org/10.1093/oxfordjournals.pcp.a029600

Ishida, K., Yamashino, T., Yokoyama, A., & Mizuno, T. (2008). Three type-B response regulators, ARR1, ARR10 and ARR12, play essential but redundant roles in cytokinin signal transduction throughout the life cycle of Arabidopsis thaliana. *Plant and Cell Physiology*, *49*(1), 47–57. https://doi.org/10.1093/pcp/pcm165

Izhaki, A., Bowman J. L., (2007). KANADI and Class III HD-Zip Gene Families Regulate Embryo Patterning and Modulate Auxin Flow during Embryogenesis in *Arabidopsis*, *The Plant Cell*, 19(2) 495–508, https://doi.org/10.1105/tpc.106.047472

Kakimoto T. (1996). CKI1, a histidine kinase homolog implicated in cytokinin signal transduction. *Science (New York, N.Y.)*, *274*(5289), 982–985. https://doi.org/10.1126/science.274.5289.982

Kakimoto T. (2001). Identification of plant cytokinin biosynthetic enzymes as dimethylallyl diphosphate:ATP/ADP isopentenyltransferases. *Plant & cell physiology*, *42*(7), 677–685. https://doi.org/10.1093/pcp/pce112

Kakimoto, T. (2003). Perception and signal transduction of cytokinins. *Annual Review of Plant Biology*, *54*, 605–627. https://doi.org/10.1146/annurev.arplant.54.031902.134802

Kang, N. Y., Cho, C., & Kim, J. (2013). Inducible expression of Arabidopsis response regulator 22 (ARR22), a Type-C ARR, in transgenic Arabidopsis enhances drought and freezing tolerance. *PLoS ONE*, *8*(11). https://doi.org/10.1371/journal.pone.0079248

Kerstetter, R. A., Bollman, K., Taylor, R. A., Bomblies, K., & Poethig, R. S. (2001). KANADI regulates organ polarity in Arabidopsis. *Nature*, *411*(6838), 706–709. https://doi.org/10.1038/35079629

Kim, S. Y., Kim, S. G., Kim, Y. S., Seo, P. J., Bae, M., Yoon, H. K., & Park, C. M. (2007). Exploring membrane-associated NAC transcription factors in Arabidopsis: Implications

for membrane biology in genome regulation. *Nucleic Acids Research*, *35*(1), 203–213. https://doi.org/10.1093/nar/gkl1068

Koenig, R. L., Morris, R. O., & Polacco, J. C. (2002). tRNA is the source of low-level trans-zeatin production in Methylobacterium spp. *Journal of bacteriology*, *184*(7), 1832–1842. https://doi.org/10.1128/JB.184.7.1832-1842.2002

Krishnaswamy, S., Verma, S., Rahman, M. H., & Kav, N. N. V. (2011). Functional characterization of four APETALA2-family genes (RAP2.6, RAP2.6L, DREB19 and DREB26) in Arabidopsis. *Plant Molecular Biology*, *75*(1), 107–127. https://doi.org/10.1007/s11103-010-9711-7

Kurakawa, T., Ueda, N., Maekawa, M., Kobayashi, K., Kojima, M., Nagato, Y., Sakakibara, H., & Kyozuka, J. (2007). Direct control of shoot meristem activity by a cytokinin-activating enzyme. *Nature*, *445*(7128), 652–655. https://doi.org/10.1038/nature05504

Kuroha, T., Tokunaga, H., Kojima, M., Ueda, N., Ishida, T., Nagawa, S., Fukuda, H., Sugimoto, K., & Sakakibara, H. (2009). Functional analyses of LONELY GUY cytokinin-activating enzymes reveal the importance of the direct activation pathway in Arabidopsis. *The Plant Cell*, *21*(10), 3152–3169. https://doi.org/10.1105/tpc.109.068676

Landrein, B., Refahi, Y., Besnard, F., Hervieux, N., Mirabet, V., Boudaoud, A., Vernoux, T., & Hamant, O. (2015). Meristem size contributes to the robustness of phyllotaxis in Arabidopsis. *Journal of Experimental Botany*, *66*(5), 1317–1324. https://doi.org/10.1093/jxb/eru482

Laux, T., Mayer, K. F., Berger, J., & Jürgens, G. (1996). The WUSCHEL gene is required for shoot and floral meristem integrity in Arabidopsis. *Development (Cambridge, England)*, *122*(1), 87–96. https://doi.org/10.1242/dev.122.1.87

Leibfried, A., To, J. P. C., Busch, W., Stehling, S., Kehle, A., Demar, M., Kieber, J. J., & Lohmann, J. U. (2005). WUSCHEL controls meristem function by direct regulation of

cytokinin-inducible response regulators. *Nature*, *438*(7071), 1172–1175. https://doi.org/10.1038/nature04270

Letham, D. S. 1963. Zeatin, a factor inducing cell division isolated from *Zea mays*. Life Sci. 2: 569-579.

Letham, D. S., I. S. Shannon and I. R. McDonald. 1964. The structure of zeatin, a factor inducing cell division. Proc. Chem. Soc. 230-231.

Letham, D. S. 1974. The cytokinins of coconut milk. Physiol. Plant. 32: 66-70.

Lu, P., Porat, R., Nadeau, J. A., & O'Neill, S. D. (1996). Identification of a meristem L1 layer-specific gene in Arabidopsis that is expressed during embryonic pattern formation and defines a new class of homeobox genes. *The Plant cell*, *8*(12), 2155–2168. https://doi.org/10.1105/tpc.8.12.2155

Mähönen, A. P., Higuchi, M., Törmäkangas, K., Miyawaki, K., Pischke, M. S., Sussman, M. R., Helariutta, Y., & Kakimoto, T. (2006). Cytokinins Regulate a Bidirectional Phosphorelay Network in Arabidopsis. *Current Biology*, *16*(11), 1116–1122. https://doi.org/10.1016/j.cub.2006.04.030

Mason, M. G., Li, J., Mathews, D. E., Kieber, J. J., & Schaller, G. E. (2004). Type-B response regulators display overlapping expression patterns in Arabidopsis. *Plant Physiology*, *135*(2), 927–937. https://doi.org/10.1104/pp.103.038109

Mayer, K. F., Schoof, H., Haecker, A., Lenhard, M., Jürgens, G., & Laux, T. (1998). Role of WUSCHEL in regulating stem cell fate in the Arabidopsis shoot meristem. *Cell*, *95*(6), 805–815. https://doi.org/10.1016/s0092-8674(00)81703-1

Meyerowitz EM. Genetic control of cell division patterns in developing plants. Cell. 1997 Feb 7;88(3):299-308. doi: 10.1016/s0092-8674(00)81868-1. PMID: 9039256.

McConnell, J. R., Emery, J., Eshed, Y., Bao, N., Bowman, J., & Barton, M. K. (2001). Role of PHABULOSA and PHAVOLUTA in determining radial patterning in shoots. *Nature*, *411*(6838), 709–713. https://doi.org/10.1038/35079635

Miller, C., F. Skoog, M. H. Von Saltza and E. M. Strong. 1955a. Kinetin, a cell division factor from deoxyribonucleic acid. J. Amer. Chem. Soc. 77: 1392.

Miller, C. 1961. A kinetin-like compound in maize. Proc. Nat. Acad. Sci. 47: 170-174.

Miyawaki, K., Matsumoto-Kitano, M., & Kakimoto, T. (2004). Expression of cytokinin biosynthetic isopentenyltransferase genes in Arabidopsis: Tissue specificity and regulation by auxin, cytokinin, and nitrate. *Plant Journal*, *37*(1), 128–138. https://doi.org/10.1046/j.1365-313X.2003.01945.x

Miyawaki, K., Tarkowski, P., Matsumoto-Kitano, M., Kato, T., Sato, S., Tarkowska, D., Tabata, S., Sandberg, G., & Kakimoto, T. (2006). Roles of Arabidopsis ATP/ADP isopentenyltransferases and tRNA isopentenyltransferases in cytokinin biosynthesis. *Proceedings of the National Academy of Sciences of the United States of America*, *103*(44), 16598–16603. https://doi.org/10.1073/pnas.0603522103

Mizuno T. (1997). Compilation of all genes encoding two-component phosphotransfer signal transducers in the genome of Escherichia coli. *DNA research : an international journal for rapid publication of reports on genes and genomes*, *4*(2), 161–168. https://doi.org/10.1093/dnares/4.2.161

Moubayidin, L., di Mambro, R., & Sabatini, S. (2009). Cytokinin-auxin crosstalk. *Trends in Plant Science*, *14*(10), 557–562. https://doi.org/10.1016/j.tplants.2009.06.010

Mok, D. W., & Mok, M. C. (2001). CYTOKININ METABOLISM AND ACTION. *Annual review of plant physiology and plant molecular biology*, *52*, 89–118. https://doi.org/10.1146/annurev.arplant.52.1.89

Müller, R., Borghi, L., Kwiatkowska, D., Laufs, P., & Simon, R. (2006). Dynamic and compensatory responses of Arabidopsis shoot and floral meristems to CLV3 signaling. *The Plant cell*, *18*(5), 1188–1198. https://doi.org/10.1105/tpc.105.040444

Müller, R., Bleckmann, A., & Simon, R. (2008). The receptor kinase CORYNE of Arabidopsis transmits the stem cell-limiting signal CLAVATA3 independently of CLAVATA1. *The Plant cell*, *20*(4), 934–946. https://doi.org/10.1105/tpc.107.057547

Nayar S. Exploring the Role of a Cytokinin-Activating Enzyme LONELY GUY in Unicellular Microalga *Chlorella variabilis*. Front Plant Sci. 2021 Jan 29;11:611871. doi: 10.3389/fpls.2020.611871. PMID: 33613586; PMCID: PMC7891180.

Nguyen, K. H., Ha, C. van, Nishiyama, R., Watanabe, Y., Leyva-González, M. A., Fujita, Y., Tran, U. T., Li, W., Tanaka, M., Seki, M., Schaller, G. E., Herrera-Estrella, L., & Tran, L. S. P. (2016). Arabidopsis type B cytokinin response regulators ARR1, ARR10, and ARR12 negatively regulate plant responses to drought. *Proceedings of the National Academy of Sciences of the United States of America*, *113*(11), 3090–3095. https://doi.org/10.1073/pnas.1600399113

Nishimura, C., Ohashi, Y., Sato, S., Kato, T., Tabata, S., & Ueguchi, C. (2004). Histidine kinase homologs that act as cytokinin receptors possess overlapping functions in the regulation of shoot and root growth in arabidopsis. *Plant Cell*, *16*(6), 1365–1377. https://doi.org/10.1105/tpc.021477

Nishiyama, R., Watanabe, Y., Fujita, Y., Le, D. T., Kojima, M., Werner, T., Vankova, R., Yamaguchi-Shinozaki, K., Shinozaki, K., Kakimoto, T., Sakakibara, H., Schmülling, T., & Tran, L.-S. P. (2011). Analysis of cytokinin mutants and regulation of cytokinin metabolic genes reveals important regulatory roles of cytokinins in drought, salt and abscisic Acid responses, and abscisic Acid biosynthesis. *The Plant Cell*, *23*(6), 2169–2183. https://doi.org/10.1105/tpc.111.087395

Nishiyama, R., Watanabe, Y., Leyva-Gonzalez, M. A., van Ha, C., Fujita, Y., Tanaka, M., Seki, M., Yamaguchi-Shinozaki, K., Shinozaki, K., Herrera-Estrella, L., & Tran, L. S. P. (2013). Arabidopsis AHP2, AHP3, and AHP5 histidine phosphotransfer proteins function as redundant negative regulators of drought stress response. *Proceedings of the National Academy of Sciences of the United States of America*, *110*(12), 4840–4845. https://doi.org/10.1073/pnas.1302265110

Nobécourt, P. 1938. Sur les proliferations spontanées de fragments de tubercules de Carotte et leur culture sur milieu synthétique. Bull. Soc. Bot. Fr. 85: 1-7.

Nobécourt, P. 1939. Sur la pérennité et l'augmentation de volume des cultures de tissus végétaux. C. R. Soc. Biol. 130: 1270-1271.

Novák, O., Hauserová, E., Amakorová, P., Doležal, K., & Strnad, M. (2008). Cytokinin profiling in plant tissues using ultra-performance liquid chromatography-electrospray tandem mass spectrometry. *Phytochemistry*, *69*(11), 2214–2224. https://doi.org/10.1016/j.phytochem.2008.04.022

O'Malley, R. C., Huang, S. S. C., Song, L., Lewsey, M. G., Bartlett, A., Nery, J. R., Galli, M., Gallavotti, A., & Ecker, J. R. (2016). Cistrome and Epicistrome Features Shape the Regulatory DNA Landscape. *Cell*, *165*(5), 1280–1292. https://doi.org/10.1016/j.cell.2016.04.038

Ogawa, E., Yamada, Y., Sezaki, N., Kosaka, S., Kondo, H., Kamata, N., Abe, M., Komeda, Y., & Takahashi, T. (2015). ATML1 and PDF2 Play a Redundant and Essential Role in Arabidopsis Embryo Development. *Plant & cell physiology*, *56*(6), 1183–1192. https://doi.org/10.1093/pcp/pcv045

Orchard CB, Siciliano I, Sorrell DA, Marchbank A, Rogers HJ, Francis D, Herbert RJ, Suchomelova P, Lipavska H, Azmi A, Van Onckelen H. Tobacco BY-2 cells expressing

fission yeast cdc25 bypass a G2/M block on the cell cycle. Plant J. 2005 Oct;44(2):290-9. doi: 10.1111/j.1365-313X.2005.02524.x. PMID: 16212607.

Perotti, M. F., Ribone, P. A., Cabello, J. v., Ariel, F. D., & Chan, R. L. (2019). AtHB23 participates in the gene regulatory network controlling root branching, and reveals differences between secondary and tertiary roots. *Plant Journal*, *100*(6), 1224–1236. https://doi.org/10.1111/tpj.14511

Pfaffl, M. W. (2001). A new mathematical model for relative quantification in real-time RT-PCR. In *Nucleic Acids Research* (Vol. 29, Issue 9).

Plong, A., Rodriguez, K., Alber, M. *et al.* CLAVATA3 mediated simultaneous control of transcriptional and post-translational processes provides robustness to the WUSCHEL gradient. *Nat Commun* **12,** 6361 (2021). https://doi.org/10.1038/s41467-021-26586-0

Proveniers, M., Rutjens, B., Brand, M., & Smeekens, S. (2007). The Arabidopsis TALE homeobox gene ATH1 controls floral competency through positive regulation of FLC. *Plant Journal*, *52*(5), 899–913. https://doi.org/10.1111/j.1365-313X.2007.03285.x

Reddy, G. V., & Meyerowitz, E. M. (2005). Stem-cell homeostasis and growth dynamics can be uncoupled in the Arabidopsis shoot apex. *Science (New York, N.Y.)*, *310*(5748), 663–667. https://doi.org/10.1126/science.1116261

Reinhardt, D., Pesce, E. R., Stieger, P., Mandel, T., Baltensperger, K., Bennett, M., Traas, J., Friml, J., & Kuhlemeier, C. (2003). Regulation of phyllotaxis by polar auxin transport. *Nature*, *426*(6964), 255–260. https://doi.org/10.1038/nature02081

Riefler, M., Novak, O., Strnad, M., & Schmülling, T. (2006). Arabidopsis cytokinin receptors mutants reveal functions in shoot growth, leaf senescence, seed size, germination, root development, and cytokinin metabolism. *Plant Cell*, *18*(1), 40–54. https://doi.org/10.1105/tpc.105.037796

Riou-Khamlichi C, Huntley R, Jacqmard A, Murray JA. Cytokinin activation of Arabidopsis cell division through a D-type cyclin. Science. 1999 Mar 5;283(5407):1541-4. doi: 10.1126/science.283.5407.1541. PMID: 10066178.

Robbins, W. J. 1922a. Cultivation of excised root-tips and stem tips under sterile conditions. Bot. Gaz. 73: 376-390.

Robbins, W. J. 1922b. Effect of autolyzed yeast and peptone on growth of excised corn root tips in the dark. Bot. Gaz. 74: 59-79.

Robinson, C. R., & Sauer, R. T. (1998). Optimizing the stability of single-chain proteins by linker length and composition mutagenesis. *Proceedings of the National Academy of Sciences of the United States of America*, *95*(11), 5929–5934. https://doi.org/10.1073/pnas.95.11.5929

Rodermel, S. (2002). Arabidopsis Variegation Mutants. *The Arabidopsis Book*, *1*, e0079. https://doi.org/10.1199/tab.0079

Sakakibara H. (2005). Cytokinin biosynthesis and regulation. *Vitamins and hormones*, *72*, 271–287. https://doi.org/10.1016/S0083-6729(05)72008-2

Sakakibara, H., Takei, K., & Hirose, N. (2006). Interactions between nitrogen and cytokinin in the regulation of metabolism and development. *Trends in Plant Science*, *11*(9), 440–448. https://doi.org/10.1016/j.tplants.2006.07.004

Sakai, H., Honma, T., Aoyama, T., Sato, S., Kato, T., Tabata, S., & Oka, A. (2001). ARR1, a transcription factor for genes immediately responsive to cytokinins. *Science (New York, N.Y.)*, *294*(5546), 1519–1521. https://doi.org/10.1126/science.1065201

Sakamoto, H., Maruyama, K., Sakuma, Y., Meshi, T., Iwabuchi, M., Shinozaki, K., & Yamaguchi-Shinozaki, K. (2004). Arabidopsis Cys2/His2-type zinc-finger proteins function as transcription repressors under drought, cold, and high-salinity stress

conditions. *Plant Physiology*, *136*(1), 2734–2746. https://doi.org/10.1104/pp.104.046599

Sawa, S., Watanabe, K., Goto, K., Liu, Y. G., Shibata, D., Kanaya, E., Morita, E. H., & Okada, K. (1999). FILAMENTOUS FLOWER, a meristem and organ identity gene of Arabidopsis, encodes a protein with a zinc finger and HMG-related domains. *Genes & development*, *13*(9), 1079–1088. https://doi.org/10.1101/gad.13.9.1079

Schaller, G. E., Street, I. H., & Kieber, J. J. (2014). Cytokinin and the cell cycle. *Current opinion in plant biology*, *21*, 7–15. https://doi.org/10.1016/j.pbi.2014.05.015

Scheres B., Laurenzio D. L., Willemsen V., Hauser M. T., Janmaat K., Weisbeek P., Benfey P. N. (1995) Mutations affecting the radial organisation of the Arabidopsis root display specific defects throughout the embryonic axis. *Development*, 121 (1): 53–62. doi: https://doi.org/10.1242/dev.121.1.53

Schoof, H., Lenhard, M., Haecker, A., Mayer, K. F., Jürgens, G., & Laux, T. (2000). The stem cell population of Arabidopsis shoot meristems in maintained by a regulatory loop between the CLAVATA and WUSCHEL genes. *Cell*, *100*(6), 635–644. https://doi.org/10.1016/s0092-8674(00)80700-x

Seo, P. J., Kim, M. J., Song, J. S., Kim, Y. S., Kim, H. J., & Park, C. M. (2010). Proteolytic processing of an Arabidopsis membrane-bound NAC transcription factor is triggered by cold-induced changes in membrane fluidity. *Biochemical Journal*, *427*(3), 359–367. https://doi.org/10.1042/BJ20091762

Sessions A., Weigel D., Yanofsky M.F. (1999) The *Arabidopsis thaliana MERISTEM LAYER1* promoter specifies epidermal expression in meristems and young primordia. *Plant J, 20,* 259-263.

Schleiden, M. J. 1838. Beiträge zur Phytogenesis. Müller Arch. Anat. und Physiol.: 137-176.

Schrick, K., Nguyen, D., Karlowski, W. M., & Mayer, K. F. (2004). START lipid/sterol-binding domains are amplified in plants and are predominantly associated with homeodomain transcription factors. *Genome biology*, *5*(6), R41. https://doi.org/10.1186/gb-2004-5-6-r41

Shen, J., Chen, X., Hendershot, L., & Prywes, R. (2002). ER stress regulation of ATF6 localization by dissociation of BiP/GRP78 binding and unmasking of Golgi localization signals. *Developmental cell*, *3*(1), 99–111. https://doi.org/10.1016/s1534-5807(02)00203-4

Smit, M. E., McGregor, S. R., Sun, H., Gough, C., Bågman, A.-M., Soyars, C. L., Kroon, J. T., Gaudinier, A., Williams, C. J., Yang, X., Nimchuk, Z. L., Weijers, D., Turner, S. R., Brady, S. M., & Etchells, J. P. (2020). A PXY-Mediated Transcriptional Network Integrates Signaling Mechanisms to Control Vascular Development in Arabidopsis. *The Plant Cell*, *32*(2), 319–335. https://doi.org/10.1105/tpc.19.00562

Sun, J., Niu, Q. W., Tarkowski, P., Zheng, B., Tarkowska, D., Sandberg, G., Chua, N. H., & Zuo, J. (2003). The Arabidopsis AtIPT8/PGA22 gene encodes an isopentenyl transferase that is involved in de novo cytokinin biosynthesis. *Plant physiology*, *131*(1), 167–176.

Suzuki, T., Imamura, A., Ueguchi, C., & Mizuno, T. (1998). Histidine-containing phosphotransfer (HPt) signal transducers implicated in His-to-Asp phosphorelay in Arabidopsis. *Plant & Cell Physiology*, *39*(12), 1258–1268. https://doi.org/10.1093/oxfordjournals.pcp.a029329

Suzuki, T., Miwa, K., Ishikawa, K., Yamada, H., Aiba, H., & Mizuno, T. (2001). The Arabidopsis sensor His-kinase, AHK4, can respond to cytokinins. *Plant and Cell Physiology*, *42*(2), 107–113. https://doi.org/10.1093/pcp/pce037

Sweere, U., Eichenberg, K., Lohrmann, J., Mira-Rodado, V., Bäurle, I., Kudla, J., Nagy, F., Schafer, E., & Harter, K. (2001). Interaction of the response regulator ARR4 with

phytochrome B in modulating red light signaling. *Science (New York, N.Y.)*, *294*(5544), 1108–1111. https://doi.org/10.1126/science.1065022

Takeda, S., Fujisawa, Y., Matsubara, M., Aiba, H., & Mizuno, T. (2001). A novel feature of the multistep phosphorelay in Escherichia coli: a revised model of the RcsC --> YojN --> RcsB signalling pathway implicated in capsular synthesis and swarming behaviour. *Molecular microbiology*, *40*(2), 440–450.

Takei, K., Ueda, N., Aoki, K., Kuromori, T., Hirayama, T., Shinozaki, K., Yamaya, T., & Sakakibara, H. (2004). AtIPT3 is a key determinant of nitrate-dependent cytokinin biosynthesis in Arabidopsis. *Plant and Cell Physiology*, *45*(8), 1053–1062. https://doi.org/10.1093/pcp/pch119

Tan, Q. K. G., & Irish, V. F. (2006). The Arabidopsis zinc finger-homeodomain genes encode proteins with unique biochemical properties that are coordinately expressed during floral development. *Plant Physiology*, *140*(3), 1095–1108. https://doi.org/10.1104/pp.105.070565

Tang, M., Li, B., Zhou, X., Bolt, T., Li, J. J., Cruz, N., Gaudinier, A., Ngo, R., Clark-Wiest, C., Kliebenstein, D. J., & Brady, S. M. (2021). A genome-scale TF-DNA interaction network of transcriptional regulation of Arabidopsis primary and specialized metabolism. *Molecular Systems Biology*, *17*(11), e10625. https://doi.org/10.15252/msb.202110625

To, J. P. C., Deruère, J., Maxwell, B. B., Morris, V. F., Hutchison, C. E., Ferreira, F. J., Schaller, G. E., & Kieber, J. J. (2007). Cytokinin regulates type-A Arabidopsis Response Regulator activity and protein stability via two-component phosphorelay. *The Plant Cell*, *19*(12), 3901–3914. https://doi.org/10.1105/tpc.107.052662

To, J. P. C., Haberer, G., Ferreira, F. J., Deruère, J., Mason, M. G., Schaller, G. E., Alonso, J. M., Ecker, J. R., & Kieber, J. J. (2004). Type-A Arabidopsis response regulators are

partially redundant negative regulators of cytokinin signaling. *The Plant Cell*, *16*(3), 658–671. https://doi.org/10.1105/tpc.018978

To, J. P. C., & Kieber, J. J. (2008). Cytokinin signaling: two-components and more. *Trends in Plant Science*, *13*(2), 85–92. https://doi.org/10.1016/j.tplants.2007.11.005

To, J. P. C., Deruère, J., Maxwell, B. B., Morris, V. F., Hutchison, C. E., Ferreira, F. J., Schaller, G. E., & Kieber, J. J. (2007). Cytokinin regulates type-A Arabidopsis Response Regulator activity and protein stability via two-component phosphorelay. *The Plant Cell*, *19*(12), 3901–3914. https://doi.org/10.1105/tpc.107.052662

Tokunaga, H., Kojima, M., Kuroha, T., Ishida, T., Sugimoto, K., Kiba, T., & Sakakibara, H. (2012). Arabidopsis lonely guy (LOG) multiple mutants reveal a central role of the LOG-dependent pathway in cytokinin activation. *Plant Journal*, *69*(2), 355–365. https://doi.org/10.1111/j.1365-313X.2011.04795.x

Tran, L. P., Urao, T., Qin, F., Maruyama, K., Kakimoto, T., Shinozaki, K., & Yamaguchi-Shinozaki, K. (2007). Functional analysis of AHK1/ATHK1 and cytokinin receptor histidine kinases in response to abscisic acid, drought, and salt stress in Arabidopsis. *Proceedings of the National Academy of Sciences of the United States of America*, *104*(51), 20623–20628. https://doi.org/10.1073/pnas.0706547105

Tran, L. S. P., Nakashima, K., Sakuma, Y., Osakabe, Y., Qin, F., Simpson, S. D., Maruyama, K., Fujita, Y., Shinozaki, K., & Yamaguchi-Shinozaki, K. (2007). Co-expression of the stress-inducible zinc finger homeodomain ZFHD1 and NAC transcription factors enhances expression of the ERD1 gene in Arabidopsis. *Plant Journal*, *49*(1), 46–63. https://doi.org/10.1111/j.1365-313X.2006.02932.x

Truskina, J., Han, J., Chrysanthou, E., Galvan-Ampudia, C. S., Lainé, S., Brunoud, G., Macé, J., Bellows, S., Legrand, J., Bågman, A. M., Smit, M. E., Smetana, O., Stigliani, A., Porco, S., Bennett, M. J., Mähönen, A. P., Parcy, F., Farcot, E., Roudier, F., …

Vernoux, T. (2021). A network of transcriptional repressors modulates auxin responses. *Nature*, *589*(7840), 116–119. https://doi.org/10.1038/s41586-020-2940-2

Ueguchi, C., Koizumi, H., Suzuki, T., & Mizuno, T. (2001). Novel Family of Sensor Histidine Kinase Genes in Arabidopsis thaliana. In *Plant Cell Physiol* (Vol. 42, Issue 2). https://academic.oup.com/pcp/article/42/2/231/1929913

Ulmasov, T., Hagen, G., & Guilfoyle, T. J. (1999). Activation and repression of transcription by auxin-response factors. *Proceedings of the National Academy of Sciences of the United States of America*, *96*(10), 5844–5849. https://doi.org/10.1073/pnas.96.10.5844

Urao, T., Miyata, S., Yamaguchi-Shinozaki, K., & Shinozaki, K. (2000). Possible His to Asp phosphorelay signaling in an Arabidopsis two-component system. *FEBS Letters*, *478*(3), 227–232. https://doi.org/10.1016/s0014-5793(00)01860-3

Vik, A., & Rine, J. (2000). Membrane biology: membrane-regulated transcription. *Current biology : CB*, *10*(23), R869–R871. https://doi.org/10.1016/s0960-9822(00)00822-8

Wang, J., Tian, C., Zhang, C., Shi, B., Cao, X., Zhang, T. Q., Zhao, Z., Wang, J. W., & Jiao, Y. (2017). Cytokinin signaling activates WUSCHEL expression during axillary meristem initiation. *Plant Cell*, *29*(6), 1373–1387. https://doi.org/10.1105/tpc.16.00579

Watanabe, K., & Okada, K. (2003). Two discrete cis elements control the Abaxial side-specific expression of the FILAMENTOUS FLOWER gene in Arabidopsis. *The Plant cell*, *15*(11), 2592–2602. https://doi.org/10.1105/tpc.015214

Went, F. W. 1926. On growth accelerating substances in the coleoptile of *Avena sativa*. Proc. Kon. Nederl. Akad. Wetensch. Amsterdam 30: 10

Werner, T., Motyka, V., Laucou, V., Smets, R., Onckelen, H. van, & Schmuelling, T. (2003). Cytokinin-Deficient Transgenic Arabidopsis Plants Show Functions of Cytokinins in the Regulation of Shoot and Root Meristem Activity. *The Plant Cell*, *15*(November), 2532–2550. https://doi.org/10.1105/tpc.014928.)

White, P. R. 1939a. Potentially unlimited growth of excised plant callus in an artificial medium. Amer. J. Bot. 26: 59-64.

White, P. R. 1939b. Controlled differentiation in a plant tissue culture. Bull. Torrey. Bot. Club 66: 507-513.

Wulfetange, K., Lomin, S. N., Romanov, G. A., Stolz, A., Heyl, A., & Schmülling, T. (2011). The cytokinin receptors of Arabidopsis are located mainly to the endoplasmic reticulum. *Plant physiology*, *156*(4), 1808–1818. https://doi.org/10.1104/pp.111.180539

Xie, M., Chen, H., Huang, L., O'Neil, R. C., Shokhirev, M. N., & Ecker, J. R. (2018). A B-ARR-mediated cytokinin transcriptional network directs hormone cross-regulation and shoot development. *Nature Communications*, *9*(1), 1–13. https://doi.org/10.1038/s41467-018-03921-6

Yadav, R. K., Perales, M., Gruel, J., Ohno, C., Heisler, M., Girke, T., Jönsson, H., & Reddy, G. V. (2013). Plant stem cell maintenance involves direct transcriptional repression of differentiation program. *Molecular systems biology*, *9*, 654. https://doi.org/10.1038/msb.2013.8

Yadav, R. K., Tavakkoli, M., Xie, M., Girke, T., & Venugopala, R. G. (2014). A high-resolution gene expression map of the arabidopsis shoot meristem stem cell niche. *Development (Cambridge)*, *141*(13), 2735–2744. https://doi.org/10.1242/dev.106104

Yang, Z. T., Lu, S. J., Wang, M. J., Bi, D. L., Sun, L., Zhou, S. F., Song, Z. T., & Liu, J. X. (2014). A plasma membrane-tethered transcription factor, NAC062/ANAC062/NTL6, mediates the unfolded protein response in Arabidopsis. *Plant Journal*, *79*(6), 1033–1043. https://doi.org/10.1111/tpj.12604

Yamada, H., Suzuki, T., Terada, K., Takei, K., Ishikawa, K., Miwa, K., Yamashino, T., & Mizuno, T. (2001). The Arabidopsis AHK4 Histidine Kinase is a Cytokinin-Binding

Receptor that Transduces Cytokinin Signals Across the Membrane. In *Plant Cell Physiol* (Vol. 42, Issue 9).

Xiong, L., Schumaker, K. S., & Zhu, J. K. (2002). Cell signaling during cold, drought, and salt stress. *The Plant cell*, *14 Suppl*(Suppl), S165–S183. https://doi.org/10.1105/tpc.000596

Zhang, K., Novak, O., Wei, Z., Gou, M., Zhang, X., Yu, Y., Yang, H., Cai, Y., Strnad, M., & Liu, C. J. (2014). Arabidopsis ABCG14 protein controls the acropetal translocation of root-synthesized cytokinins. *Nature communications*, *5*, 3274. https://doi.org/10.1038/ncomms4274

Zhang, F., May, A., & Irish, V. F. (2017). Type-B ARABIDOPSIS RESPONSE REGULATORs Directly Activate WUSCHEL. *Trends in Plant Science*, *22*(10), 815–817. https://doi.org/10.1016/j.tplants.2017.08.007

Zhao, Z., Andersen, S. U., Ljung, K., Dolezal, K., Miotk, A., Schultheiss, S. J., & Lohmann, J. U. (2010). Hormonal control of the shoot stem-cell niche. *Nature*, *465*(7301), 1089–1092. https://doi.org/10.1038/nature09126

Zubo, Y. O., Blakley, I. C., Yamburenko, M. v., Worthen, J. M., Street, I. H., Franco-Zorrilla, J. M., Zhang, W., Hill, K., Raines, T., Solano, R., Kieber, J. J., Loraine, A. E., & Schaller, G. E. (2017). Cytokinin induces genome-wide binding of the type-B response regulator ARR10 to regulate growth and development in Arabidopsis. *Proceedings of the National Academy of Sciences of the United States of America*, *114*(29), E5995–E6004. https://doi.org/10.1073/pnas.1620749114

Zürcher, E., Tavor-Deslex, D., Lituiev, D., Enkerli, K., Tarr, P. T., & Müller, B. (2013). A robust and sensitive synthetic sensor to monitor the transcriptional output of the cytokinin signaling network in planta. *Plant Physiology*, *161*(3), 1066–1075. https://doi.org/10.1104/pp.112.211763